

Spring 5-6-2016

## Scalable Three-Dimensional Grasping Mechanism

Ikya Mamidala  
*Bowling Green State University*

Follow this and additional works at: [https://scholarworks.bgsu.edu/ms\\_tech\\_mngmt](https://scholarworks.bgsu.edu/ms_tech_mngmt)



Part of the [Applied Mechanics Commons](#), and the [Computer-Aided Engineering and Design Commons](#)

---

### Recommended Citation

Mamidala, Ikya, "Scalable Three-Dimensional Grasping Mechanism" (2016). *Master of Technology Management Plan II Graduate Projects*. 21.

[https://scholarworks.bgsu.edu/ms\\_tech\\_mngmt/21](https://scholarworks.bgsu.edu/ms_tech_mngmt/21)

This Thesis is brought to you for free and open access by the College of Technology, Architecture and Applied Engineering at ScholarWorks@BGSU. It has been accepted for inclusion in Master of Technology Management Plan II Graduate Projects by an authorized administrator of ScholarWorks@BGSU.

**SCALABLE THREE-DIMENSIONAL GRASPING MECHANISM**

Ikyu Mamidala

A Major Project

Submitted to the Graduate College of Bowling Green  
State University in the partial fulfillment of  
the requirements for the degree of

MASTER OF TECHNOLOGY MANAGEMENT

May 2016

Committee:

Dr. Mohammad Mayyas, Advisor

Dr. Sri Kolla

## ABSTRACT

Dr. Mohammad Mayyas, Advisor

In this work, we develop a scalable end-effector mechanism for grasping three-dimensional objects with sizes ranging from micrometer to millimeter scale. The design architecture of the gripper comprises an array of identical fingers patented in a circular fashion. Each finger is designed from a novel linkage mechanism whose end effector is manipulated by two independent actuators. In this research, we study three finger gripper device, where each is obtained from a 3 - linkage mechanism. The device is controlled by three independent piezo actuators, and one electro-magnetic solenoid common to each mechanism. The gripping capability depends on how fingers are controlled collectively and on the mechanical flexibility, which together provide variety of gripping performances that are necessary to handle a wide variety of objects. The gripping performance is defined here by grasping force at contact, motion range, and bandwidth. Optimization is done to design the link lengths for the best Geometric Advantage (GA), and the functionality evaluated using finite element analysis software, ANSYS.

Key words: Robotics, End-effector, Grasping mechanism, Flexibility, Scalability

## **ACKNOWLEDGEMENTS**

I would like to extend my sincere thanks to all of them who supported and helped me in making this project a success.

Foremost, I would like to express my special gratitude and thanks to my advisor Dr. Mohammad Mayyas for his guidance and constant supervision by providing required information for the project and also for his support, motivation, and patience in reviewing and completing the project.

I would like to thank my project committee member Dr. Sri Kolla for his critical advice and guidance in compiling the project.

I would also like to thank the faculty and staff in College of Technology, Architecture and Applied Engineering for their continuous support.

Last but not least I would like to thank my family and friends for providing encouragement during the preparation of this project.

## TABLE OF CONTENTS

ABSTRACT .....	ii
ACKNOWLEDGEMENTS .....	iii
TABLE OF CONTENTS .....	iv
LIST OF FIGURES .....	vii
LIST OF TABLES .....	xi
<b>CHAPTER 1: INTRODUCTION</b> .....	<b>1</b>
1.1 Context of the Problem .....	1
1.2 Problem Statement .....	3
1.3 Project Objectives .....	4
1.4 Significance of the Study .....	5
1.5 Definition of Terms .....	5
<b>CHAPTER 2: LITERATURE REVIEW</b> .....	<b>6</b>
2.1 Historical Perspective .....	6
2.2 Theoretical Topics .....	8
2.2.1 Actuation sources .....	8
2.2.2 Operating parameters of grippers.. .....	10
2.2.3 Mechanical mechanisms for grippers .....	15
2.2.4 Flexible gripping techniques .....	17
2.2.5 3D printable materials .....	21
2.2.6 Finite Element Method for analysis .....	22

2.3 Current Research Topics in Grasping Technology .....	25
2.4 Summary .....	26
<b>CHAPTER 3: METHODOLOGY .....</b>	<b>27</b>
3.1 Restatement of the Problem .....	27
3.2 Specific Aims .....	27
3.3 Procedure.....	29
3.3.1 Functionality.....	29
3.3.2 Flexibility .....	41
3.3.3 Scalability .....	42
<b>CHAPTER 4: FINDINGS .....</b>	<b>43</b>
4.1 Functionality.....	43
4.1.1 Analysis of line model.....	43
4.1.1.1 Optimization .....	49
4.1.2 Analysis of 3-D model.....	52
4.1.2.1 Meshing.....	52
4.1.2.2 Static Structural Analysis.....	54
4.1.2.3 Buckling analysis .....	64
4.1.2.4 Modal analysis. ....	75
4.1.2.5 Transient analysis.....	76
4.1.2.6 Static structural analysis with the object grasped .....	83
4.2 Flexibility .....	85

4.2.1 Grasping small size object.....	86
4.2.2 Grasping large size object.....	87
4.3 Scalability.....	88
4.3.1 Scalability under constant input displacement. ....	89
4.3.2 Scalability under varying input displacement .....	90
<b>CHAPTER 5: SUMMARY AND DISCUSSION .....</b>	<b>92</b>
5.1 Summary .....	92
5.2 Future work .....	93
<b>REFERENCES.....</b>	<b>94</b>

## LIST OF FIGURES

<b>Figure 1.1:</b> iRobot Warrior 710.....	2
<b>Figure 2.1:</b> Victor Schienman Stanford arm .....	6
<b>Figure 2.2:</b> Parallel gripper .....	7
<b>Figure 2.3:</b> Angular gripper .....	7
<b>Figure 2.4:</b> Barrett hand .....	8
<b>Figure 2.5:</b> Parallel gripper .....	12
<b>Figure 2.6:</b> Slider-crank mechanism .....	16
<b>Figure 2.7:</b> Gear and rack actuated mechanism .....	16
<b>Figure 2.8:</b> Cam actuated mechanism .....	16
<b>Figure 2.9:</b> Linkage actuated mechanism .....	16
<b>Figure 2.10:</b> (2) is the jaw to accommodate gripper fingers (1) .....	17
<b>Figure 2.11:</b> Multi-Gripper .....	18
<b>Figure 2.12:</b> Universal gripper handling different shaped objects.....	18
<b>Figure 2.13:</b> (a) 2 fingers (b) 3 fingers (c) 5 fingers robot gripper .....	19
<b>Figure 2.14:</b> Passive compliant gripper .....	20
<b>Figure 2.15:</b> Modular robot handling different sized objects .....	20
<b>Figure 2.16:</b> Automation gripper .....	22
<b>Figure 3.1:</b> 3D model of the gripper (by Dr. Mayyas).....	29
<b>Figure 3.2:</b> Detailed representation of links and base.....	30
<b>Figure 3.3:</b> Line model of a finger in Workbench .....	31
<b>Figure 3.4:</b> Workbench home page (Project Schematic and Tool box).....	32
<b>Figure 3.5:</b> Displacement through Electro-magnetic actuation .....	34



<b>Figure 3.6:</b> Displacement through piezo actuation .....	35
<b>Figure 3.7:</b> Force application (upwards) through EM actuation .....	37
<b>Figure 3.8:</b> Force application (downwards) through EM actuation .....	38
<b>Figure 3.9:</b> Force application (upwards) through piezo-electric actuation .....	39
<b>Figure 4.1:</b> Un-optimized line model .....	44
<b>Figure 4.2:</b> Input EM load and support in open mode (line model) .....	45
<b>Figure 4.3:</b> Output results under EM actuation in open mode (line model) .....	46
<b>Figure 4.4:</b> Input PE load and support in close mode (line model) .....	46
<b>Figure 4.5:</b> Output results under PE actuation in close mode (line model) .....	47
<b>Figure 4.6:</b> Input EM load and support in close mode (line model) .....	47
<b>Figure 4.7:</b> Output results under EM actuation in close mode (line model) .....	48
<b>Figure 4.8:</b> Optimized geometries .....	51
<b>Figure 4.9:</b> Mesh convergence .....	54
<b>Figure 4.10:</b> Input EM load in open mode .....	55
<b>Figure 4.11:</b> Directional deformation under EM actuation in open mode .....	56
<b>Figure 4.12:</b> Relationship between horizontal tip displacement and force in open mode .....	56
<b>Figure 4.13:</b> Equivalent stress under EM actuation in open mode .....	57
<b>Figure 4.14:</b> Relationship between equivalent stress and force in open mode .....	57
<b>Figure 4.15:</b> Input EM load in close mode for coarse movement .....	58
<b>Figure 4.16:</b> Directional deformation under EM actuation in close mode .....	59
<b>Figure 4.17:</b> Relationship between horizontal tip displacement and force in close mode under EM actuation .....	59
<b>Figure 4.18:</b> Equivalent stress under EM actuation in close mode .....	60

<b>Figure 4.19:</b> Relationship between stress and force in close mode under EM actuation.....	60
<b>Figure 4.20:</b> Input PE load in close mode for fine movement .....	61
<b>Figure 4.21:</b> Directional deformation under PE actuation in close mode .....	62
<b>Figure 4.22:</b> Relationship between horizontal tip displacement and force in close mode under PE actuation .....	62
<b>Figure 4.23:</b> Equivalent stress under PE actuation in close mode .....	63
<b>Figure 4.24:</b> Relationship between stress and force in close mode under PE actuation .....	63
<b>Figure 4.25:</b> Buckling modes in open mode under EM actuation .....	65
<b>Figure 4.26:</b> Buckling modes in close mode under EM actuation .....	66
<b>Figure 4.27:</b> Buckling modes in close mode under PE actuation .....	67
<b>Figure 4.28:</b> Buckling modes for fixed finger tips under EM actuation .....	68
<b>Figure 4.29:</b> Buckling modes for fixed finger tips under PE actuation .....	70
<b>Figure 4.30:</b> Buckling modes for frictionless support at tips under EM actuation .....	72
<b>Figure 4.31:</b> Buckling modes for frictionless support at tips under PE actuation .....	73
<b>Figure 4.32:</b> Effect of buckling load under EM actuation for various supports at tips.....	74
<b>Figure 4.33:</b> Effect of buckling load under PE actuation for various supports at tips .....	74
<b>Figure 4.34:</b> Mode shapes under pre-stressed condition.....	76
<b>Figure 4.35:</b> Input force vs time (Case-1).....	77
<b>Figure 4.36:</b> Output horizontal tip displacement vs time (Case-1).....	78
<b>Figure 4.37:</b> Input force vs time (Case-2).....	80
<b>Figure 4.38:</b> Output horizontal tip displacement vs time (Case-2).....	80
<b>Figure 4.39:</b> Input force vs time (Case-3).....	82
<b>Figure 4.40:</b> Output horizontal tip displacement vs time (Case-3).....	82

<b>Figure 4.41:</b> Gripper with the bead and its contact region.....	83
<b>Figure 4.42:</b> Contact status.....	84
<b>Figure 4.43:</b> Contact pressure .....	84
<b>Figure 4.44:</b> Output total deformation with the bead grasped .....	85
<b>Figure 4.45:</b> Output equivalent stress with the bead grasped .....	85
<b>Figure 4.46:</b> Gripper capable of grasping small sized object under EM actuation .....	86
<b>Figure 4.47:</b> Gripper capable of grasping small sized under EM and PE actuation .....	87
<b>Figure 4.48:</b> Gripper capable of grasping large sized object under EM actuation.....	88
<b>Figure 4.49:</b> Effect of scalability on output deformation under constant input displacement .....	89
<b>Figure 4.50:</b> Effect of scalability on equivalent stress under constant input displacement .....	90
<b>Figure 4.51:</b> Effect of scalability on output deformation under varying input displacement .....	91
<b>Figure 4.52:</b> Effect of scalability on equivalent stress under varying input displacement .....	91

## LIST OF TABLES

<b>Table 2.1:</b> Actuator and its input quantities .....	9
<b>Table 2.2:</b> Macro-size gripper actuation sources .....	9
<b>Table 2.3:</b> Micro-size gripper actuation sources .....	10
<b>Table 2.4:</b> Micro-size gripper characteristics.....	12
<b>Table 2.5:</b> Specifications of piezo actuators.....	13
<b>Table 2.6:</b> Electro-magnetic actuators specifications.....	14
<b>Table 2.7:</b> Macro-size gripper characteristics .....	14
<b>Table 2.8:</b> Material properties .....	21
<b>Table 3.1:</b> Objectives and aims of the project.....	28
<b>Table 3.2:</b> Preliminary dimensions extracted from the 3D model using Solidworks .....	31
<b>Table 3.3:</b> Material properties of ABS plastic taken for feasibility study .....	33
<b>Table 4.1:</b> Static structural analysis results of an un-optimized line model.....	48
<b>Table 4.2:</b> Input details for optimization and its output results.....	50
<b>Table 4.3:</b> Updated dimensions of a 3D model.....	51
<b>Table 4.4:</b> Mesh methods and its skewness .....	52
<b>Table 4.5:</b> Mesh statistics .....	53
<b>Table 4.6:</b> Buckling load under EM actuation in open mode.....	64
<b>Table 4.7:</b> Buckling load in close mode under EM actuation .....	65
<b>Table 4.8:</b> Buckling load in close mode under PE actuation .....	66
<b>Table 4.9:</b> Buckling load for fixed finger tips under EM actuation .....	68
<b>Table 4.10:</b> Buckling load for fixed finger tips under PE actuation .....	69
<b>Table 4.11:</b> Buckling load for frictionless support at tips under EM actuation .....	71

<b>Table 4.12:</b> Buckling load for frictionless support at tips under PE actuation.....	73
<b>Table 4.13:</b> Natural frequencies for un-pre-stress and pre-stress conditions .....	75
<b>Table 4.14:</b> Input EM load for transient analysis (Case-1) .....	77
<b>Table 4.15:</b> Input EM load for transient analysis (Case-2) .....	79
<b>Table 4.16:</b> Input PE load for transient analysis (Case-3).....	81
<b>Table 4.17:</b> Input parameters – scalability .....	89

# CHAPTER 1

## INTRODUCTION

### 1.1 Context of the Problem

In the present life of advancements, robots are being used in several industry and service applications because of their consistency, precision, and repeatability with which they perform the tedious operations. In robotic platform, end effector is connected at the end of a robot arm, like our fingers to the arm. The advantages of using industrial robots are to avoid faulty movements, save time, reduce cost, and improve quality. Therefore, the main motive for using robots can be to perform precise and repetitive operations, which are difficult for humans to directly implement them. These can be applicable in the variable environment conditions or unreachable locations such as very hot, very chilled temperatures, and at high altitude, deeper, minute parts, etc. According to the application of robot, material, size, and mechanism of the robot can be chosen. For example, to hold a hot wafer with a cold vacuum gripper, material of low thermal conductivity should be chosen. In present day applications, robots are used in:

- Manufacturing industries: Uses Cylindrical, Spherical, SCARA, Articulated robots equipped with grippers and tools as end effectors for handling, welding, assembly, dispensing, processing, maintenance, and packaging (Karabegović, Karabegović, & Husak, 2013).
- Security and military services: Uses drones with cameras fitted to the end effector for patrolling, unmanned ground/air vehicles in warfare. Robots such as iRobot's Warrior 710 uses hand with gripper for bomb disposal, carrying heavy weights, climb and rollover uneven surfaces as shown in Figure 1.1.



**Figure 1.1:** iRobot Warrior 710  
(Source: gizmag.com)

- Medical field: Mostly micro robots are used for surgeries, and removing blood clots in parts such as brain, and fatty deposits in arteries according to Rubinstein (2000). As this application is diverse and as it needs accuracy and precision, end effectors are customized based on the purpose.
- Nuclear industries: Mobile robots are used for maintenance tasks in environments not suitable for humans since it is harmful for humans to get exposed to radiations during productions or when accidents occur. As this requires remote maintenance at various temperatures, material of end effector matters the most, and it can be in the form of multi-fingered gripper that can take pictures at the location.
- Railways, construction industries, mining: Robots equipped with the required equipment at the end of robot arm are used for repairing roads, removing snow, collecting data about the road conditions, traffic incidents, laying roads, for handling and mixing materials during construction, deep mining and data collection of underground resources (Parker & Draper, 1998).
- Deep space and underwater services: Tele-robots with special cameras fitted as end of arm tooling are used to explore the remote areas such as space and underwater (Goradia,

Xi, & Elhajj, 2005). For example, the surface properties of Mars are explored by a MER A Spirit rover.

Every company has to upgrade its manufacturing and production processes periodically to put themselves in a competitive position in the market (Hoshizaki & Bopp, 1990).

The end effector is an important mechanical link of a robotic system, which is used to handle the parts. Based on the application, end effector is to be customized. End effectors are generally classified into two types: grippers and tools (Groover, Weiss, & Nagel, 1986).

- Grippers: These type of end effectors are used to grasp the parts for picking and placing objects in applications such as loading and unloading machines and conveyors, and arranging parts at the required position (Reddy & Suresh, 2013).
- Tools: The tool required can be mounted on the wrist or the gripper itself. Tools as end effector can be brushes, cameras, cutting tools, drills, magnets, sanders, screw drivers, spray guns, welding guns, vacuum cups.

Robots being used in manufacturing industries since 1989 were generally for mass production (MacDuffie, & Pil, 1997), which utilized fixed automation concept for a single product, and later during the developments in technology, batch production has been introduced which required flexible automation able to accommodate variety of part configurations (MacDuffie, Sethuraman, & Fisher, 1996). Flexible gripping by robots in the assembly line is employed to tackle this. Variable strategies of flexible gripping have been researched for this purpose, which have been discussed in the next chapter.

## **1.2 Problem Statement**

There is a need to develop a gripper capable of handling different sized objects, especially in pick and place operations of small parts in semiconductor assembly technology.



The approach will involve optimizing the line model of the gripper for its maximum tip displacement, followed by updating the 3-D model of the gripper with the optimized dimensions. Functionality, scalability, and flexibility of the 3-D model is studied, which involves analysis such as static structural, buckling, modal and transient analysis to simulate its performance. The dimensions of proposed gripper are 20.553 x 17.799 x 37.557 mm. Maximum input piezo-electric (PE) force and displacement applied are 190N and 0.008mm respectively, while the maximum electro-magnetic (EM) force and displacement are 0.04N and 3mm respectively. At last, scalability of the gripper is studied.

### **1.3 Project Objectives**

The goal is to develop a multipurpose device capable of grasping different sized objects whose size vary from micrometer to millimeter scale, and achieve flexibility in gripping by combining features in one design mechanism using two different actuation sources, i.e., PE and EM forces.

To achieve this, we will:

- Study various actuation sources and operating parameters for grippers.
- Study various flexible gripping procedures.
- Propose a gripper mechanism, able to accommodate variable object sizes for gripping.
- Create a simplified line model to optimize it for the maximum tip displacement of gripper by evaluating Geometric Advantage (GA) of it.
- Perform the simulation of 3-D model of the gripper using ‘ANSYS Workbench’ to study its functionality and scalability.
- Evaluate the gripping range for open and close positions of the fingers to study its flexibility.

## **1.4 Significance of the Study**

The findings of this study will help in the development of a flexible gripper along with optimization to find the best options for gripper dimensions. Robots are playing an important role in every field such as manufacturing, construction, military, medicine, security, and defense. Robot grippers have significant applications in each and every field. Thus, this study uncovers the major strategies for flexible gripping, useful to accommodate product variety for use in electronic industries for handling different-sized objects.

## **1.5 Definition of Terms**

1. Actuator: A mechanical device that transforms energy into force and motion for driving various equipment (Huber, Fleck, & Ashby, 1997)
2. CAD: Computer Aided Design
3. CAE: Computer Aided Engineering
4. DOF: Degrees of Freedom: Number of independent inputs required to define a engineering system (Yan, 1998)
5. FEM: Finite Element Method/Modeling
6. FEA: Finite Element Analysis
7. GA: Geometric Advantage
8. SMA: Shape Memory Alloy
9. PE: Piezo – Electric
10. EM: Electro-Magnetic

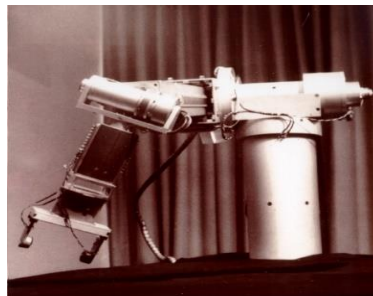
## CHAPTER 2

### LITERATURE REVIEW

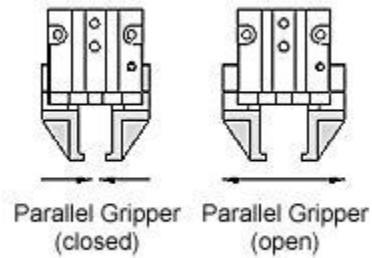
This chapter gives us a review of literature for the background required to understand and deliver the project objectives discussed in Chapter 1. The first section provides a historical perspective of grippers and the gradual developments involved in it. The next section discusses the theoretical topics which involve the comparison of actuation sources, discussion of flexible gripping methods, and importance of finite element method for simulation. The final section provides the topics involved in the current research pertaining to the field of robot grippers.

#### 2.1 Historical Perspective

A robot without a gripper cannot handle or grasp objects. For gripping, it needs actuation source, controls, and sensors for robotic handling refinement. The actual first controllable gripper came in 1969, developed by Stanford University mechanical engineering student Victor Scheinman (Nikoobin & Niaki, 2012). Uncontrollable grippers were developed before which were fast but dangerous. The controllable gripper developed had 6 degrees of freedom, and used DC motors. Then in early 1980s, this design was taken with some modifications in feedback control elements, and were produced in mass for industrial applications. Pneumatic source was used for actuation, which is still in use as of today.

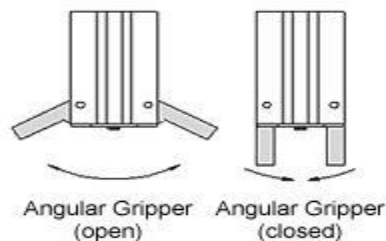


**Figure 2.1:** Victor Schienman Stanford arm. (Source: infolab.stanford.edu)



**Figure 2.2:** Parallel gripper.  
(Source: OMEGA-Engineering Technical Reference)

The arm by Stanford University used a type of gripper which is two-fingered called as parallel gripper. It is a gripper, which has two parallel straight bar fingers, which slide together or apart to grasp and place objects. Then in 1970s, a different type of gripper called angular gripper was developed, which opens and closes on a pivot like a claw. The difference between parallel and angular grippers is that parallel gripper force remains the same throughout the stroke. And, moreover it has short stroke and high gripping force.



**Figure 2.3:** Angular gripper.  
(Source: OMEGA-Engineering Technical Reference)

In late 1980s, a 3-fingered gripper was developed by Massachusetts Institute of Technology, and its design is now known as the Barrett hand shown in the Figure 2.4 (since Barrett Technology Inc. owned the product's license), which used servo controllers, communication, and brushless motors. In 2009, Barrett Technology owned the license of a hand which is built of polymer with flexible joints, which conforms to the shape and mass of the

object to be grasped (Eitel, 2010). For flexible applications, 3-fingered grippers have been widely used thereafter.



**Figure 2.4:** Barrett hand.  
(Source: Robotiq.com)

## 2.2 Theoretical Topics

In building a robot gripper, selection of actuation sources, mechanisms, and operation parameters (force, stroke, and bandwidth range) are considered as very important. A review of the actuation sources, performance characteristics, and mechanisms of grippers are surveyed, followed by flexible gripping techniques. As the gripper has to be analyzed for its functionality, the use of Finite Element Method for this purpose is discussed in later sections.

**2.2.1 Actuation sources.** The device, which is used for driving something (here, robot end effector) is called as actuation source. Source of movement can be electric, hydraulic, pneumatic, shape memory effect, etc. (Daerden & Lefeber, 2002). Input quantities which drive different types of actuators are listed in Table 2.1, for which the output is force and displacement.

**Table 2.1:** Actuator and its input quantities.

<b>Actuator</b>	<b>Input Quantity</b>
Electro-magnetic	Electric voltage and current
Electro-static	Electric voltage and current
Hydraulic	Oil Pressure
Pneumatic	Air Pressure
Thermal	Temperature
Piezo-electric	Electric voltage and current
Shape memory alloy	Temperature

The actuation sources are found to be different for large and small size grippers, since more accuracy, precision, and less force is required for micro size gripper compared to macro size. Table 2.2 and Table 2.3 list the actuation sources for general macro-size and micro-size grippers respectively.

**Table 2.2:** Macro-size gripper actuation sources. (Source: Robotiq.com)

<b>Gripper Actuation Source</b>	<b>Applications and Features</b>
Electric/Servo Grippers	Handling, picking, and machine control in a particular way, i.e., flexible automation involving high variety, gripping feedback, good force and speed control, and cleaner environment.
Pneumatic Grippers	Low-variety, more space, high volume, non-programmable, high speed, and low cost applications. Low pressure/forces, speed control are difficult to achieve to grab delicate parts.
Suction cups	Material handling applications except for perforated parts, objects like glass or mirror, curved, sharp, and porous surfaces.
Magnetic Grippers	Handling ferrous materials, perforated materials, flexible shape parts with high grabbing speed and low maintenance. Quick movements are not allowed to avoid slipping of parts.

**Table 2.3:** Micro-size gripper actuation sources.

Gripper Actuation Source	Features
Electro-static Actuators	Electricity is converted to force (mechanical strain). Ease of fabrication on silicon wafers, high electric fields and rotation speeds can be obtained. Favors scaling down of electrostatic force. Circuit board can be designed on the same chip. Drive-size was found to be from 10 micro-meters to multiples of 100 micro-meters. (Monkman, Hess, Steinmann, & Schunk, 2007)
Electro-magnetic Actuators	Magnetic flux density decreases for small sizes. Drive trains (reduction gears) are used to produce required torque and it is hard to fabricate at micro scale. Drive size was found to be from 10 micro-meters to multiples of 100 micro-meters. (Sam, Kumar, Tetteh, & Braineard, 2014)
Piezo-electric Actuators	Electricity is converted to force (mechanical strain) through inverse piezo-electric effect. Commonly used piezo-electric materials are lead zirconate titanate and lead magnesium niobate. Can give small displacements, provide high pressures, and the response is quick. Possibility of creep and hysteresis. (Hunter, Hollerbach, & Ballantyne, 1991)
Electro-pneumatic or Electro-hydraulic Actuators	Pressure is converted to force. Smooth operation. Response is quick, and high $\frac{output}{weight}$ ratio. Easily scalable to small size and many degree of freedom are possible. (Hunter, Hollerbach, & Ballantyne, 1991)
Shape Memory Alloy Actuators	Thermal energy is converted into mechanical energy (kinetic energy). Compact, high power to weight ratio. Thermo-elastic transformation can be resulted from the voltages accessible. Electric resistance difference is used to track/detect the position of actuator and force. Heat dissipation element should also be included. (Hunter, Hollerbach, & Ballantyne, 1991)

**2.2.2 Operating parameters of grippers.** For accurate handling of objects, care should be taken such that there is minimum deviation from the required operation. So the study of the following factors is made, which gives the general idea of the gripper performance characteristics (Nikoobin & Niaki, 2012).

Material: Based on the application, material for the robot can be selected. For example, if there is a need to operate gripper in high temperature conditions, then a material suitable for that

application should be selected. In the same way, strength of material can be taken into account to decide the type of material suitable for the application load. There should be compatibility between the gripping surface and the object to be gripped (Appleton & Williams, 2012).

Materials such as Aluminum (high yield strength and modulus of resilience), silicon (for electro-thermal applications), SU8 (mainly used for micro-size grippers, which is a photo resist material (Seidemann, Rabe, Feldmann, & Büttgenbach, 2002), stainless steel (high yield stress and low cost) can be used.

Gripping Stroke: It is the maximum length of the stroke of gripping jaw. It is generally aimed for optimum stroke, which can be done by changing the position of flexural hinges (Nikoobin & Niaki, 2012).

Gripping Range: It is the maximum and minimum size of objects handled by the gripper. For irregular-sized objects, large gripping range and stroke are required. For micro-size applications, gripping range should be small for more accurate movements of the gripper (Nikoobin & Niaki, 2012).

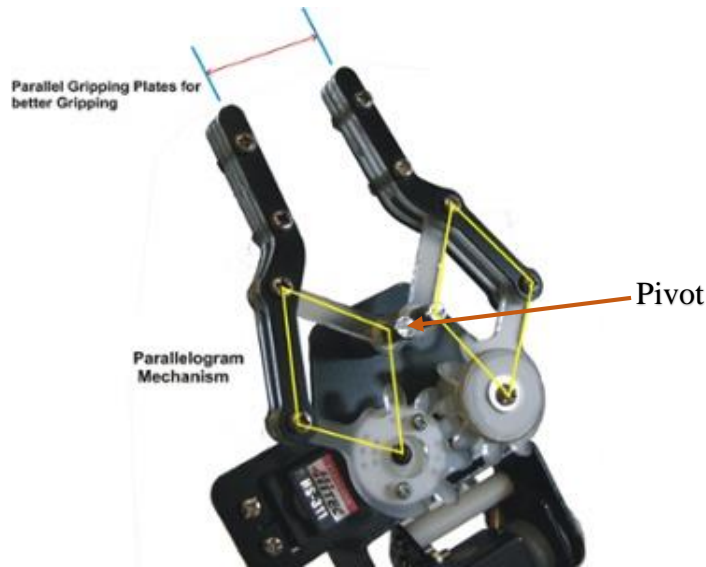
Gripping Force: It is the force applied by the end-effector on the object. This is used to hold the object from slipping during motion.

Bandwidth: It is the frequency at which it lowers the input by 3dB. As the bandwidth increases, the time response is faster. For example, if the bandwidth is 11Hz, the actuator will try to achieve speed at specified value, and it can make adjustments 11 times per second. Higher bandwidth improves the position control, which indicates that actuator is more capable of handling disturbances (Buzuayene, 2008).

Parallel and Non-Parallel Grippers: Non-parallel motion is generally referred to as rotational motion, in which the x-component of the reaction force allows the gripper to hold the object,



while its y-component forces the object out of the gripper. So, in parallel grippers, y-component is eliminated to improve the precision in grasping objects. Parallel motion of the gripper jaws is achieved by using the parallelogram structure for the mechanism (Nikoobin & Niaki, 2012).



**Figure 2.5:** Parallel gripper.  
(Source: robotiq.com)

Above discussed parameters are tabulated below according to the specifications obtained from robotic manufacturing firms.

**Table 2.4:** Micro-size gripper characteristics. (Castillo-León, Svendsen, & Dimaki, 2011; Nikoobin & Niaki, 2012; Wu, Lee, Cao, & Shen, 2005)


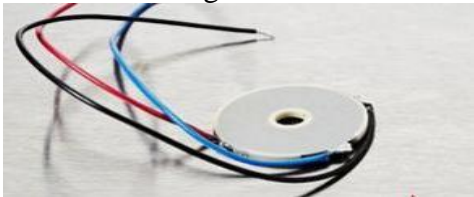


Structure Material	Actuation Source	Dimensions (mm)	Stroke ( $\mu\text{m}$ )	Range ( $\mu\text{m}$ )	Force (mN)	Band width
Stainless steel	Electro-magnetic	15.x5.22x0.5	300	-	130-18	High(>1 KHz)
Brass	Piezo-electric	29.2x20.91x3	515	100-1000	159	
Stainless steel	SMA	20x20x1	-	Max is 123	330	Low(<1K HZ)
SU8	Electro-thermal	2x2x0.2	18	-	10	

From Table 2.4, we can say that SMA actuators have more gripping force, while less gripping range, and low force, and the high band width of EM actuators makes them more suitable for accurate gripping in micro-size applications. Piezo-electric actuators with low stroke and high band-width are used for accurate grasping. Therefore, the specifications of various

piezo-electric and EM actuators are discussed below, which can be used for analysis in the following chapters.

According to Noliac (piezo actuator manufacturing company), piezo actuators can be in the form of ring stacks, plate stacks, plate benders, or ring benders. Specifications of some of its products are given in Table 2.5.

**Table 2.5:** Specifications of piezo actuators. (Source: Noliac.com)

Product Type	Dimensions (mm)	Operating Voltage (volts)	Max. Stroke (mm)	Max. Force (N)
Plate Bender 	50 x 7.8 x 1.3 (Length x width x height)	200	0.85	1.6
Ring Bender 	40 x 8 x 0.7 (outer dia. X inner dia. X height)	200	0.185	13
Plate Stacks 	15 x 15 x (4-150)	200	0.003 – 0.244	9450
	3 x 2 x 9 (Source: Physikinstrumente.com)	120	0.008	190
Ring Stacks 	20 x 12 x (4-200)	200	0.003 – 0.327	8450

Some of the commonly used EM actuators and their specifications are given in Table 2.6.

**Table 2.6:** Electro-magnetic actuators specifications.


Product	Dimensions (mm)	Operating Voltage DC (V)	Max. Stroke (mm)	Max. Force (N)
Push-Pull Solenoid Electro-magnet 	Push bar dia. = 6 Frame size (L x W x H) = 30 x 17 x 14 (Source: Jameco Electronics)	12	10	10
Pull Solenoid Electromagnet	Push bar dia. = 5 Frame size = 30 x 15 x 13 (Source: Jameco Electronics)	12	10	5
High Power Actuator with output arm	5 mm dia x 5 mm length (Source: microflierradio)	60 ohms @ 3.7V	3	0.04

Table 2.7 gives the characteristics for macro-size grippers.

**Table 2.7:** Macro-size gripper characteristics. (Romheld Automation, n.d.)

Structure Material	Actuation Source	Dimensions (mm)	Stroke	Force (N)	Weight (kg)	Operating range	Type
Aluminum	Pneumatic	-	9.5 mm	62	0.08	20-100 psi	2 Jaw Parallel
		-	25.4 mm	445	0.9		
Heat treated steel	Pneumatic	-	10 mm	1474	1	30-100 psi	3 Jaw Parallel
		-	30 mm	2838	5.3		
Heat treated steel	Pneumatic	-	90 deg	272	0.72	40-100 psi	2 Jaw Angular, 180 deg
		-	90 deg	651	1.82		
Aluminum	Electric	-	25 mm	111	0.53	24VDC	-
-	Pneumatic-magnetic	130x80	-	1100	-	50.8 psi	-
-	Magnetic-vacuum	100x63	-	640	-		-

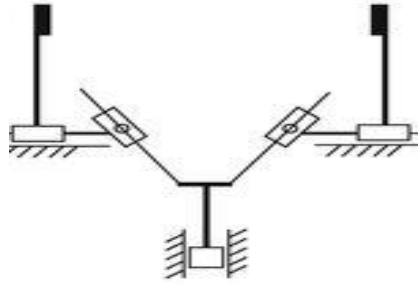
From the information provided in Table 2.7, we can draw conclusions that pneumatic source can give a large range of gripping forces with variable speed, but electric source has fixed speed. Electric actuators have low force to weight ratio, while pneumatic actuators have high force to weight ratio. And, the fact that electric actuators have repeatability and can precisely control and position the parts leads to flexibility in processes.

**2.2.3 Mechanical mechanisms for grippers.** To perform a grasping operation, design problems include a proper selection of mechanism for gripper. Classification can be made based on the motion of fingers. So, the actuation of fingers can be made based on motions:

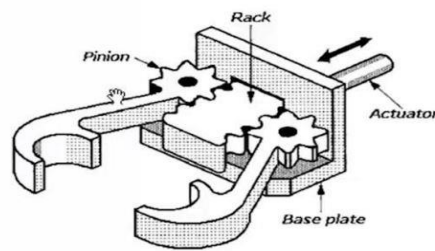
- Pivoting motion: Open and close movements of the fingers are achieved by finger rotation about the fixed pivot of the gripper of a linkage mechanism as shown in Figure 2.5.
- Linear motion: Slider and crank mechanism (Figure 2.6) is used to open and close the fingers of the gripper.

Classification can also be made based on the device type used for actuation as follows.

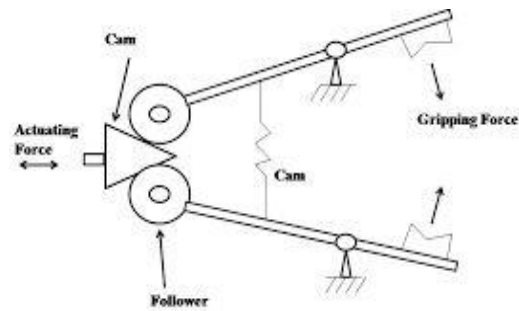
- Linkage actuation: There are several designs for linkage mechanisms used for actuating (opening and closing) fingers of the gripper (Lanni & Ceccarilli, 2009), some of them are given in Figure 2.9.
- Gear and rack actuation: Linear motion of rack is obtained by converting the rotary motion of gears, and this facilitates the opening and closing of grippers as given in Figure 2.7.
- Cam actuation: The reciprocating motion of the cam results in the movement of follower, which allows the gripper attached to follower to open and close, as shown in Figure 2.8.



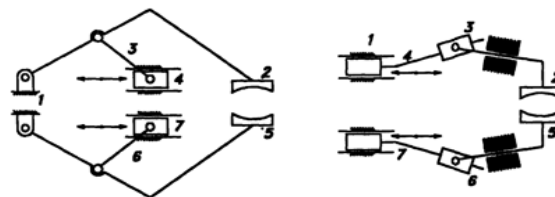
**Figure 2.6:** Slider-crank mechanism.  
(Source: RoboticsBible)



**Figure 2.7:** Gear and rack actuated mechanism. (Nair, 2009)



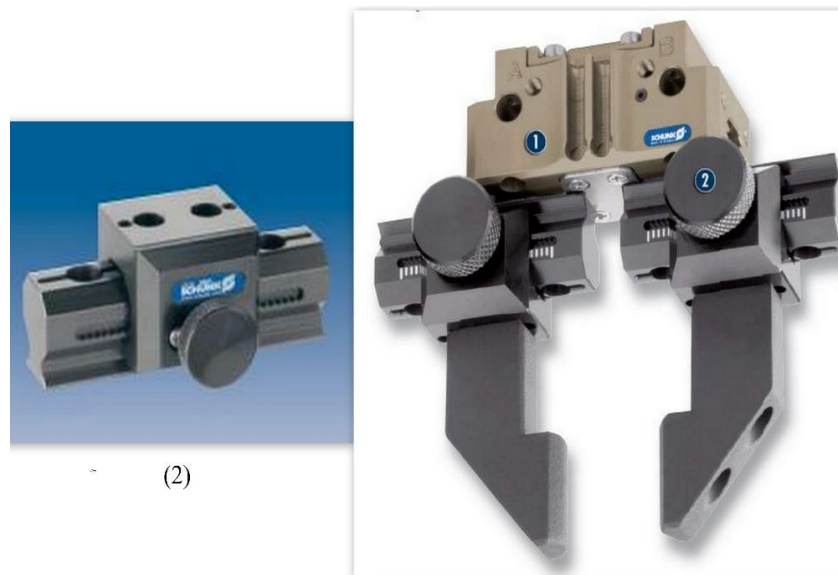
**Figure 2.8:** Cam actuated mechanism. (Nair, 2009)



**Figure 2.9:** Linkage actuated mechanism. (Belfiore & Pennestrì, 1997)

**2.2.4 Flexible gripping techniques.** In assembly operations, robot grippers are used to handle a variety of products. Therefore, the options for cost-effective flexible gripping are surveyed in this section:

1. Replacement of fingers of gripper: In this technique, sets of different fingers are maintained, and set in specific positions. According to the requirement, the desired set of fingers are attached to the gripper base by some quick and efficient mechanical means. In this way, gripper is made capable for handling variety of products. For example, Figure 2.10 is the jaw designed by Schunk, used for quick gripper finger replacement.



**Figure 2.10:** (2) is the jaw to accommodate gripper fingers (1). (Schunk.com)

2. Replacement of gripper: When a gripper cannot handle a range of objects, then there is a need to change the gripper itself. Then, this technique is helpful. Many manufacturing industries such as Schunk, Accurpress Automation, and ATM Automation and Robotics manufacture mounts for facilitating quick gripper replacement.
3. Multi-gripper: In this method, end of the robot arm has more than one gripper attached to it. Selection of the desired gripper can be done by indexing the mechanism holding it.

Since, more grippers are attached, more payload is already attached. Therefore, handling lighter weights is recommended, mostly in electronics industry for assembling circuit boards by handling small and lightweight parts such capacitors, resistors, etc. (Pham & Yeo, 1991).



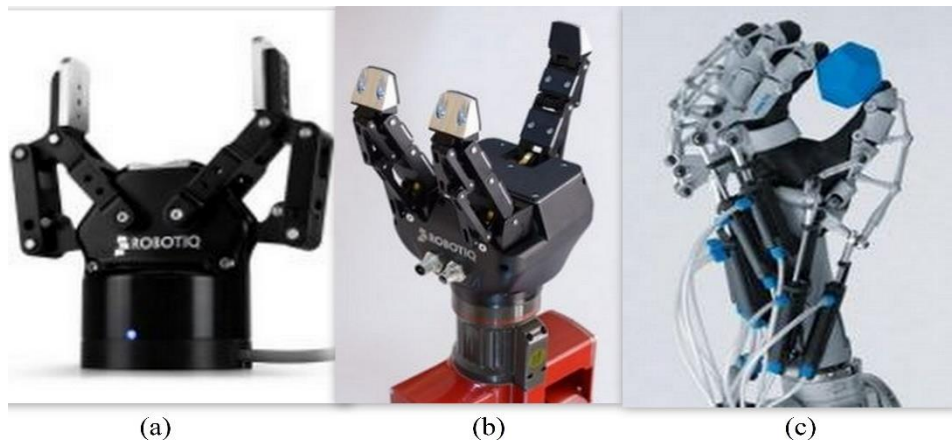
**Figure 2.11:** Multi-gripper.  
(Source: Schunk.com)

4. Universal/Adaptive passive gripper: These grippers are capable of handling different shaped objects, by deforming itself to fit to the shape of the object to be handled. Accurate positioning of the objects is not possible with this type of grippers, making it available only for simple picking and placing operations. John used granular material in an elastic material to achieve flexibility (Amend, Brown, Rodenberg, Jaeger, & Lipson, 2012).



**Figure 2.12:** Universal gripper handling different shaped objects.  
(Source: GRABCAD)

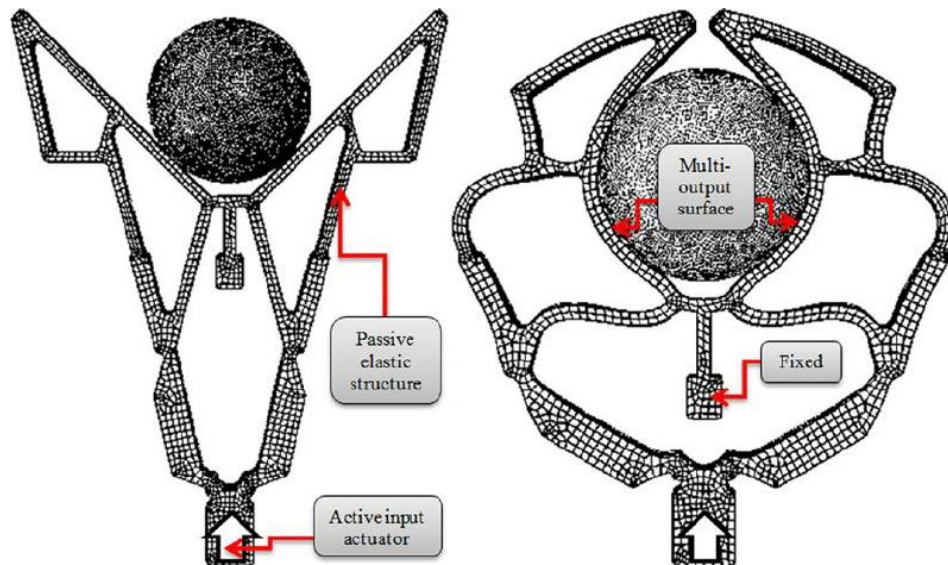
5. Adaptive multi-fingered gripper: To achieve the flexibility like a human hand, various grippers have been developed. According to the research conducted by Robotiq (2015), a manufacturing company, 2-fingered grippers can adapt to both rectangular and cylindrical, and since the workpiece is always at the same place in the gripper, programming is easier. A 3-fingered gripper is found to have more flexibility and repeatability. It can carry more payload, and grasp a wide range of objects because of its three modes: scissor, wide, and regular. A 4/5-fingered gripper has more flexibility than the others, but it cannot handle more payload and the repeatability was found to be less.



**Figure 2.13:** (a) 2 fingers (b) 3 fingers (c) 5 fingers robot gripper.  
(Source: Robotiq.com)

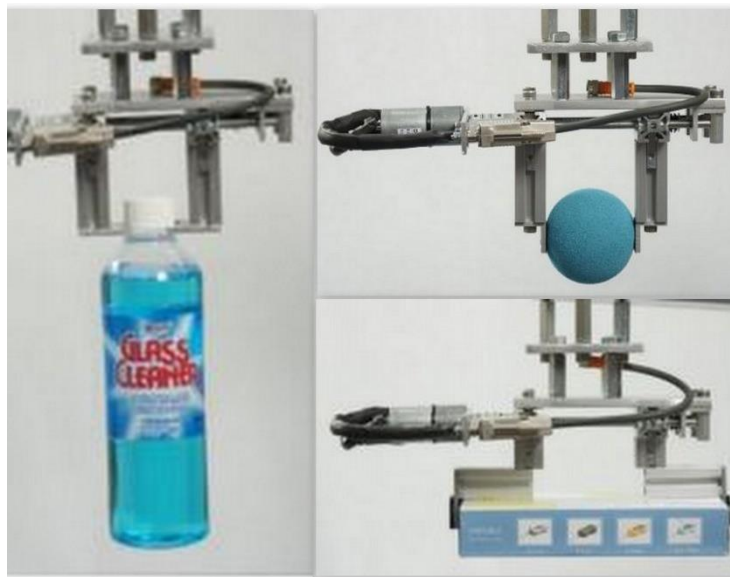
6. Compliant gripper: The gripper with the compliant mechanism is made of a single piece, without joints, facilitating low maintenance and no wear. Compliance of the fingers reduces the contact forces avoiding collisions (Petković, Pavlović, Shamshirband, & Anuar, 2013). As there are no joints, it is flexible and can conform to the shape of the workpiece to be handled as shown in the Figure 2.14.





**Figure 2.14:** Passive compliant gripper. (Petković et al., 2013)

7. Modular gripper: Modular robots are made of several modules which have physical connections among them, and can be reconfigured into different shapes by changing connectivity between modules, promoting flexibility.



**Figure 2.15:** Modular robot handling different sized objects.  
(Source: Universal Robots)

**2.2.5 3D printable materials.** There are flexible materials which can be 3D printed, which allows flexible grippers to be built. 3D printing avoids assembling of parts, i.e., can be printed in one piece. It allows printing of complex shapes, and wide range of materials can be used. It is also cost-effective and maintenance free. Table 2.8 gives the list of materials that can be 3D printed for gripper manufacturing.

**Table 2.8:** Material properties.

S. No.	Material	Tensile Modulus (Mpa)	Tensile Strength (Mpa)	Elongation at Break (%)	Flexural Modulus (Mpa)	Heat deflection (deg C)	Melting Temperature (deg C)	Ref
1	<b>Polyamide PA12</b>	1650 +/-150	48 +/-3	20 +/-5	1500 +/-130	86 (1.82Mpa)	-	(Materialise)
2	<b>Rubber like TPU 92A-1</b>	-	27 (x-direction) 22 (z-direction)	400 (x-direction) 370 (z-direction)	9 (x-direction) 10 (z-direction)	-	160	
3	<b>ABS Plastic</b>	1627	22	6	1834	90 (0.45 Mpa) 76 (1.81 Mpa)	-	
4	<b>Silicone Rubber</b>	50	8	800	-	-	-	(Matbase)

Polyamide is a strong and flexible material, which was first used by Materialise for 3D printing a gripper designed by ABB in the year 2015 (Materialise, 2015). Later, they used Thermoplastic Polyurethane (TPU) which is rubberlike, highly flexible, and more durable than polyamide. This gripper is mostly suitable for electronics and food industry for handling delicate

parts. ABS thermoplastic is UV resistant and can be used to design structures with more accuracy. Silicone rubber is resistant to heat, cold, oil, and other solvents.



**Figure 2.16:** Automation gripper.  
(Source: Materialise.com)

**2.2.6 Finite element method for analysis.** Finite Element Method (FEM) is used to simulate the performance of the proposed gripper. In this method, a physical system is represented in the form of a mathematical model. A model is the one which is used for simulations to predict its behavior instead of testing the actual product. Performing tests on the actual product may lead to wear and tear. Mathematical models of each physical system are not easy to solve as they involve complex equations with boundary conditions having infinite number of degrees of freedom. So, number of degrees of freedom is reduced to a finite number giving rise to discrete model. The popular method for discretization is found to be FEM. So in this method, the complexity of the mathematical model is reduced by subdividing it into simple geometry components called elements/finite elements. The response of all the elements are individually collected to approximate the overall response of the mathematical model (Felippa,

2004). The software packages which use FEM include ANSYS, Abaqus, and Adina. In this project, ANSYS was used for simulations. It is used for static structural, buckling, dynamic analysis such as modal analysis, and also non-linear analysis for contact interaction analysis.

Optimization is also a part of simulation and is about evaluating the best choice for design parameters while designing a new product or modifying the existing product.

Optimization of each part is easy, instead of whole assembly as it may involve several design parameters. Optimization techniques are used by engineers, managers, researchers in CAE (Computer-aided Engineering) department to evaluate designs via simulations, to re-engineer business processes, and to design innovative products (Miccoli, 2004).

Optimization techniques can be:

1. Traditional: Algorithms used here are deterministic, which has some set of rules to move from one solution to the other to find the best solution. Examples: Non-linear programming, Dynamic Programming, Quadratic Programming, etc. These cannot solve problems with more constraints and multi-objective problems.
2. Advanced: Algorithms used here are probabilistic. These techniques are mostly used to solve complex problems having several constraints and variables. Examples: Genetic Algorithm, Artificial Immune Algorithm, Differential Evolution, Particle Swarm Optimization, Harmony Elements Algorithm, etc. The most widely used technique is Genetic Algorithm for multi-objective optimization and the principle behind this is Darwin's theory of survival of the fittest and theory of evolution in human beings (Rao & Savsani, 2012).
3. Plug-ins: Third party software and plug-ins can be used to optimize the problems (Miccoli, 2004). Examples: optiStruct, optiSLang, SAS, smartDO, MATLAB, ANSYS,

Solidworks. All these use deterministic and probabilistic algorithms for solving optimization problems.

Optimization methods available in ANSYS Workbench are:

1. NLPQL: Non-linear Programming Quadratic Lagrangian is used for single objective functions and continuous input parameters. This method uses a gradient based algorithm to give us local optimization result.
2. Adaptive Single Objective: This also uses a gradient based algorithm to give us global optimization result. This can take single objective and continuous input parameters.
3. Adaptive Multiple Objective: This supports multiple objectives and gives global optimization result by taking continuous input parameters.

MISQP: Mixed Integer Sequential Quadratic Programming. This method is used for continuous non-linear optimization problems. It can handle integer variables also. Mixed integer non-linear programming problem is of the form

$$\text{Minimize } f(x, y) \text{ where } x \in \mathbb{R}, y \in \mathbb{N} \dots \dots \dots (2.1)$$

$$\text{Subject to } g_j(x, y) = 0, j = 1, \dots, m_c$$

$$g_j(x, y) \geq 0, j = m_c + 1, \dots, m.$$

Where,  $f$  and  $g$  are continuously differentiable functions.

4. Screening: This uses sample and sort approach, which supports multiple objectives and all types of input parameters.
5. MOGA: Multi-objective Genetic Algorithm can take multiple objectives and gives global optimization result (Lee, 2015).

### 2.3 Current Research Topics in Grasping Technology

Currently, research is mostly focused on the precision micro-grippers, their fabrication, and flexibility in terms of material and design. Following are some of the research topics, which depict the requirements of the gripper in the industry.

- “Design of Asymmetric Flexible Micro-Gripper Mechanism Based on Flexure Hinges”

This paper discussed the requirements of assembling micro parts. Asymmetric flexible gripper is introduced and the output displacement amplified by the four-bar linkage mechanism, which is shown by ‘Finite Element Analysis’. Pneumatic source is used for actuation (Qingsong, 2015).

- “Analysis and Design Optimization of a Robotic Gripper Using Multi-objective Genetic Algorithm”

This paper discussed the non-linear, multi-modal, multi-objective optimization problem, which is used to optimize the dimensions of the links, and the angle of a gripper. Electric source is used for actuation, and the force-voltage relationship is obtained, which is used to estimate the voltage to be applied according to the required application (Datta, Pradhan, & Bhattacharya, 2016).

- “Design, Manufacturing and Mechatronics: Proceedings of the 2015 International Conference”

This book included the details regarding the optimization design for compliant gripper based on variable density method. A compliant gripper with an objective of eliminating the assembly of parts to build a gripper has been introduced. 3D printing has been mentioned for this purpose. Using variable density method, structural topology is converted into optimal material distribution problem (Shahhosseini, 2015).

- Disney Research has published some articles regarding soft skinned robotic grippers and adaptive grippers. Soft skin development with an air-tight cavity can be used to sense the air pressure. Soft skin is developed to get along with the minute size and safety requirements to handle sensitive and soft objects. This reduces the impact force on collision. 3D printing has been suggested to build this model (Kim, Alspach, & Yamane, 2015).

## **2.4 Summary**

From the literature review and the ongoing research, we can tell that industry needs precision grippers with flexibility in both design and material. This requirement is mainly in the medical industry, which needs micro grippers for handling micro and nano objects. In general manufacturing industries, speed of operations along with the accuracy and flexibility required to handle different sized objects is the main issue. So, scalability and optimization are considered as challenging tasks in this project.

## **CHAPTER 3**

### **METHODOLOGY**

This chapter deals with the procedures used to address the problem statement. The problem is restated and specific aims are stated, followed by the detailed explanation of the approach towards achieving them.

#### **3.1 Restatement of the Problem**

Achieve mechanical flexibility by proposing a new mechanism. Optimize the proposed mechanism of the gripper, and study its functionality. It is then examined for its flexibility in grasping objects ranging from micrometer to millimeter scale. Scalability of the proposed mechanism is also investigated.

Functionality is the assessment of behavior of gripper in terms of tip displacement, time response, and stresses generated for the applied actuation force. Flexibility states the wide gripping range of the gripper for handling objects. Scalability feature deals with the study and comparison of changes in gripper performance and functionality, when the gripper dimensions are scaled up.

#### **3.2 Specific Aims**

The problem stated can be explained with the help of three objectives. Aims are then established for each objective, which are tabulated as given below.



**Table 3.1:** Objectives and aims of the project.

	<b>Specific Aims</b>
<p><b>Objective-1:</b></p> <p>To optimize the proposed mechanism of the gripper and study its functionality</p>	<ol style="list-style-type: none"> <li>1. Propose the line model of the gripper and study its Geometric Advantage (GA), which is the ratio of output and input displacement of the gripper</li> <li>2. Optimize the above line model for its maximum GA, i.e., maximum tip displacement</li> <li>3. Take the optimized gripper dimensions of second step and perform analysis on its 3D model to study its functionality</li> </ol>
<p><b>Objective-2:</b></p> <p>To examine the flexibility of the gripper in grasping objects of size ranging from micrometer to millimeter scale</p>	<ol style="list-style-type: none"> <li>1. Study the maximum tip displacement of the gripper while closing and opening of its fingers in its functionality and state its flexibility</li> </ol>
<p><b>Objective-3:</b></p> <p>To study the scalability of the gripper</p>	<ol style="list-style-type: none"> <li>1. Scale up the above used 3D model of the gripper by a set of factors</li> <li>2. For each scaled model, perform the same type of analysis as done for the base model</li> <li>3. Compare the analysis results of the base model and scaled models to study the trend in results from analysis of different scaled grippers</li> </ol>

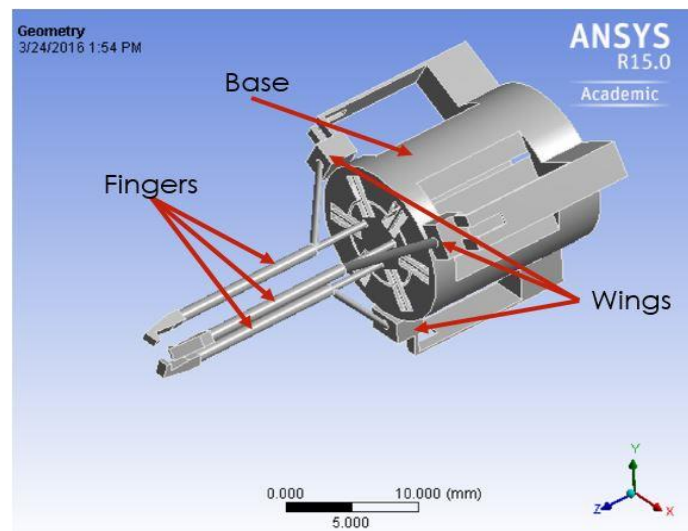
### 3.3 Procedure

To achieve the above mentioned aims, a procedure is laid down, which is given below in detail. Aims are studied under the three areas, namely ‘Functionality’, ‘Flexibility’, and ‘Scalability’, which address objectives of this project. ‘ANSYS Workbench’ software is employed for finite element analysis and optimization of the gripper.

**3.3.1 Functionality.** Evaluating functionality of gripper is about analyzing the behavior (functioning) of fingers in terms of output tip displacement of fingers, which is used for grasping objects. It is studied in the following steps by initially proposing a 3D model of the gripper, followed by optimization of a 2D line model, and then performing static structural, transient analysis of the gripper along with contact analysis of object with the gripper.

#### 1. Proposed 3D model of the gripper

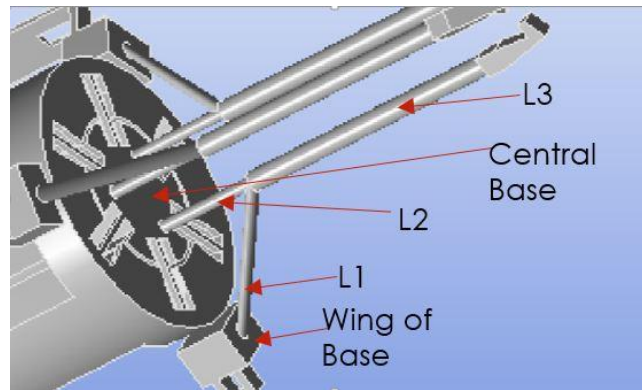
Below is the 3D model of the gripper selected for analysis. This is a micro gripper, with its dimensions Base and width-20.574 mm, Height-37.592 mm if enclosed in a volume.



**Figure 3.1:** 3D model of the gripper (by Dr. Mayyas).

As seen in Figure 3.1, the gripper has three fingers and a base with three wings. Each finger is comprised of three links with its two links on the base as depicted in the Figure 3.2. One

link (Link-1) is attached to the wing of the base, while the other link (Link-2) is attached to the main base. Link-3 is the output link connected at the joint of Link-1 and Link-2, whose tip



**Figure 3.2:** Detailed representation of links and base.

displacement is used for grasping objects. The mechanism of the three links is discussed below.

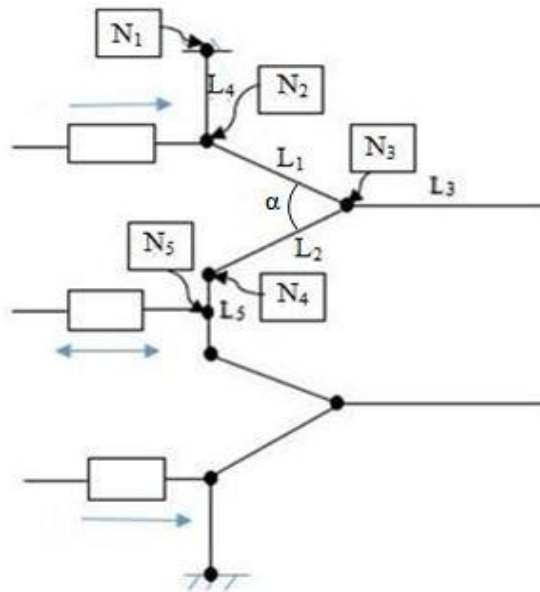
**Link 1:** One end of Link 1 is connected to the wing, where a linear piezo-electric actuator is attached to it. Piezo-electric actuator provides linear stroke. Piezo-electric actuation is considered one-directional and provides low stroke range. This provides precision motion at each tip of the finger (Link-3).

**Link 2:** One end of Link 2 is connected to the center of the base, which is supported vertically by an EM actuator. This type of actuation is bi-directional providing a wide range of gripping, where all fingers can be displaced simultaneously.

**Link 3:** This link, connected to Link 1 and Link 2, gets displaced and grasps objects according to the force applied at the ends of Link-1 and Link-2 on the base. When fingers get coarsely displaced simultaneously with EM actuation, Piezo-electric actuation is used to achieve finer displacement of each finger and therefore promoting accurate grasp.

## 2. Line model of the gripper mechanism

Initially, linkage mechanism of a single finger is taken, and its line model is created in ANSYS workbench. This reduces the computation time, and this doesn't reduce the accuracy of the model. This just removes the extra physical dimensions from the equations, and replaces them with parameters. Finite element analysis uses the simple finite elements such as 2-node bar or 2-node beam element (Boeraeve, 2010). Static Structural analysis is then performed on this model in the next step.



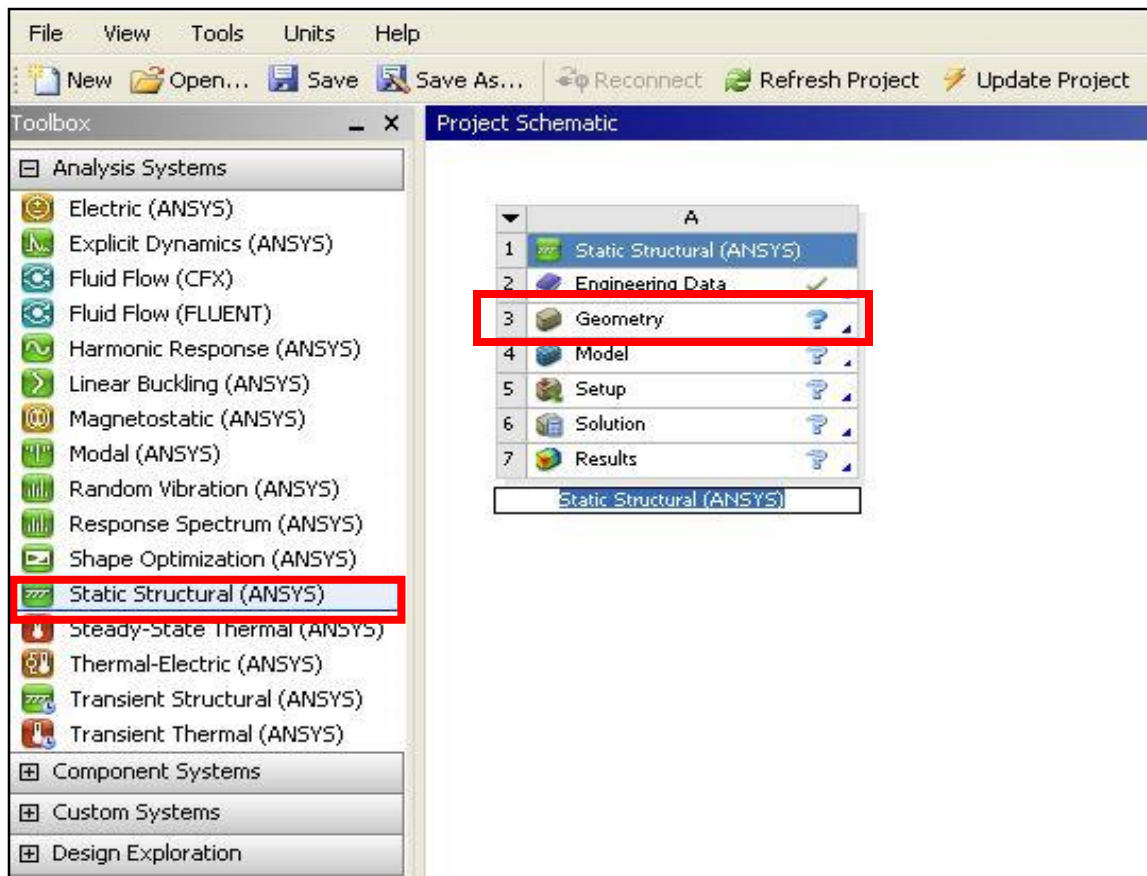
**Figure 3.3:** Line model of a finger in Workbench.

The dimensions of a finger, extracted from the 3D model of the gripper, are used to build this line model. The dimensions are given in Table 3.2.

**Table 3.2:** Preliminary dimensions extracted from the 3D model using Solidworks.

Link	Length (mm)	Radius (mm) – Cross-section
L <sub>1</sub>	7.14	0.40 – Circular
L <sub>2</sub>	5.00	0.30 – Circular
L <sub>3</sub>	13.00	0.50 – Circular

Cross-section is taken circular with a radius of 0.3 mm. ' $\alpha$ ' is the angle between links 'L1' and 'L2'. The home page of ANSYS workbench is shown below in Figure 3.4, and the type of analysis here is 'Static Structural'. Then, for sketching the line model, 'Geometry' is selected from the Project schematic, which opens the design modeler, where the line model is sketched.



**Figure 3.4:** Workbench home page (Project Schematic and Tool box).

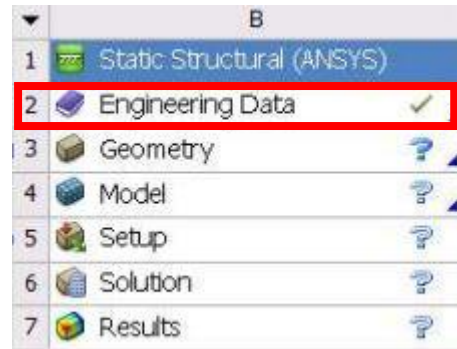
### 3. Analysis of the line model

Static structural analysis is performed on the above built line model, and the required steps for analysis are discussed here.

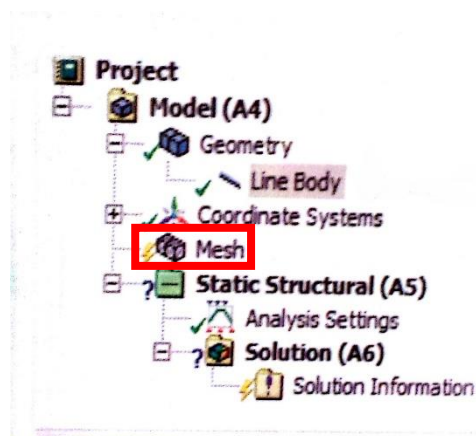
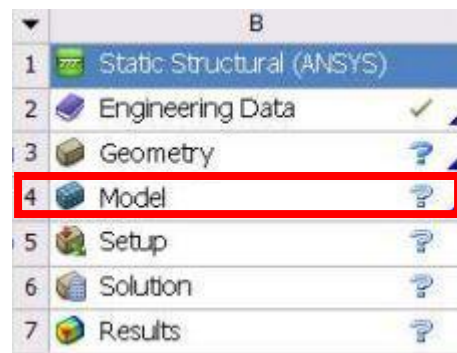
- Assigning Material Properties: ABS plastic was chosen as the material, and its properties taken from literature review were tabulated below, which were then used to insert them in the 'Engineering data' of the project schematic.

**Table 3.3:** Material properties of ABS plastic taken for feasibility study. (Source: Accura)

Physical Property	Value
Tensile Modulus	1625 MPa
Density	1.2 g/cm <sup>3</sup>
Bulk Modulus	1805.6 MPa
Shear Modulus	601.85 MPa
Poisson ratio	0.35
Ultimate Tensile Strength	42 MPa



- Generate Mesh: For mesh generation and for analysis settings, 'Model' is started up.



It can be meshed by default, and then improved to fine mesh under its details.

- Specifying Fixed supports and Displacement:

For the following two cases, analysis is to be performed to evaluate Total deformation and Direct-stress. According to Rubinstein (2000), Geometric Advantage (GA) is given by,

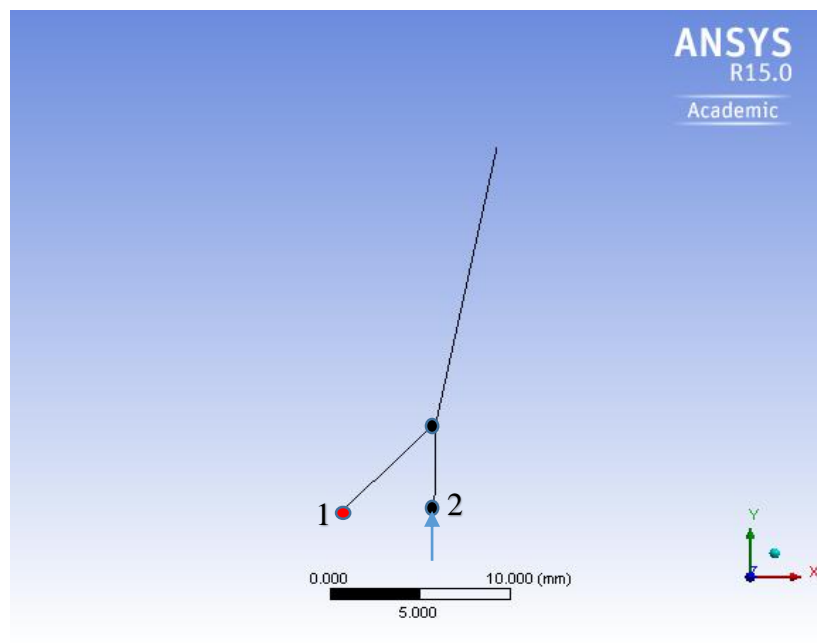
$$GA = \frac{U_o}{U_i} \dots\dots\dots (3.1)$$

Where,

$U_o$  = Output Displacement

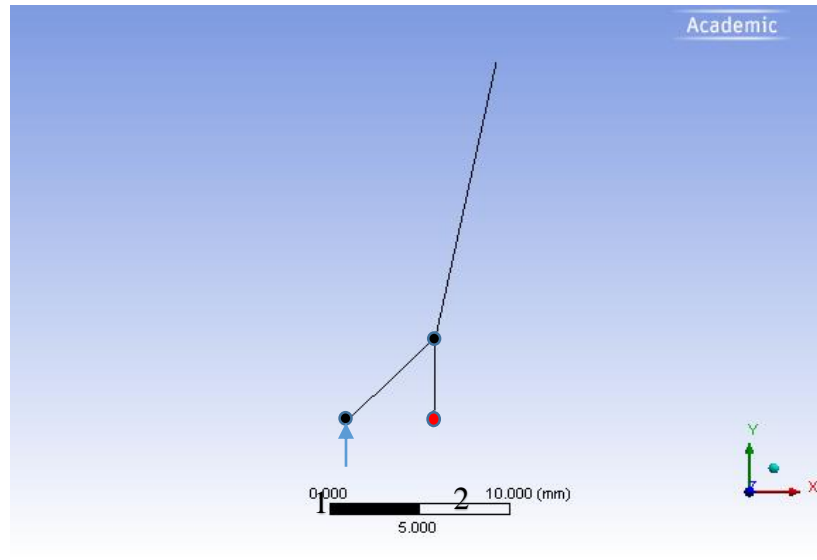
$U_i$  = Input Displacement

Case-1: Node-1 is fixed, and node-2 is given a displacement ( $U_i$ ) of **3 mm**, which correspond to a force of 0.04N (Specifications of an Electro-magnet solenoid actuator taken from literature review).  $U_o$  (Total Deformation) is found through static structural analysis and  $GA_1$  is calculated.



**Figure 3.5:** Displacement through electro-magnetic actuation.

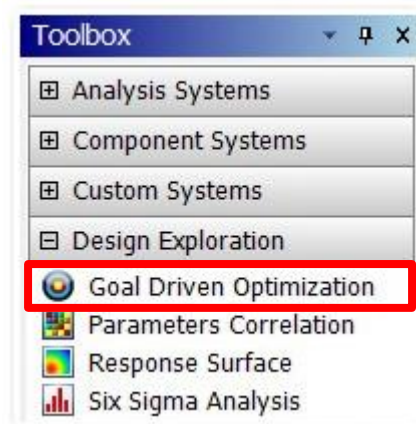
Case-2: Node-2 is fixed and node-1 is given a displacement ( $U_i$ ) of **0.008 mm** corresponding to a force of 190 N (Specifications of a Piezo actuator taken from literature review). Find  $U_o$  and Calculate  $GA_2$ .



**Figure 3.6:** Displacement through piezo actuation.

#### 4. Optimization of the line model

For the better functionality of the gripper,  $GA_1$  and  $GA_2$  have to be increased, i.e., tip displacement of the finger can be maximized, which can be performed by ‘Goal driven optimization’ under ‘Design Exploration’ in ANSYS Workbench.





Objective function: Maximize  $U_{o1}(A, l_i, \alpha)$  ..... (2.2)

Maximize  $U_{o2}(A, l_i, \alpha)$  ..... (3.3)

Subject to:  $\sigma < 42$  MPa (Ultimate tensile strength of ABS Plastic)

$$A > 0$$

$$\alpha > 0$$

$$l_i > 0, (i=1,2,3)$$

Where,

$U_{o1}$  = Output tip displacement (Total deformation from analysis results)  
corresponding to  $GA_1$

$U_{o2}$  = Output tip displacement corresponding to  $GA_2$

$\sigma$  = Equivalent stress

$A$  = Cross-sectional area of the link

$\alpha$  = angle between Link-1 and Link-2

$l_i$  = link length

In Workbench,

$A, l_i, \alpha$  are entered as driving/input parameters

$\sigma$  is entered as output parameter

$U_{o1}$  and  $U_{o2}$  are taken as Maximization objectives

Optimization method: Multi-Objective Genetic Algorithm (MOGA), since there are two objective functions.

## 5. Analysis of 3D model

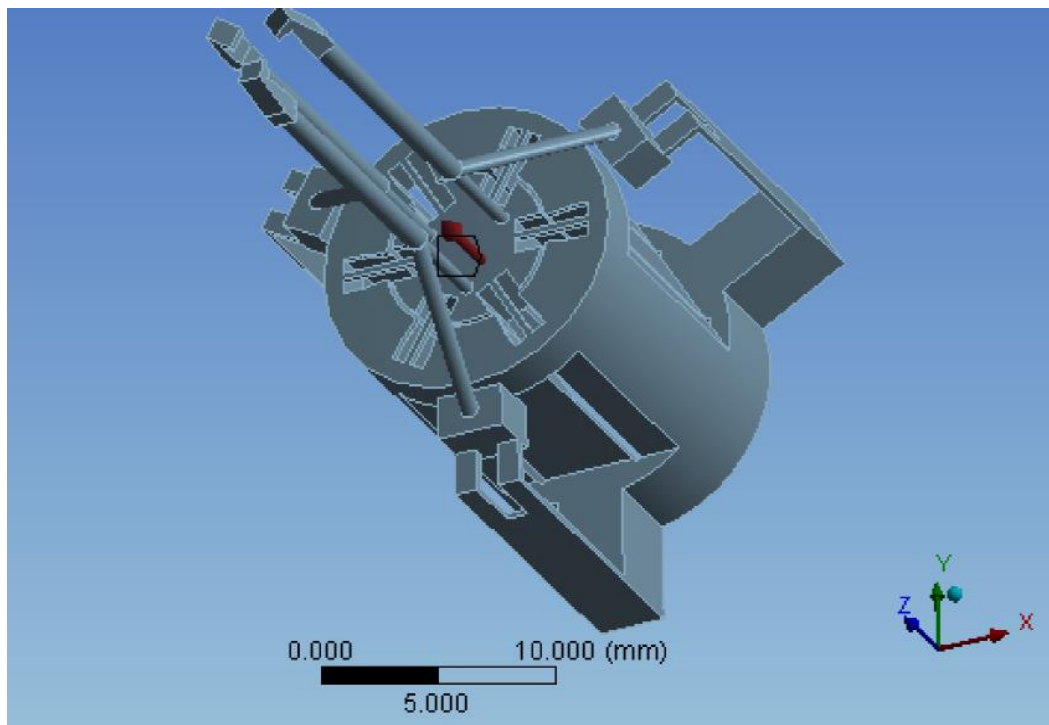
From the above optimization problem, we get the optimal values of input parameters  $A_i$ . These values can be updated in the 3D model of the gripper and the simulation schematic is discussed below.

### **Case 1: With no object grasped**

a) **Static Structural Analysis:** Static Structural analysis is performed to find the gripping range by solving for the maximum total deformation in the two positions mentioned below.

#### Position 1: Opening of finger tips

Force of 0.04N (EM actuation force) applied on the central base in the upper direction. This corresponds to an input displacement of 3mm used in the line model in step-3.

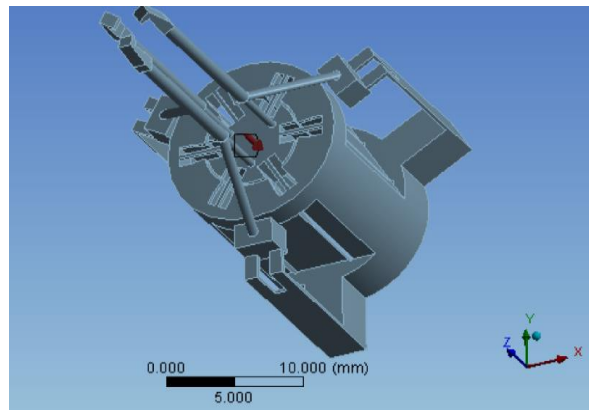


**Figure 3.7:** Force application (upwards) through EM actuation.

Position 2: Closing of finger tips

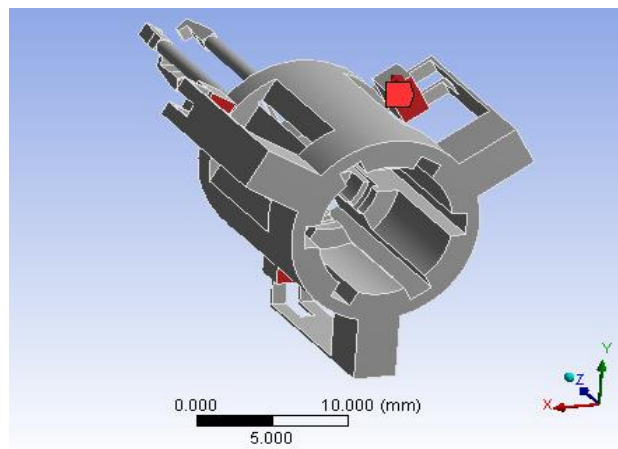
i) **Coarse Movement of tips:** Force of  $-0.04\text{N}$  (EM actuation force) corresponding to a displacement of  $-3\text{mm}$  applied at the central base of the gripper, i.e., in the downward direction.

Find the maximum total deformation in this position.



**Figure 3.8:** Force application (downwards) through EM actuation.

ii) **Fine Movement of tips:** Force of  $190\text{N}$  (Piezo-electric actuation force) is applied in the upward direction which corresponds to an input displacement of  $0.008\text{mm}$  used in the line model analysis.



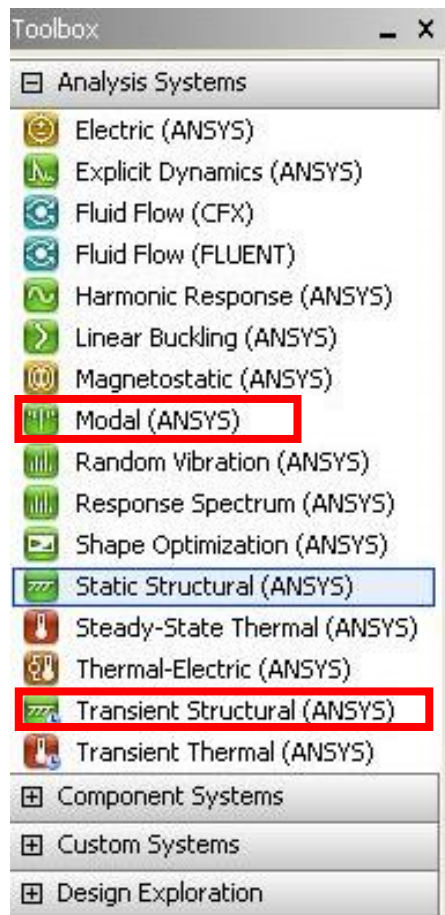
**Figure 3.9:** Force application (upwards) through piezo-electric actuation.

## b) Transient analysis

This analysis is performed to evaluate the band-width i.e. time response of the tip displacement, when given a step input force. Before transient analysis, modal analysis is performed to use its natural frequency for the calculation of Integration Time Step (ITS). Integration time step is  $1/20^{\text{th}}$  of the response period, which is given by the following equation (3.4).

$$\text{ITS} = \frac{1}{20f} \dots \dots \dots (3.4)$$

Where,  $f$  = natural frequency obtained from modal analysis.



Modal analysis is a dynamic simulation to find out the frequencies with which the gripper vibrates under pre-stressed and un-pre-stressed conditions. We can check the difference between the natural frequencies for both conditions. Even though pre-stress is negligible, it is considered more practical since the load might affect stiffness.

No pre-stress condition: It involves free vibrations of the gripper, when no external forces are applied. The whole base of the gripper is fixed, i.e., wings and central base. Maximum number of modes can be taken as six. Total deformation value has no significant meaning here, but the shape of vibration modes generated with its natural frequencies matter in this analysis.

Pre-stress condition: It involves the generation of vibration modes when external forces are applied. Here external forces are considered and the modal analysis is performed for the two positions of gripper as mentioned in static structural analysis section. Then, frequencies are found for both of these positions and used in transient analysis for the calculation of ITS as given in equation (3.4).

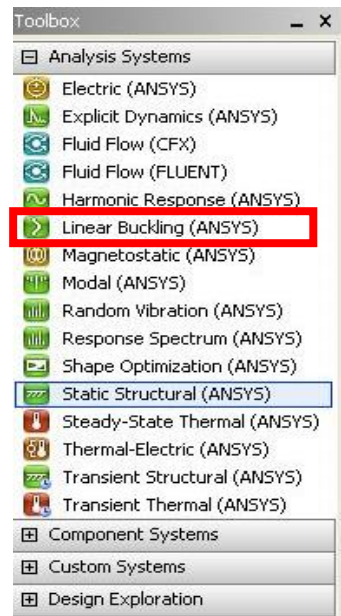
*Transient structural simulation:*

Step end time, i.e., total simulation time for tip displacement is assumed to be 1 second. ITS is calculated and Stiffness coefficient value of ABS plastic is found to be  $7.9e-5$  (Takemoto, 2002). These values are used for analysis settings. Transient analysis is performed for both positions (open and close) of gripper as given in static structural simulation. Time response for total deformation (i.e., tip displacement) and equivalent stress is studied and plotted.

**c) Buckling analysis:**

To analyze the stability of gripper structural members under axial compressive loads, buckling analysis is performed. As the compressive stress increases, stiffness of the member

decreases to zero and becomes weak to handle any lateral force and fails. The load at which it fails is called as buckling load and the related deformation is called as buckling mode.



In Workbench, linear buckling simulation is performed. Buckling loads can be obtained upon solving and its mode shapes can be obtained. For the two positions (open and close) of the gripper, this analysis is performed.

### **Case 2: With object grasped**

Consider an object such as a bead with a diameter of 4 mm. Create a new geometry of bead and then a plane of symmetry for the gripper. Set up the initial contact point. The bead is modeled as a rigid body, as it doesn't deform. Here, contact body is gripper and the target is bead, and the contact between them is frictionless. Consider position-1 (closing of the gripper) and perform static structural simulation to evaluate the contact pressure.

**3.3.2 Flexibility.** Flexibility is stated by investigating the maximum tip displacement values in open and close position of the gripper. Maximum opening of the gripper indicates the value of maximum size of the object the gripper can grasp. In the same way, maximum tip displacement of the gripper while closing indicates the minimum size of the object it can grasp.

Based on this range, the flexibility of gripper in grasping micrometer and millimeter scale objects is stated.

**3.3.3 Scalability.** Scalability of the gripper model is discussed by scaling up the model by a set of factors such as 5 or 10. Static structural simulation is performed in the same way as done for the basic model. The results are then compared with the base model, and can be plotted as 'Total deformation/stress' vs 'scaling factor'.

## CHAPTER 4

### FINDINGS

This chapter provides the results of simulation according to the methodology laid out in Chapter 3. The first section discusses the functionality of the gripper by performing the analysis of line model and 3D model. The following sections detail the flexibility and scalability aspects of the analyzed 3D model.

#### 4.1 Functionality

This section consists of the results of the line model analysis. Then, optimization of link lengths is performed by varying input parameters for the maximum tip displacement resulting in maximum gripping range. One of the optimized line models is taken for 3D analysis, and its results are discussed.

**4.1.1 Analysis of line model.** Figure 4.1 gives us the initial dimensions of the link lengths taken for analysis as mentioned in Chapter 3. This model is driven by two actuation sources namely piezo-electric and electro-magnetic. As discussed in the previous chapter, piezo-electric actuation source is applied at the wings, i.e., at node-2 ( $N_2$ ), while electro-magnetic actuation is applied at the central base, i.e., on Link-5 ( $L_5$ ) as shown in Figure 4.1. Actuation loads are taken from the literature review, which are the specifications of the actuators given by the manufacturing industries as given in Table 2.5 and Table 2.6. Input force and displacement of the actuators have a linear relationship varying by a constant, given by the following equation (4.1).

$$F_i = kX_i \dots\dots\dots (4.1)$$

Where,

$F_i$  = Input Force,  $X_i$  = Input Displacement,  $k$  = constant



For the chosen electro-magnetic actuator,

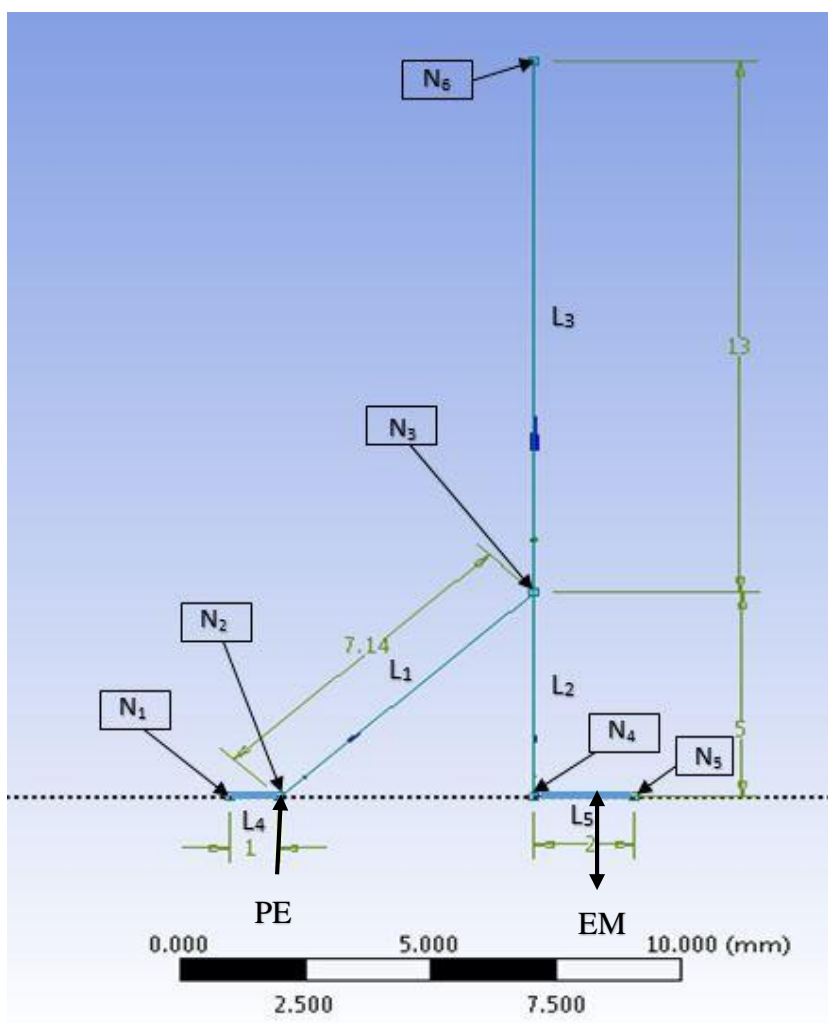
$$F_i = 0.04\text{N}, X_i = 3\text{mm}.$$

$$k = F_i/X_i = 0.0133 \text{ (From equation (4.1))} \dots\dots\dots (4.2)$$

For the chosen piezo-electric actuator,

$$F_i = 190\text{N}, X_i = 0.008\text{mm}.$$

$$k = F_i/X_i = 23750 \text{ (From equation (4.1))} \dots\dots\dots (4.3)$$

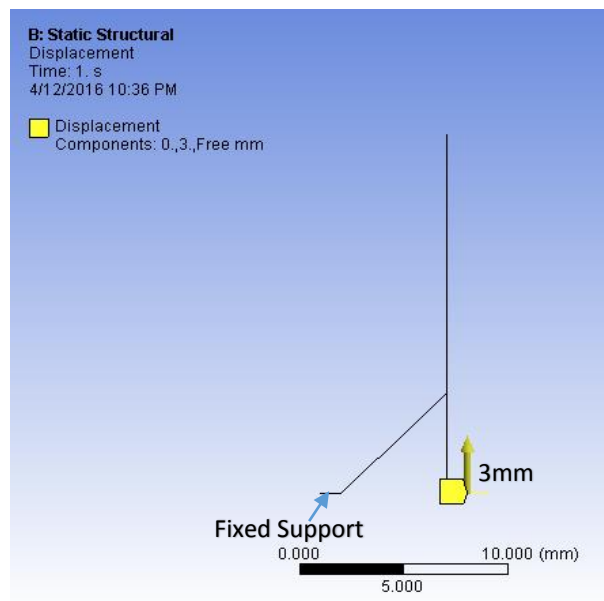


**Figure 4.1:** Un-optimized line model.

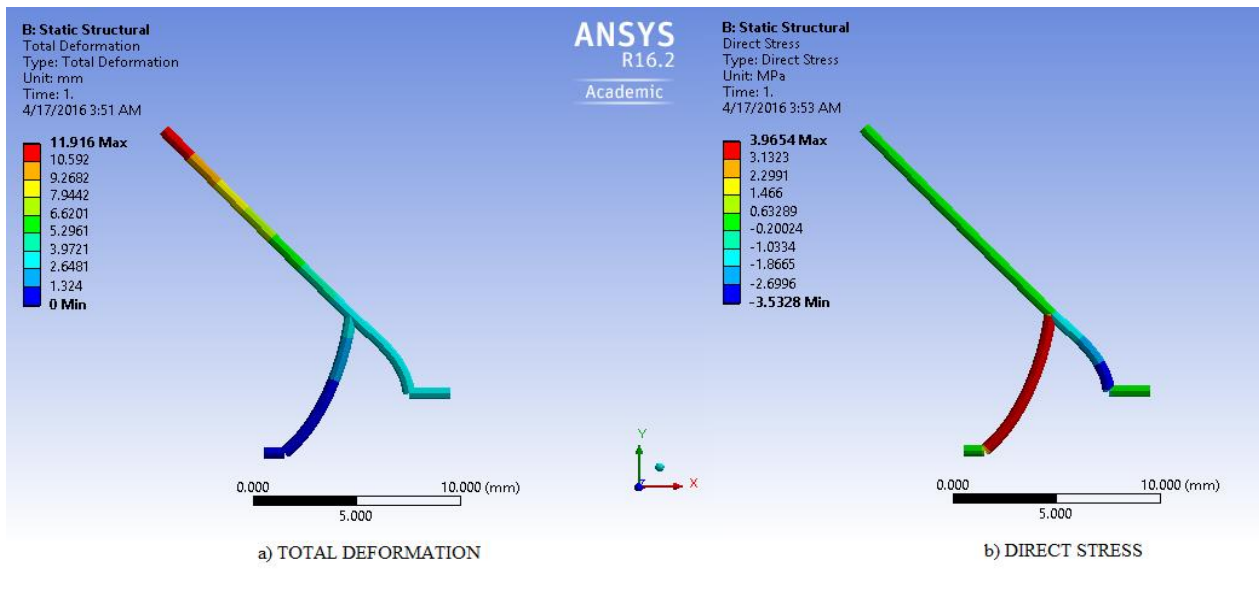
The following cases are considered which facilitate opening and closing modes of a single finger in the gripper. Output total deformation and direct stress results are obtained for line model. Line model uses structural beams, and it is said to be under direct stress when the members are under either compressive or tensile loading.

**Case-1:** Open mode under EM actuation

Input displacement of 3mm on L<sub>5</sub> in upward direction is applied with fixed support on L<sub>4</sub>, as shown in Figure 4.2.



**Figure 4.2:** Input EM load and support in **open mode** (line model).

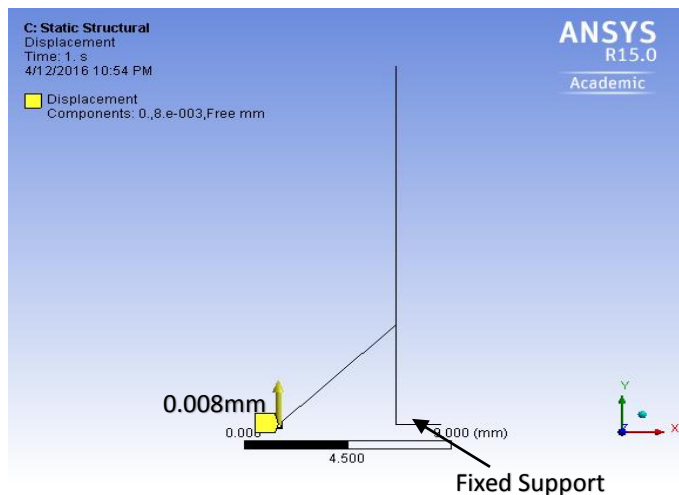


**Figure 4.3:** Output results under EM actuation in **open mode** (line model).

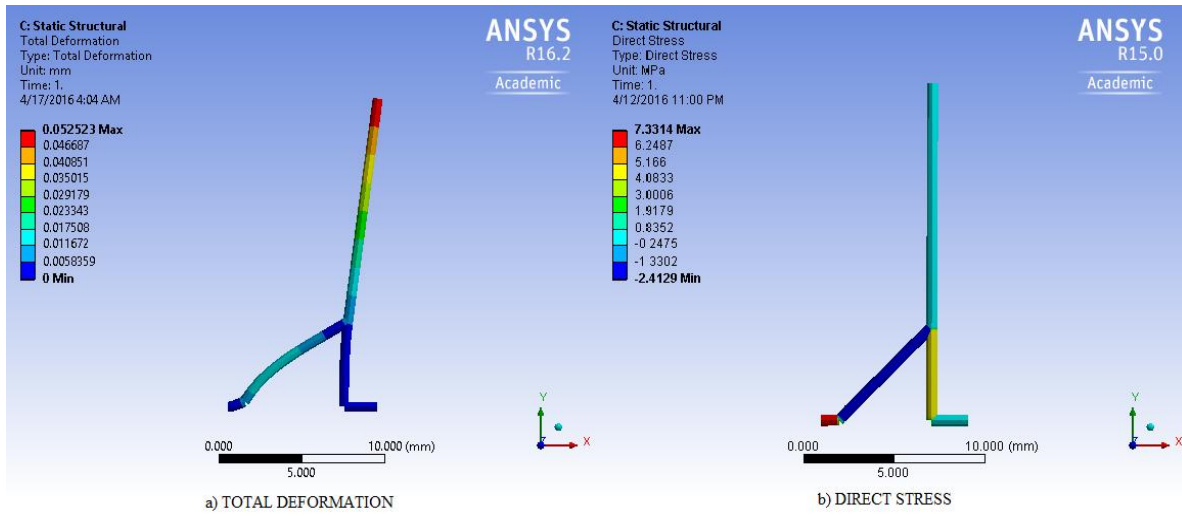
Output results are shown in Figure 4.3. Maximum total deformation of 11.916 mm is observed at the tip of the finger, with the maximum direct stress of 3.9654MPa generated in Link-1.

**Case 2:** Close mode under Piezo-electric actuation

Input displacement of 0.008 mm at  $N_2$  in upward direction is applied with fixed support at  $N_1$  and  $L_5$  as shown in Figure 4.4.



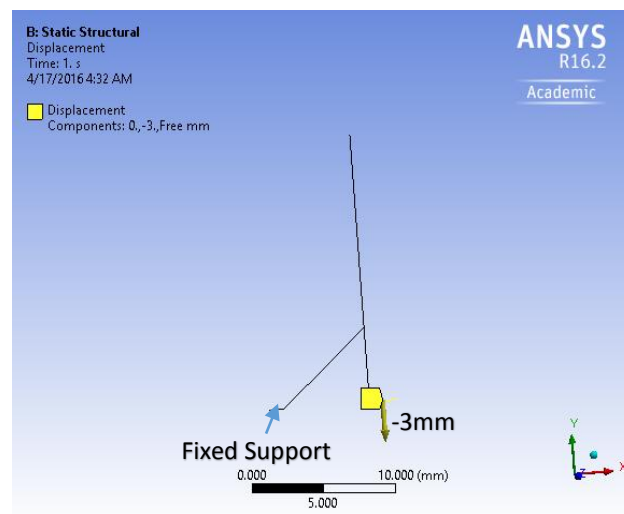
**Figure 4.4:** Input PE load and support in **close mode** (line model).



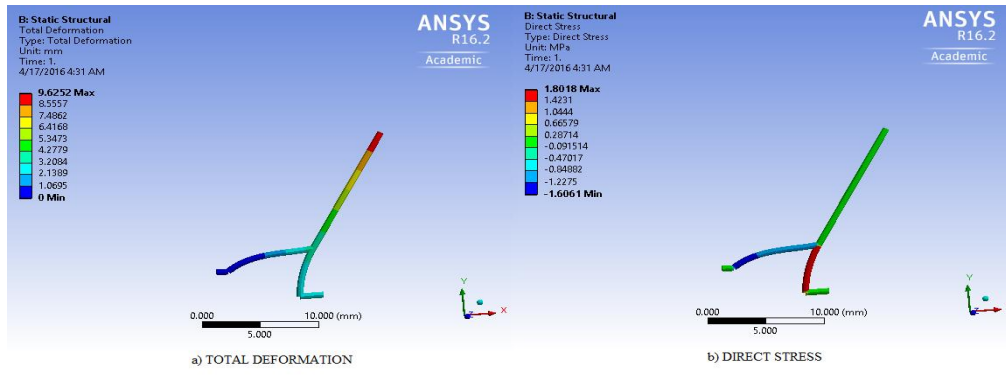
**Figure 4.5:** Output results under PE actuation in **close mode** (line model).

Output results are shown in Figure 4.5. Maximum total deformation of 0.052523 mm is observed at the tip of the finger with the direct stress of 7.3314 MPa generated in Link-4.

**Case 3:** Close mode under EM actuation. EM is bi-directional and changing current direction would change the direction of EMF, and generate force in the opposite direction. Input displacement of -3 mm on  $L_5$  in downward direction is applied with fixed support at  $L_4$ .



**Figure 4.6:** Input EM load and support in **close mode** (line model).



**Figure 4.7:** Output results under EM actuation in **close mode** (line model).

Output results are shown in Figure 4.7. Maximum total deformation of 9.6252 mm is observed at the tip of the finger, with the direct stress of 1.8018 MPa generated in Link-2.

In this case, maximum total deformation of the tip exceeds the right-side boundary of the mechanism, which may result in collision with other fingers of gripper. Link-5 is of 2 mm, so input displacement in this case has to be chosen based on the size of the object to be held, with the tip deflection not exceeding the right end of link-5, during simulation of 3D model.

Results of all the above cases are tabulated in Table 4.1 below.

**Table 4.1:** Static structural analysis results of an un-optimized line model.

	Mode	Actuation source	Input		Output (Maximum)		
			U <sub>i</sub> , Displacement (mm) – Location (Link/node)	Fixed Support	U <sub>o</sub> , Total Deformation (mm) at tip	Direct stress (Mpa) - Location	GA (U <sub>o</sub> /U <sub>i</sub> )
Case-1	Open	Electro-magnetic	↑ 3 - L5	L4	11.916	3.9654 – L1	3.972
Case-2	Close	Piezo-electric	↑ 0.008 - N2	N1, L5	0.052523	7.3314 - L4	6.5653
Case-3	Close	Electro-magnetic	↓ 3 - L5	L4	9.6252	1.8018 - L2	3.2084

From Table 4.1, if we look at electro-magnetic (EM) actuation, GA of case-1 and case-3 are almost similar, and as we are concerned only with open mode, GA of case-1 can be increased, which is considered as an objective. Case-3 is not taken into account, since it gives more tip displacement, which might result in collision with other fingers. In case-1, link-1 is mostly stressed for opening, while in case-3 link-2 is stressed for closing, due to which a small difference is observed in GA values of both the cases even if the magnitude of input displacement is same. Taking piezo-electric (PE) actuation into account, its GA also can be increased, which is considered as the other objective for optimization. Piezo-electric actuation gives more GA when compared to electro-magnetic. Therefore, PE actuation is used for giving fine movements of gripper tip, while EM actuation is used for coarse movements.

**4.1.1.1 Optimization.** Optimization is performed to maximize the output total deformation of the tip for both electro-magnetic and piezo-electric actuation sources. Following are the conditions taken during optimization.

- Size of the mechanism is fixed.
- Node-3 is chosen as input parameter, where its x and y coordinates are manipulated to get various set of optimized link lengths and shapes.
- Multi-objective Genetic algorithm is used for entire optimization.
- Case-3 of line model analysis is ignored as it gives larger displacement than required.

Table 4.1 lists two different sets of optimization results when input parameters are varied. Its grasping capability is measured by evaluating the maximum radius of the object that the gripper can hold, which is given by equation (4.4).

$$R = X_p + (9 - X) \dots\dots\dots (4.4)$$

Where,

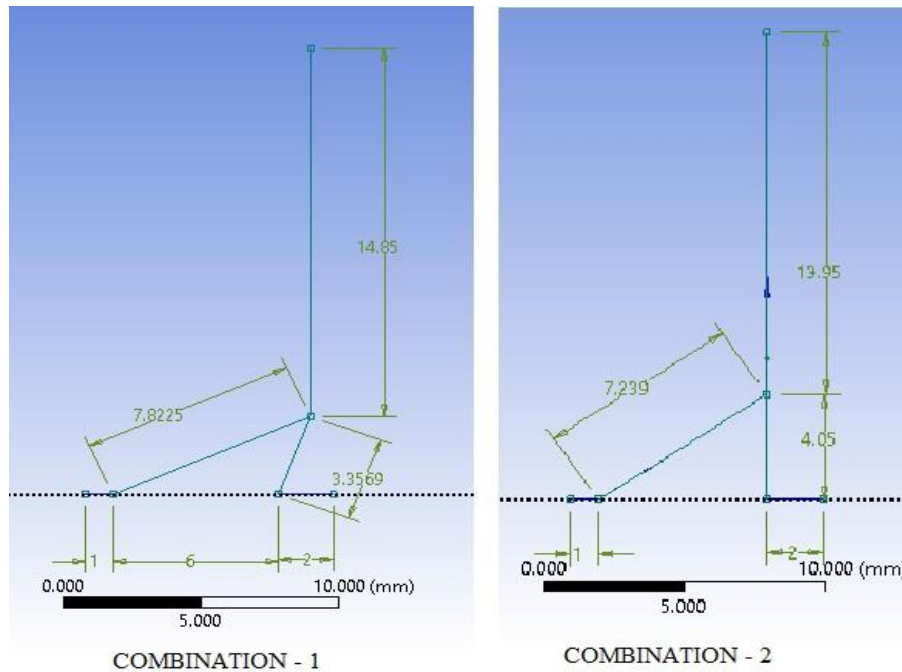
$R$  = Maximum radius of the object handled by the gripper

$X_p$  = X-directional deformation at the chosen candidate point

$X$  = x-coordinate of optimized node 3

**Table 4.2:** Input details for optimization and its output results.

	<b>Set - 1</b>	<b>Set - 2</b>
<b>Objective Function</b>	Maximize – Output Total Deformation in Case-1	Maximize - Output Total Deformation in Case-1
	Maximize – Output Total Deformation in Case -2	Maximize – Output Total Deformation in Case -2
<b>Constraints</b>	Direct stress in case-1 $\leq$ 42 MPa	Direct stress in case-1 $\leq$ 42 MPa
	Direct stress in case-2 $\leq$ 42 MPa	Direct stress in case-2 $\leq$ 42 MPa
<b>Input Parameters</b>	X co-ordinate of node-3; Lower bound = 0 mm, Upper bound = 9 mm	Y co-ordinate of node-3; Lower bound = 0 mm, Upper bound = 18 mm
	Y co-ordinate of node-3; Lower bound = 0 mm, Upper bound = 18 mm	
<b>Best Candidate point obtained (optimized)</b>	At node3, X co-ordinate = 8.1602, Y co-ordinate = 3.15	At node3, Y co-ordinate = 4.05
<b><math>X_p</math></b>	13.218 mm	12.143 mm
<b>Link lengths (Optimized)</b>	$L_1 = 7.8225\text{mm}; L_2 = 3.3569\text{mm}; L_3 = 14.85\text{mm}$	$L_1 = 7.239\text{mm}; L_2 = 4.05\text{mm}; L_3 = 13.95\text{mm}$
<b>R</b>	$13.218 + (9 - 8.1602) = 14.0578\text{mm}$	$12.143 + (9 - 7) = 14.143\text{mm}$



**Figure 4.8:** Optimized geometries.

The optimized geometries of the both sets are represented in Figure 4.8. Candidate point obtained for set-2 is chosen, since its gripping capability is more when compared to set-1. The link lengths are updated in the 3D model of the gripper with the following changes as given in the Table 4.3.

**Table 4.3:** Updated dimensions of a 3D model.

Link	Dimension (mm)
L <sub>1</sub>	7.239
L <sub>2</sub>	4.05
L <sub>3</sub>	13.95
Radius	0.3



**4.1.2 Analysis of 3-D model.** This section consists of the analysis of the 3-D model of the gripper updated with optimized geometry dimensions given in Table 4.3. The purpose of this analysis is to simulate and visualize the behavior of the gripper when input actuation load is applied and also to evaluate the maximum safe load. Time response of the gripper is also studied. All these analyses are performed considering the gripper tips are free with no object held. Later, contact stresses are evaluated for the object held by the gripper.

**4.1.2.1 Meshing.** To perform analysis, meshing is performed initially. Size of mesh here is selected by low skewness and by the convergence of the output total deformation for the input of 3mm displacement. As the number of elements/nodes increase, mesh becomes finer and gives more accurate solution. Skewness is a mesh quality metric, which enhances by refining elements. Skewness is nothing but the deviation from the ideal element shape, and it should be as low as possible. It varies from 0 to 1. Skewness values for different mesh methods are tabulated below.

**Table 4.4:** Mesh methods and their skewness.

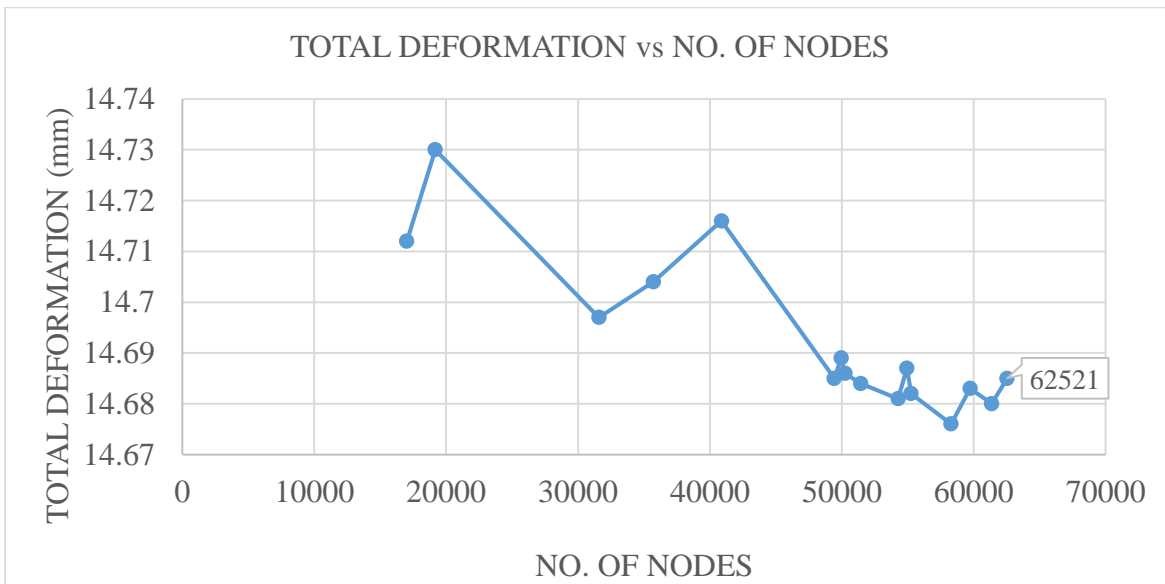
<b>Mesh Method</b>	<b>Skewness</b>
Patch conforming	0.999306176
Hex-dominant	0.999999504
Multi-zone	Unsuccessful
Patch independent	Unsuccessful

Multi-zone method transforms non-sweepable body to sweepable bodies and then sweeps elements during meshing. Patch conforming meshes triangular elements on outer face and then moves inwards to create tetrahedral elements, while Patch independent method meshes elements inside out. Hex dominant method combines tetrahedra of patch conforming to form hexahedra. The above Table 4.4 shows that skewness is very large for these methods. Multi-zone and Patch independent methods were unsuccessful in mesh generation. So, mesh convergence method is used to determine the mesh size. Higher order tetrahedrons are used for this method. Number of

nodes are increased, i.e., element size is decreased and the output total deformation is plotted against the number of nodes as given in Figure 4.9. The element size at which the output remains same/gets converged is taken for meshing throughout the analysis.

**Table 4.5:** Mesh statistics.

<b>ELEMENT SIZE (mm)</b>	<b>NO. OF NODES</b>	<b>NO. OF ELEMENTS</b>	<b>SKEWNESS</b>	<b>TOTAL DEFORMATION (mm)</b>
3	17010	8211	0.999976435	14.712
2	19174	9206	0.99981985	14.73
1	31584	16003	0.999728036	14.697
0.9	35705	18418	0.999282745	14.704
0.8	40872	21276	0.999647254	14.716
0.7	49426	26168	0.999602427	14.685
0.69	49952	26462	0.99546465	14.689
0.68	50238	26696	0.999473457	14.686
0.67	51421	27357	0.99813511	14.684
0.66	54267	29042	0.997293266	14.681
0.65	54935	29409	0.997688144	14.687
0.64	55247	29550	0.99878229	14.682
0.63	58286	31369	0.999557386	14.676
0.62	59720	32211	0.994346826	14.683
0.61	61361	33269	0.99737108	14.68
0.6	62521	33908	0.995613124	14.685



**Figure 4.9:** Mesh convergence.

From Figure 4.9, we can say that it is converging at node number, 62521. Element size at this point is 0.6 mm (from Table 4.5). Moreover, skewness of 0.99561312 is also found to be low, when compared to the skewness values in other methods given in Table 4.4.

Initially, without the object being grasped, static structural, buckling, modal, and transient analyses are performed, followed by evaluation of contact stresses of the gripper with the object grasped.

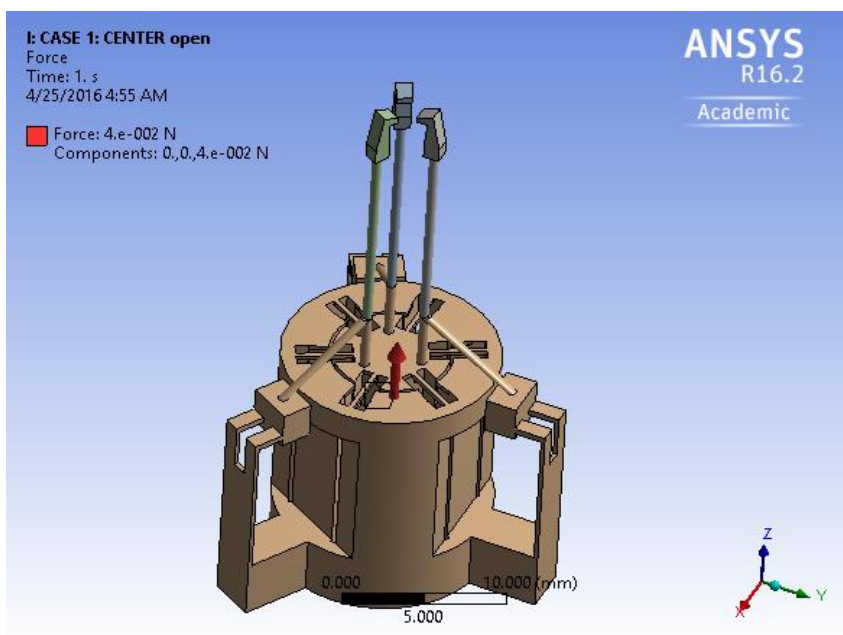
**4.1.2.2 Static Structural Analysis.** In this analysis, total deformation, horizontal deformation at the tip, and the maximum stress output are obtained. Under the input load, the resulting stresses are studied to see that they are not exceeding the ultimate tensile strength of the material. If they exceed, it can be said that the material fails under the given load. Ultimate tensile strength of ABS Plastic = 42 MPa. Input actuation loads are taken from the literature review, which are the specifications of the actuators given by the manufacturing industries.

Two positions are considered throughout the analyses, i.e., ‘open mode’ and ‘close mode’.

- ‘Open mode’ indicates the opening of gripper under the electro-magnetic actuation.
- ‘Close mode’ indicates the closing of gripper under electro-magnetic actuation for coarse movement of tips, while for fine movements piezo-electric actuation is applied.

a) Static structural analysis in open mode under EM actuation

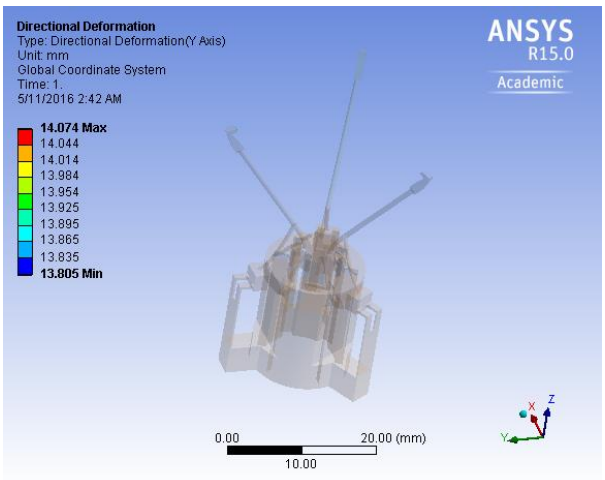
Input force of 0.04N and a displacement of 3mm are applied in upward direction at the central base as shown below in Figure 4.10, with fixed support at three wings and bottom base.



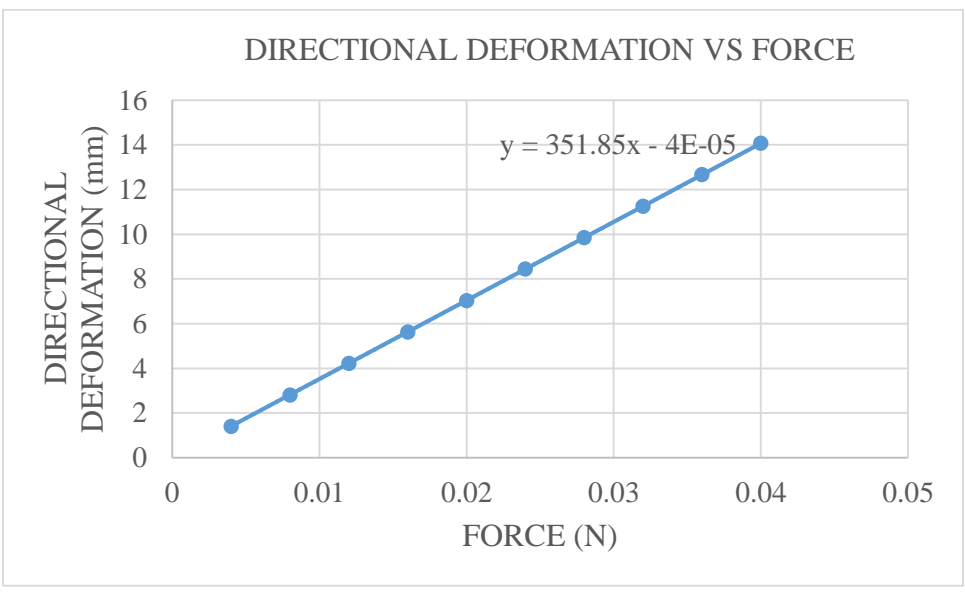
**Figure 4.10:** Input EM load in open mode.

Output result with maximum directional deformation of 14.074 mm is observed at the tip as shown in Figure 4.11. A graph (Figure 4.12) is plotted, and the following equation (4.5) is obtained with a linear fit.

$$y = 351.85x - 4E-05 \dots\dots\dots (4.5)$$



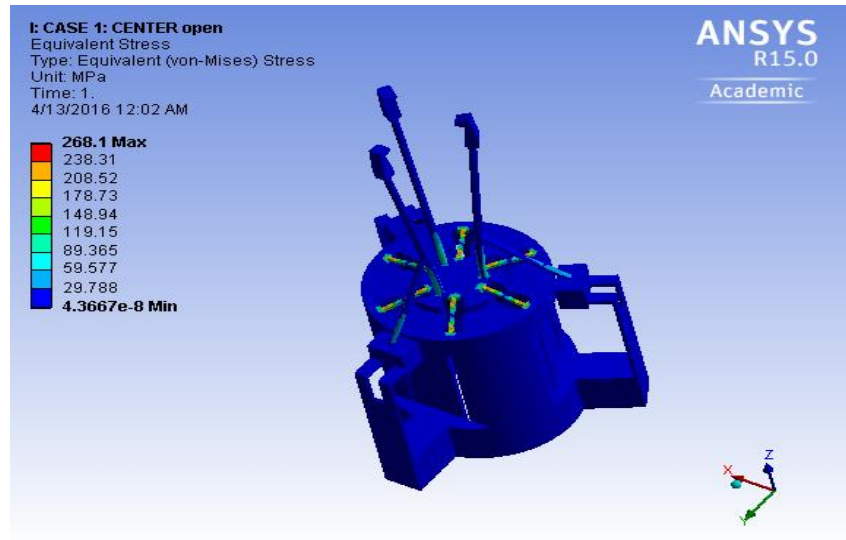
**Figure 4.11:** Directional deformation under EM actuation in **open mode**.



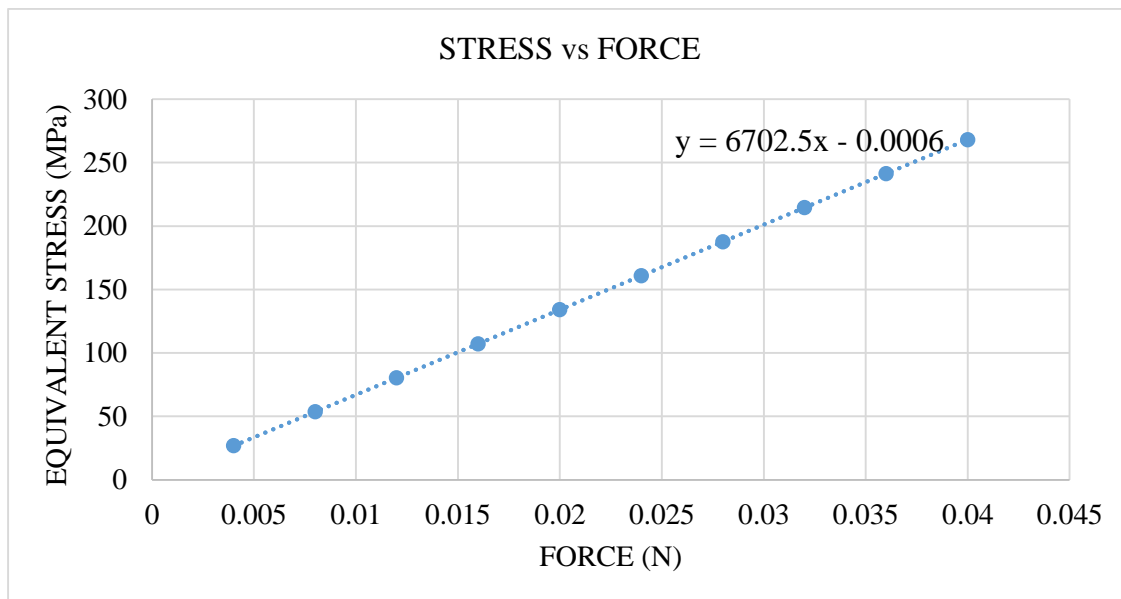
**Figure 4.12:** Relationship between horizontal tip displacement and force in **open mode**.

Maximum equivalent stress generated is 268.1MPa and is indicated by red color in Figure 4.13. A graph (Figure 4.14) is plotted, from which equation (4.6) is obtained.

$$y = 6702.5x - 0.0006 \dots\dots\dots (4.6)$$



**Figure 4.13:** Equivalent stress under EM actuation in **open mode**.

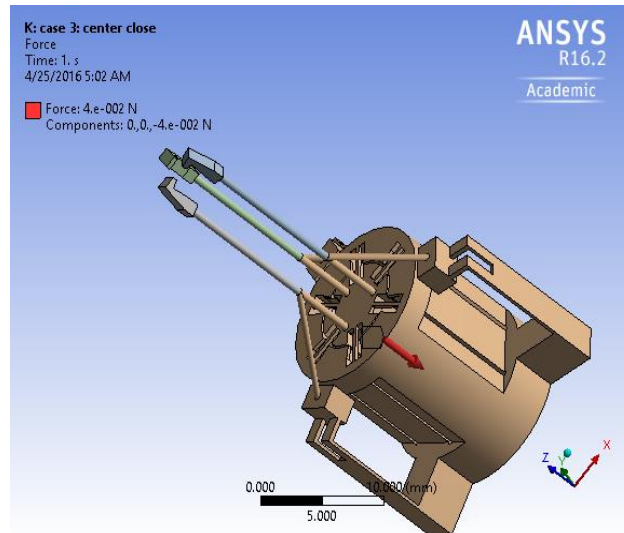


**Figure 4.14:** Relationship between equivalent stress and force in **open mode**.

Maximum equivalent stress generated, i.e., 268.1MPa is greater than the ultimate tensile strength of the material (42MPa). Therefore, for 42MPa, the maximum force input we can give is 0.006266N according to equation (4.6). Output Directional deformation for this input force of 0.006266N is 2.20465 mm, according to equation (4.5).

### Static Structural analysis in close mode under EM actuation for coarse movement

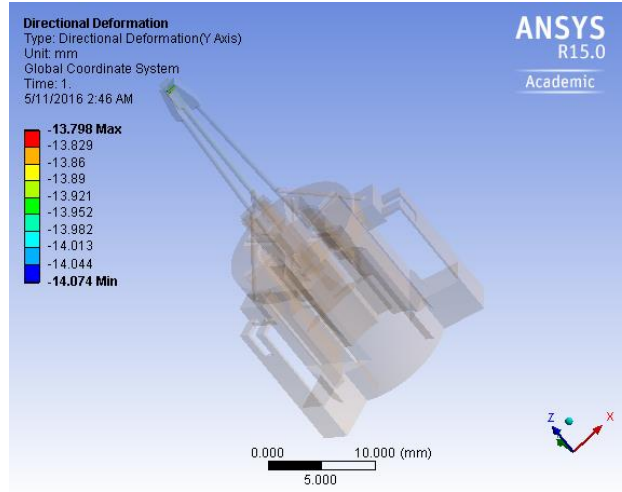
Input load of 0.04N and a displacement of 3mm are applied at the central base in downward direction, with fixed support at three wings and bottom base.



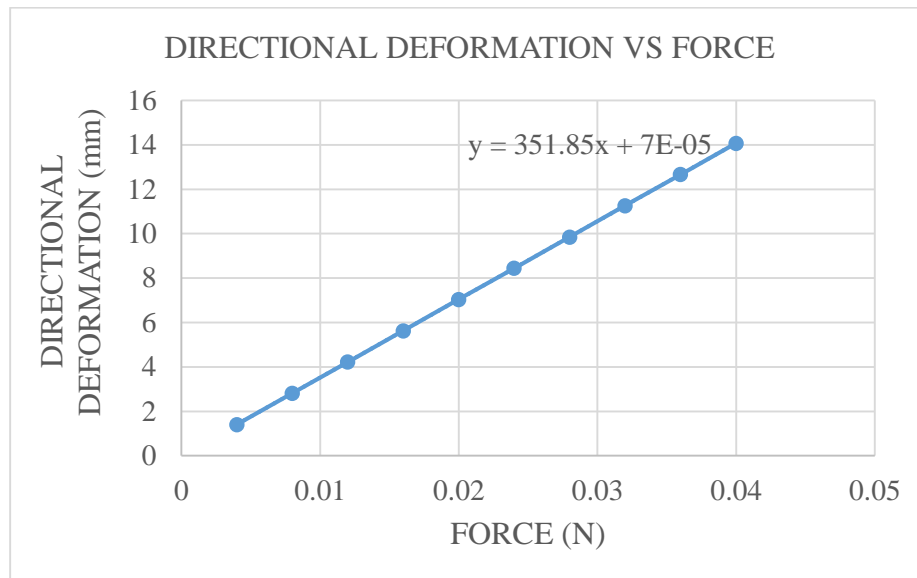
**Figure 4.15:** Input EM load in **close mode** for coarse movement.

Maximum output directional deformation of 14.074 mm is observed at the tip of fingers as shown in Figure 4.16. A graph (Figure 4.17) is plotted, from which the following equation (4.7) is obtained with a linear fit.

$$y = 351.85x + 7E-05 \dots\dots\dots (4.7)$$



**Figure 4.16:** Directional deformation under EM actuation in **close mode**.

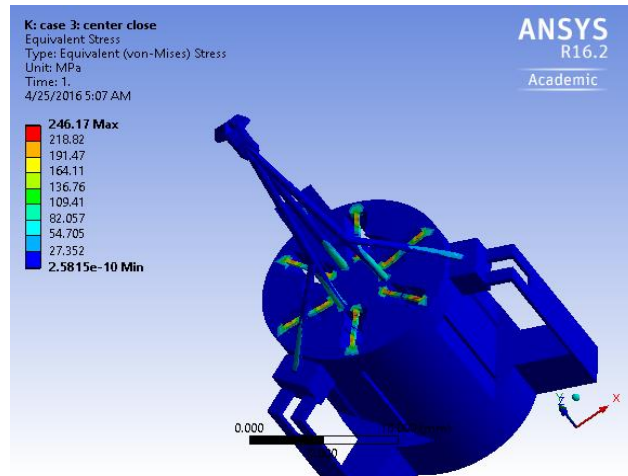


**Figure 4.17:** Relationship between horizontal tip displacement and force in **close mode** under EM actuation.

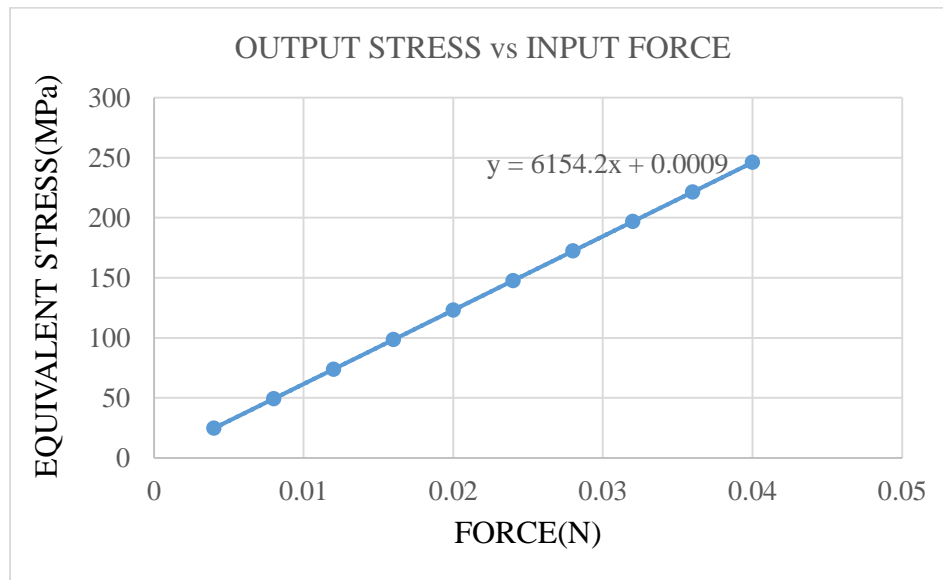
Output deformation of the tip in this case is very high. Therefore, input force should be selected in such a way that output directional deformation is less than 2 mm to avoid collision with other fingers. Horizontal distance of the tip from the center is 1.016 mm. So, for the tip displacement of 1mm, input force can be 0.002842N, according to equation (4.7).



Maximum equivalent stress of 246.17MPa is generated in the connecting members of the base indicated by red color, which is more than ultimate tensile strength of the material as shown in Figure 4.18.



**Figure 4.18:** Equivalent stress under EM actuation in close mode.



**Figure 4.19:** Relationship between stress and force in close mode under EM actuation.

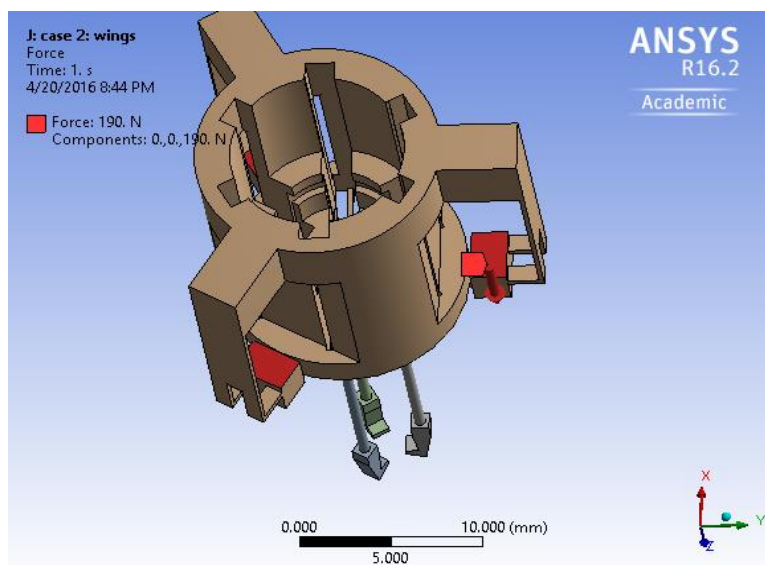
For the ultimate tensile strength of the material of 42 MPa, maximum input we can give is 0.006825N according to equation (4.8) obtained from graph (Figure 4.19).

$$y = 6154.2x + 0.0009 \dots\dots\dots (4.8)$$

But this is greater than the maximum input force we calculated in the previous section, i.e., 0.002784N. Therefore, for the force of 0.002784N, stress generated is 17.13MPa (from equation (4.8)), which is safe.

b) Static Structural analysis in close mode under PE actuation for fine movement

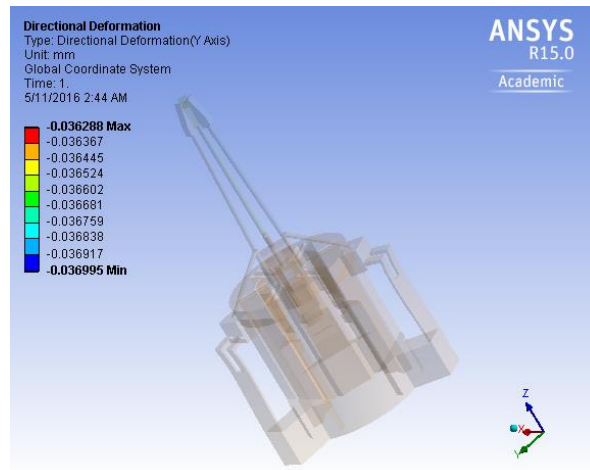
Input load of 190N and a displacement of 0.008mm are applied in the upward direction at three wings as shown in Figure 4.20, with fixed support at the central and bottom base.



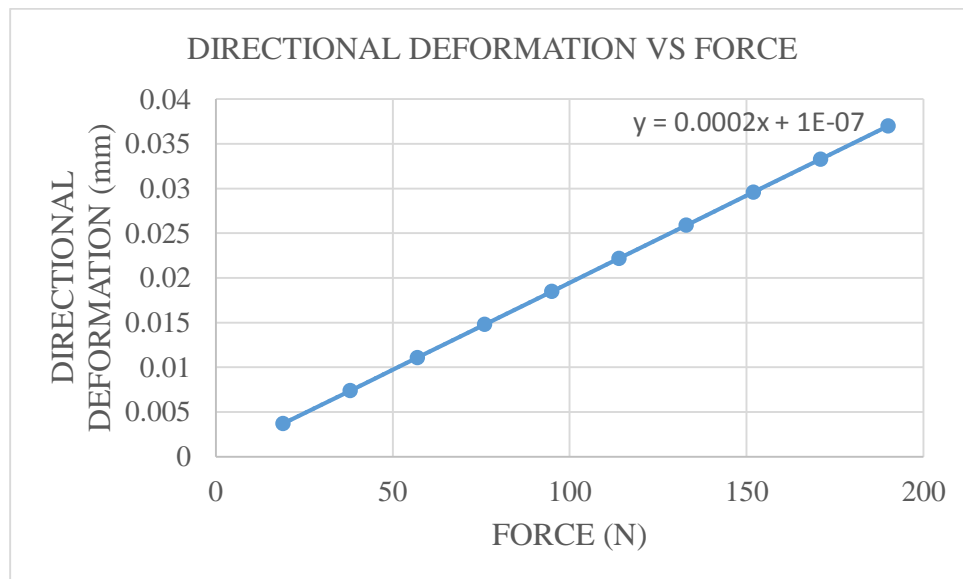
**Figure 4.20:** Input PE load in **close mode** for fine movement.

Maximum directional deformation at the tip is 0.036995 mm, which gives fine movements for closing finger tips as shown in Figure 4.21. A graph (Figure 4.22) is plotted, from which the following equation (4.9) is obtained through linear fit.

$$y = 0.0002x + 1E-07 \dots\dots\dots (4.9)$$



**Figure 4.21:** Directional deformation under PE actuation in **close mode**.



**Figure 4.22:** Relationship between horizontal tip displacement and force in **close mode** under PE actuation.

Maximum stress of 1.3888MPa is generated, which is less than ultimate tensile strength of the material (42 MPa), and the location is indicated in Figure 4.23.

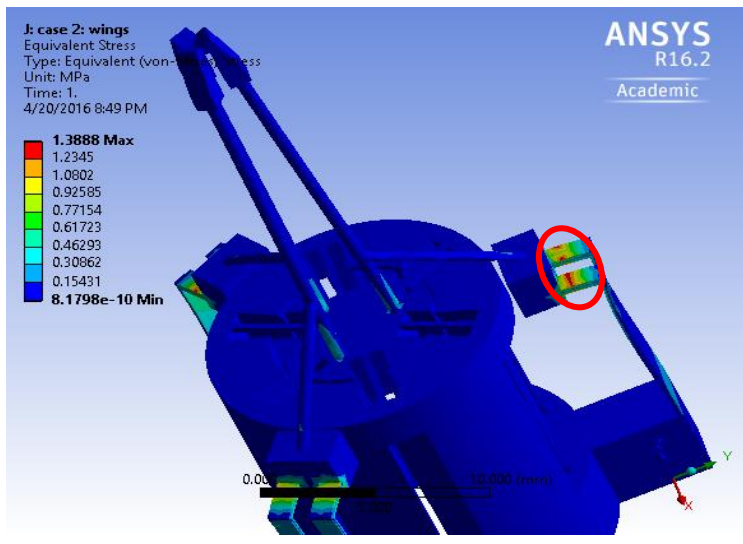


Figure 4.23: Equivalent stress under PE actuation in **close mode**.

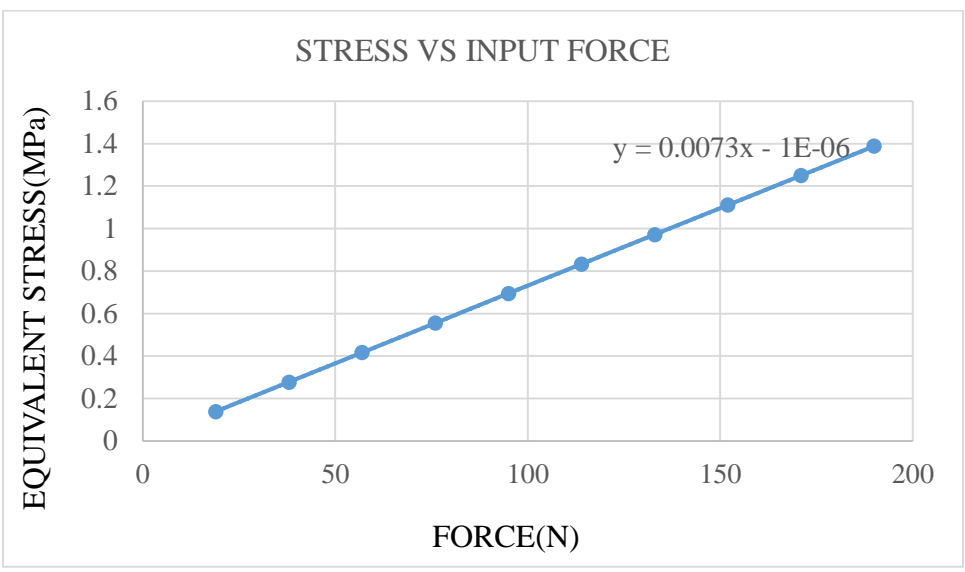


Figure 4.24: Relationship between stress and force in **close mode** under PE actuation.

For the stress of 42MPa, input force required is 5753.425N, according to equation (4.10) obtained from the graph (Figure 4.24).

$$y = 0.0073x - 1E-06 \dots\dots\dots (4.10)$$

For this force of 5753.424N, output directional deformation is 1.15069mm according to equation (4.9).

**4.1.2.3 Buckling analysis.** Gripper has three fingers which are thin and long and are subjected to axial compressive stress. As the compressive stress increases, bending stiffness decreases. Bending stiffness of zero value indicates that it is an unstable structure, i.e., a small load would result in large deflection. This is known as buckling and is said to occur when the bending stiffness in a structural member reaches zero due to the high compressive stress generated. The load at which buckling occurs is called buckling load. The deformation corresponding to this load is called buckling mode. In this section, we will evaluate the buckling load and buckling modes for the finger tips with free end, fixed end, and frictionless support.

***Buckling with finger tips having free end.*** Tips are left free, without any support, and following analysis is performed.

a) Open mode under EM actuation

Input load of 0.04N and displacement of 3 mm are applied in the upward direction on central base with wings and bottom base fixed as shown in Figure 4.10.

Upon simulation, we get the load multipliers for the first two modes of buckling as given below in Table 4.6.

**Table 4.6:** Buckling load under EM actuation in open mode.

Mode	Load Multiplier	Buckling load (N)
1	2.5654	0.102616
2	2.5776	0.103104

Buckling load is calculated by using the below given equation (4.11).

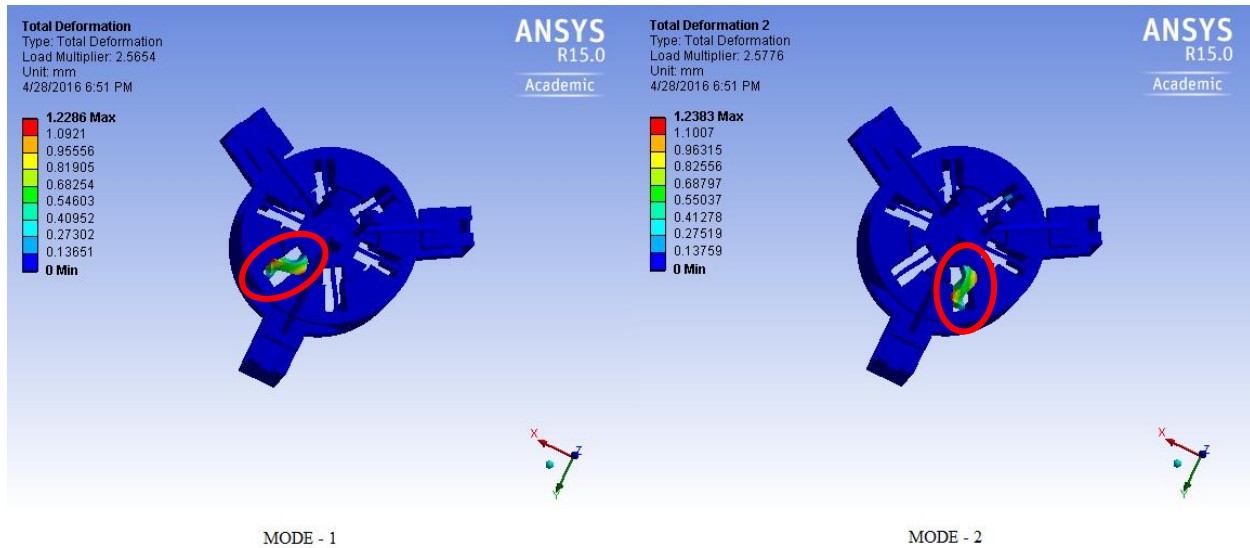
$$P_b = M \times P \dots\dots\dots (4.11)$$

Where,  $P_b$  = Buckling load

$M$  = Load Multiplier

$P$  = Applied input load

Buckling mode shapes obtained are illustrated below in Figure 4.25. Here, the deformation values have no significance, since they are scaled by ANSYS Workbench. Only the mode shapes are considered useful.



**Figure 4.25:** Buckling modes in **open mode** under EM actuation.

b) Close mode under EM actuation

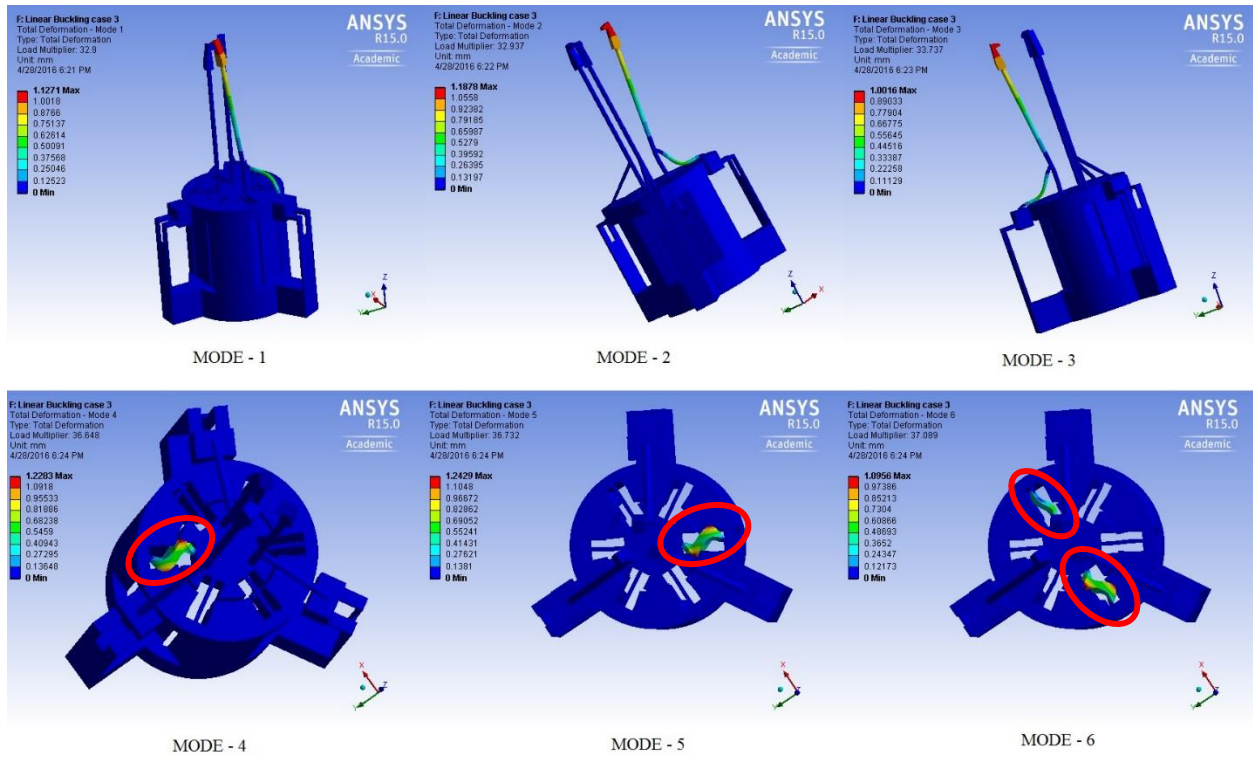
Input load of 0.002784 N and displacement of 0.208811mm (the safe input load, which avoids collision of fingers calculated in the section 4.1.2.2 [b]) is taken, which are applied in the downward direction on central base with wings and bottom base fixed as shown in Figure 4.15.

Output is obtained in the form of load multipliers, from which buckling load is calculated by equation (4.11) and tabulated in Table 4.7.

**Table 4.7:** Buckling load in close mode under EM actuation.

Mode	Load Multiplier	Buckling load (N)
1	32.9	-0.0915936
2	32.937	-0.091696608
3	33.737	-0.093923808
4	36.648	-0.102028032
5	36.732	-0.102261888
6	37.089	-0.103255776

Buckling mode shapes obtained under this load are illustrated in Figure 4.26.



**Figure 4.26:** Buckling modes in **close mode** under EM actuation.

c) Close mode under PE actuation

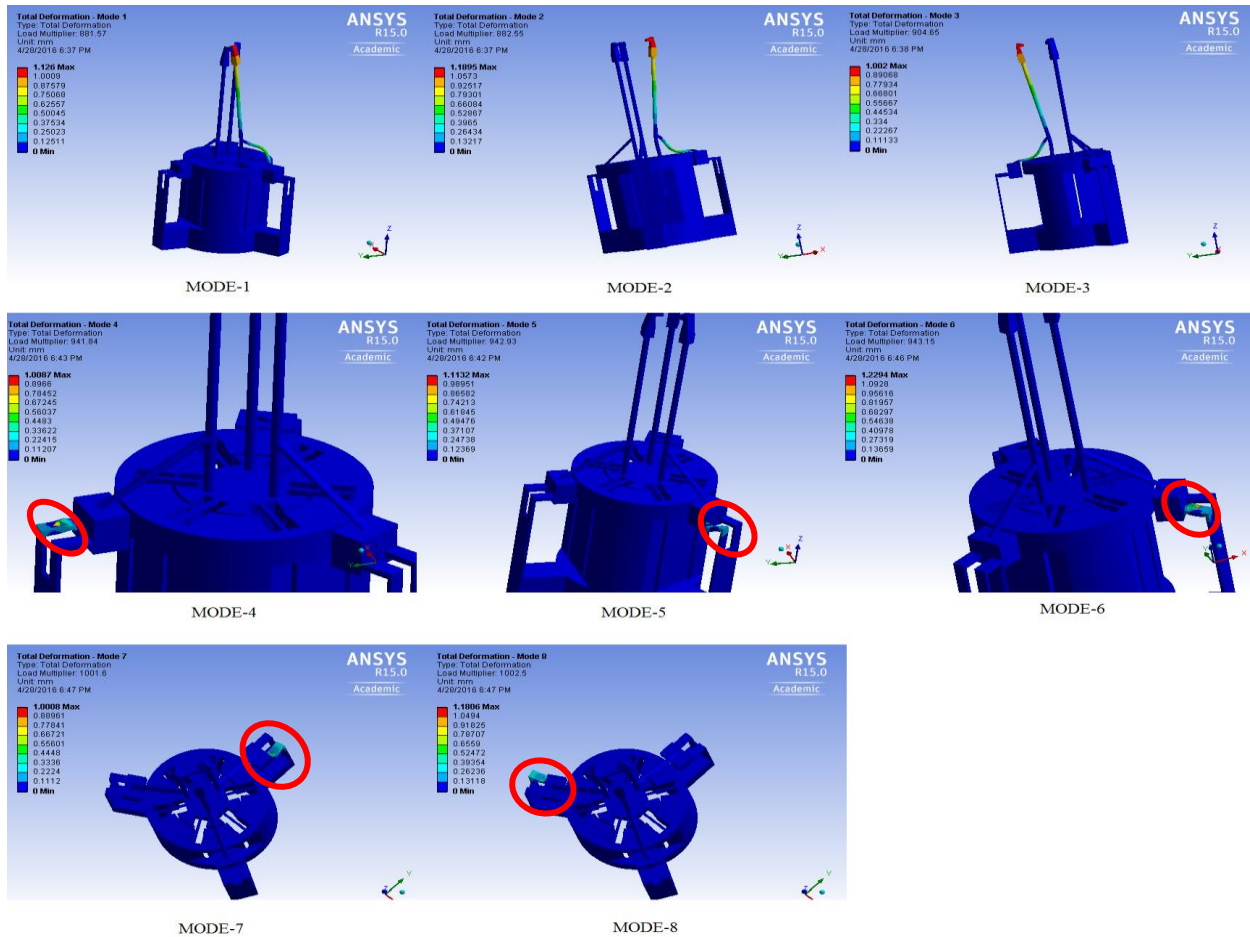
Input load of 190N and displacement of 0.008 mm are applied on wings with fixed support on central and bottom base in the upward direction as shown in Figure 4.20.

Output load multipliers are obtained, from which buckling load is calculated by equation (4.11) and tabulated in Table 4.8 as given below.

**Table 4.8:** Buckling load in close mode under PE actuation.

Mode	Load Multiplier	Buckling load (N)
1	881.57	167498.3
2	882.55	167684.5
3	904.65	171883.5
4	941.84	178949.6
5	942.93	179156.7
6	943.15	179198.5
7	1001.6	190304
8	1002.5	190475

Buckling mode shapes obtained under this load are illustrated below.



**Figure 4.27:** Buckling modes in close mode under PE actuation.

From all the above results of (a), (b), (c), we can say that the lowest buckling load obtained is 0.102616N for EM actuation, while for PE actuation it is 167498.3N. Under EM actuation, areas prone to buckling are the three fingers and the thin connecting structures on the top base. Under PE actuation, the areas affected are the connecting points at the wings, whose links are connected to the bottom base.

***Buckling with finger tips fixed.*** In this case, it is assumed that the object is being grasped and the contact is fixed. So, the analysis is performed by fixing the tips of the gripper for close mode under EM and PE actuation.



a) Close mode under EM actuation

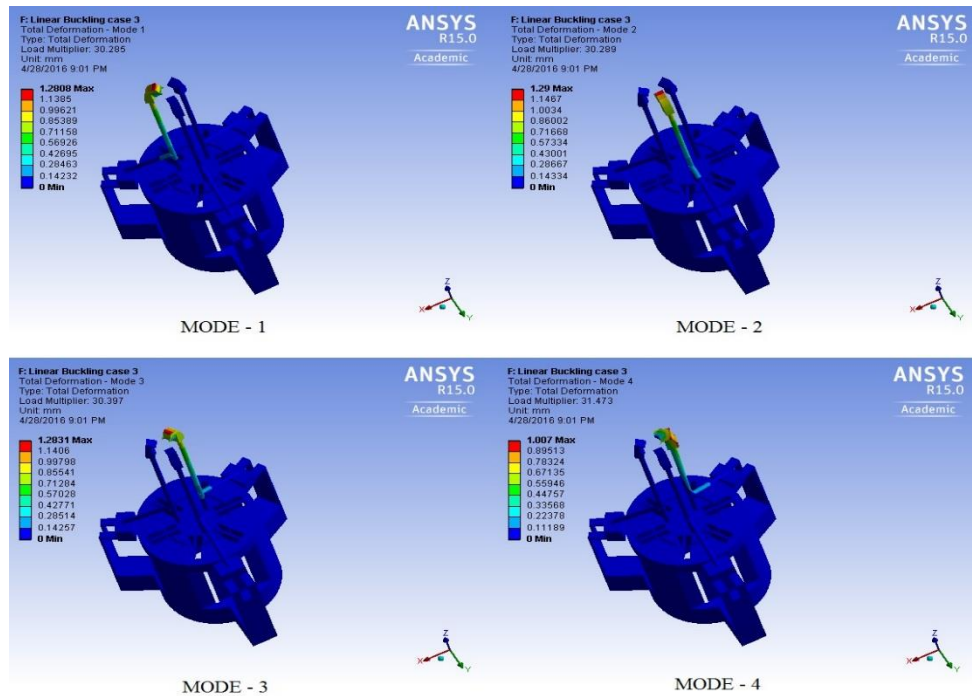
Input load of 0.002784N and displacement of 0.208811 mm are applied in the downward direction on the central base with wings and bottom base fixed as shown in Figure 4.15.

Output load multipliers are obtained, from which buckling load is calculated by equation (4.11) and tabulated in Table 4.9 as given below.

**Table 4.9:** Buckling load for fixed finger tips under EM actuation.

Mode	Load Multiplier	Buckling load (N)
1	30.285	-0.08431344
2	30.289	-0.084324576
3	30.397	-0.084625248
4	31.473	-0.087620832

The corresponding buckling modes are illustrated in Figure 4.28.



**Figure 4.28:** Buckling modes for fixed finger tips under EM actuation.

b) Close mode under PE actuation

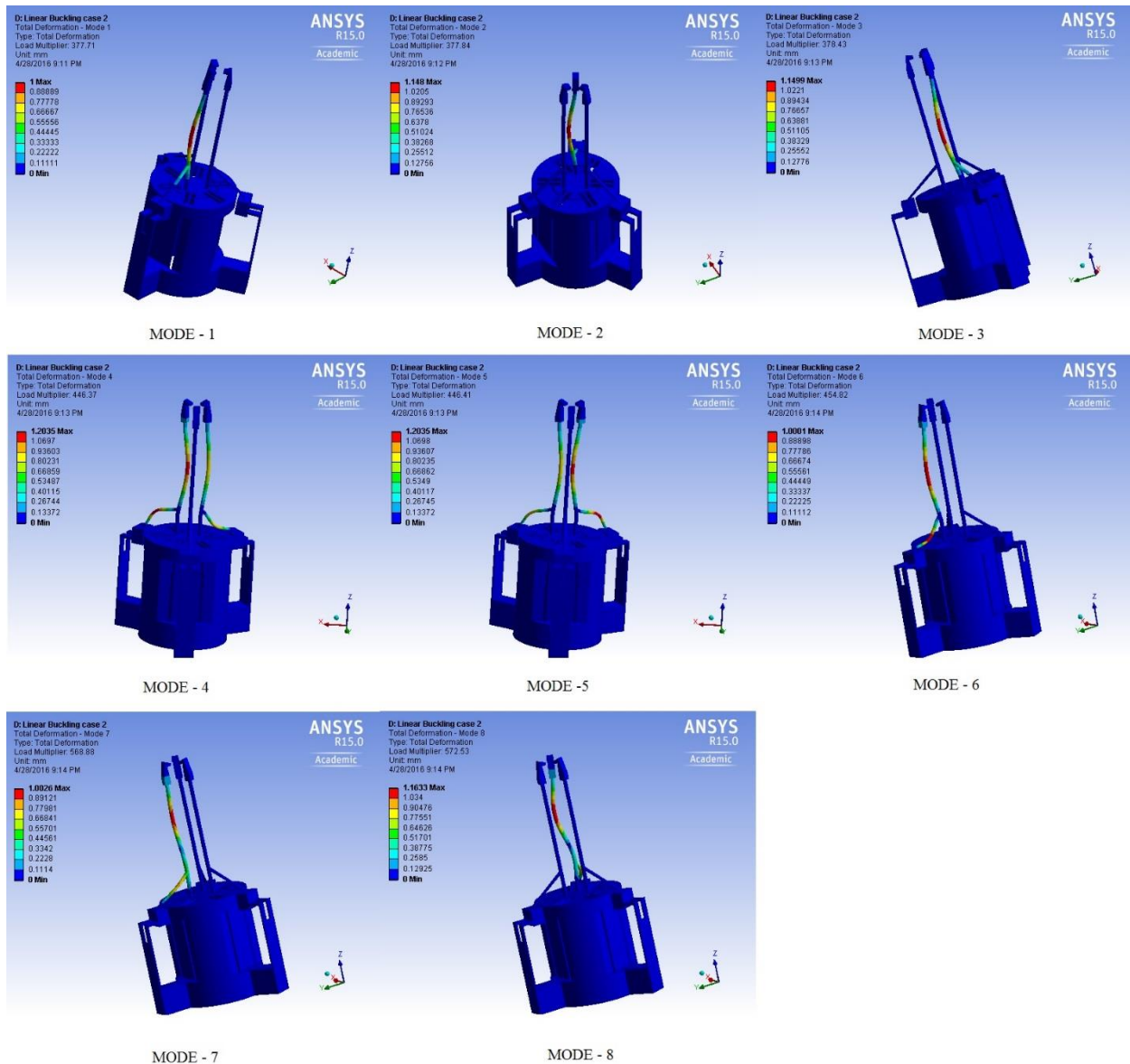
Input load of 190N and displacement of 0.008 mm are applied in the upward direction at three wings as shown in Figure 4.20, with fixed support on central and bottom base.

Output load multipliers are obtained, from which buckling load is calculated by equation (4.11) and tabulated in Table 4.10 as given below.

**Table 4.10:** Buckling load for fixed finger tips under PE actuation.

Mode	Load Multiplier	Buckling load (N)
1	377.71	71764.9
2	377.84	71789.6
3	378.43	71901.7
4	446.37	84810.3
5	446.41	84817.9
6	454.82	86415.8
7	568.88	108087.2
8	572.53	108780.7

The corresponding buckling modes are illustrated in Figure 4.29.



**Figure 4.29:** Buckling modes for fixed finger tips under PE actuation.

***Buckling with tips having frictionless support.*** In this case, with the assumption of object being grasped and the contact frictionless, analysis is performed by giving frictionless support at the tips of the gripper for close mode under EM and PE actuation. In frictionless contact, two faces in this contact can be separated freely, while in contact they slide in tangential direction without any frictional force.

a) Close mode under EM actuation

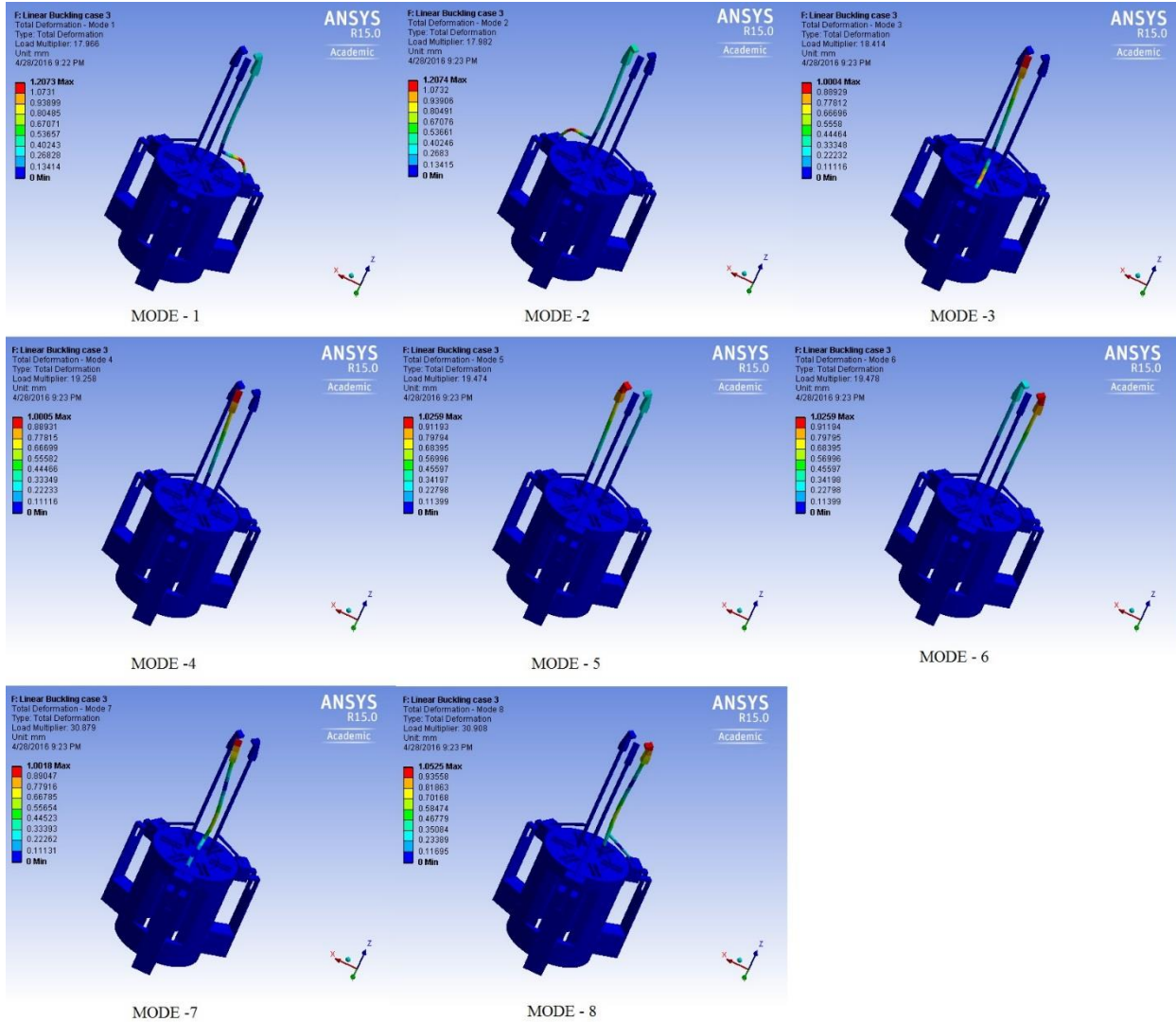
Input load of 0.002784N, and displacement of 0.208811 mm are applied in the downward direction on the central base as shown in Figure 4.15.

Output load multipliers are obtained from which buckling load is calculated by equation (4.11) and tabulated in Table 4.11 as given below.

**Table 4.11:** Buckling load for frictionless support at tips under EM actuation.

Mode	Load Multiplier	Buckling load (N)
1	17.966	-0.050017344
2	17.982	-0.050061888
3	18.414	-0.051264576
4	19.258	-0.053614272
5	19.474	-0.054215616
6	19.478	-0.054226752
7	30.879	-0.085967136
8	30.908	-0.086047872

The corresponding buckling modes are illustrated in the Figure 4.30.



**Figure 4.30:** Buckling modes for frictionless support at tips under EM actuation.

b) Close mode under PE actuation

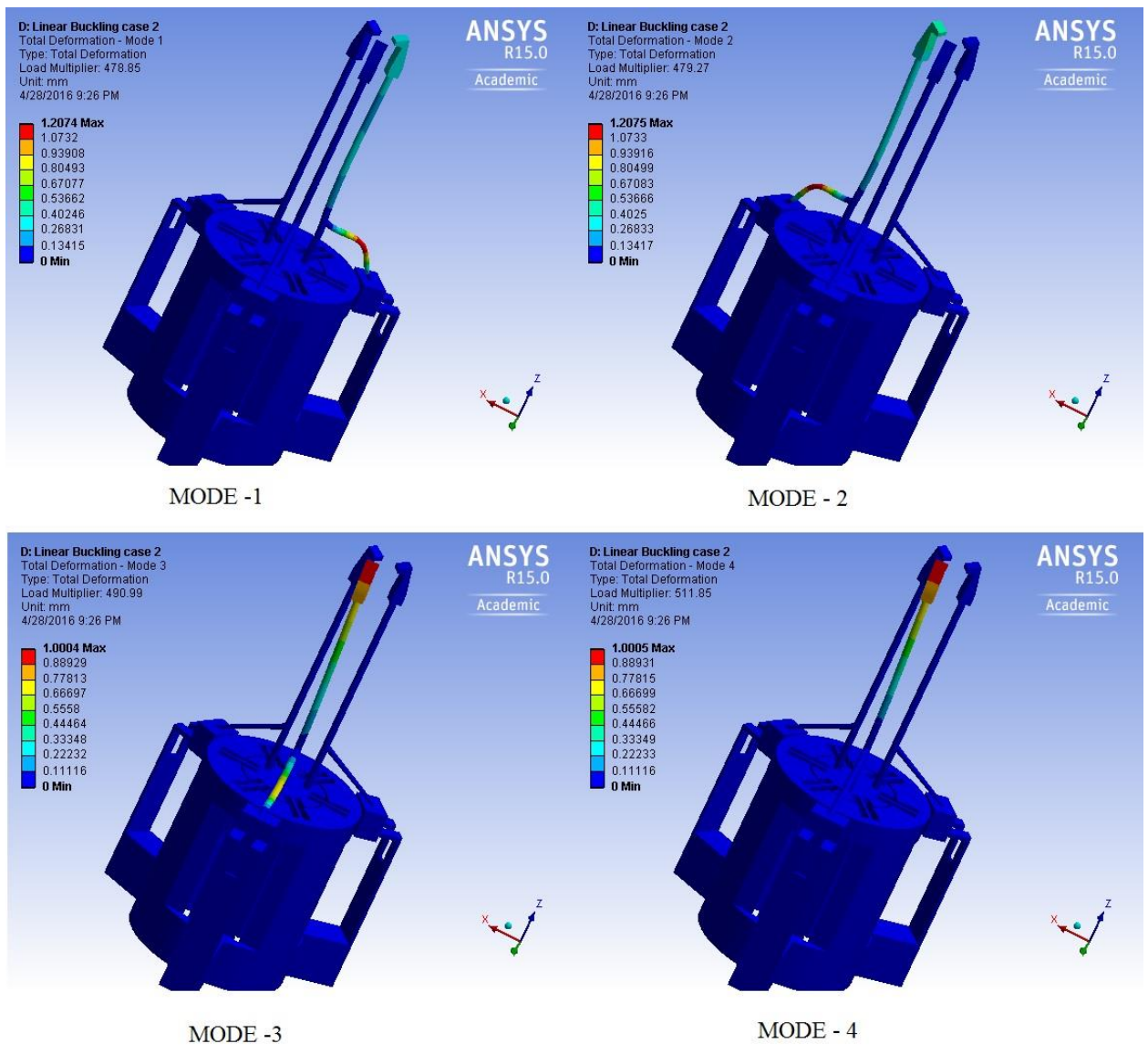
Input load of 190N and displacement of 0.008 mm are applied in the upward direction at three wings as shown in Figure 4.20.

Output load multipliers are obtained from which buckling load is calculated by equation (4.11) and tabulated in Table 4.12.

**Table 4.12:** Buckling load for frictionless support at tips under PE actuation.

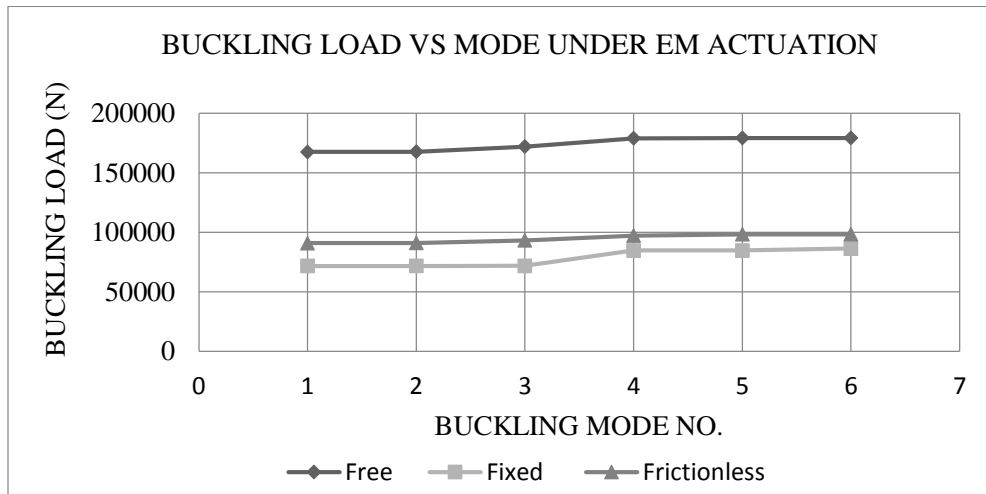
Mode	Load Multiplier	Buckling Load (N)
1	478.85	90981.5
2	479.27	91061.3
3	490.99	93288.1
4	511.85	97251.5

The corresponding buckling modes are illustrated by the following Figure 4.31.



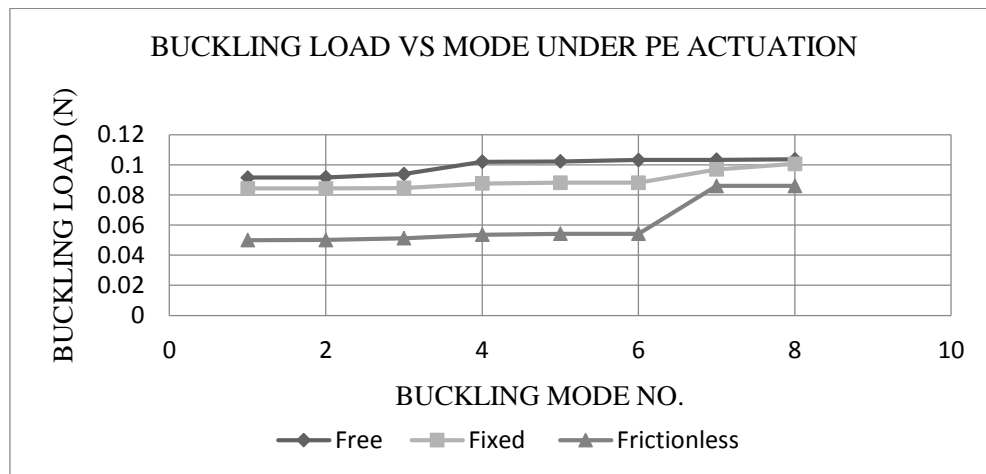
**Figure 4.31:** Buckling modes for frictionless support at tips under PE actuation.

Till now, buckling analysis has been performed for three conditions, i.e., with the tips having free end, fixed support, and the frictionless support. Buckling loads for all three cases are plotted against the mode number in Figure 4.32 and Figure 4.33 for EM and PE actuation respectively.



**Figure 4.32:** Effect of buckling load under EM actuation for various supports at tips.

From the above graph, we can say that the least buckling load is obtained when finger tips are fixed, i.e., when the object is tightly grasped.



**Figure 4.33:** Effect of buckling load under PE actuation for various supports at tips

From the above graph, we can say that the least buckling load is obtained when finger tips have frictionless support, i.e., when the object has frictionless contact with the gripper.

**4.1.2.4 Modal analysis.** Modal analysis is performed to study the simulation of vibrations in the gripper under pre-stressed and un-pre-stressed conditions. Open mode under EM actuation is considered and the analysis is performed. Natural frequencies are obtained, whose fundamental frequency is used in the calculation of Integration Time Step, given by equation (3.4). This is used for transient simulation in ANSYS Workbench.

**Un-pre-stress condition:** Three wings, central base, and bottom base are fixed, i.e., no external excitation is applied on the gripper.

**Pre-stress condition:** Input displacement of 3 mm and load of 0.04 N are applied in upward direction on the central base as shown in Figure 4.10, with fixed support at three wings and bottom base. Modal analysis uses only the stiffness matrix obtained from static structural analysis.

Following modes are obtained under un-pre-stressed and pre-stressed conditions.

**Table 4.13:** Natural frequencies for un-pre-stress and pre-stress conditions.

Mode	Un-pre-stress Frequency (Hz)	Pre-stress Frequency (Hz)
1	156.41	154.27
2	156.47	154.34
3	156.5	154.39
4	201.15	201.88
5	201.17	201.89
6	201.29	202.02

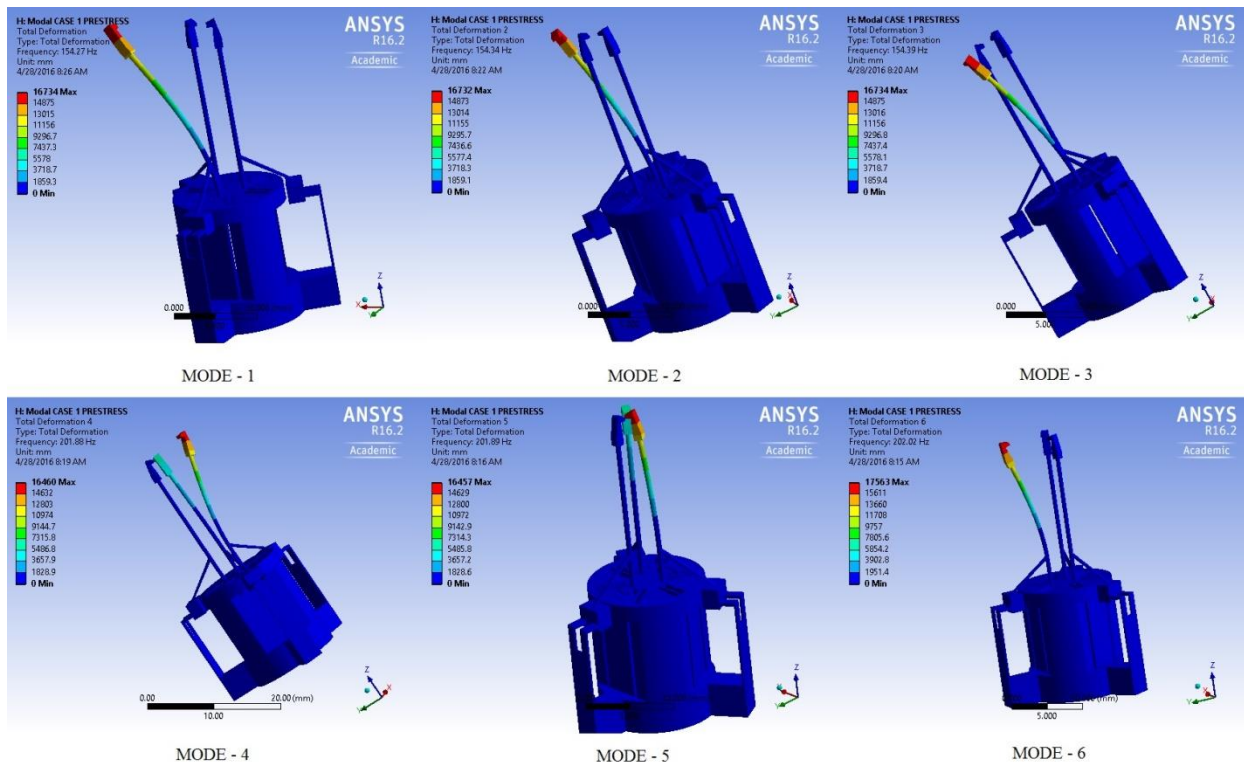
From Table 4.13, we can say that there is little difference between the values under no pre-stress and pre-stressed conditions. Therefore, pre-stress effects are found to be negligible.

Integration Time Step according to equation (3.4) is



$$ITS = 1/(20*154.27) = 0.000324 \text{ sec} \dots\dots\dots(4.12)$$

Modes obtained under pre-stressed condition are illustrated below.



**Figure 4.34:** Mode shapes under pre-stressed condition.

From Figure 4.34, it is evident that the fingers of the gripper are most sensitive to vibrations.

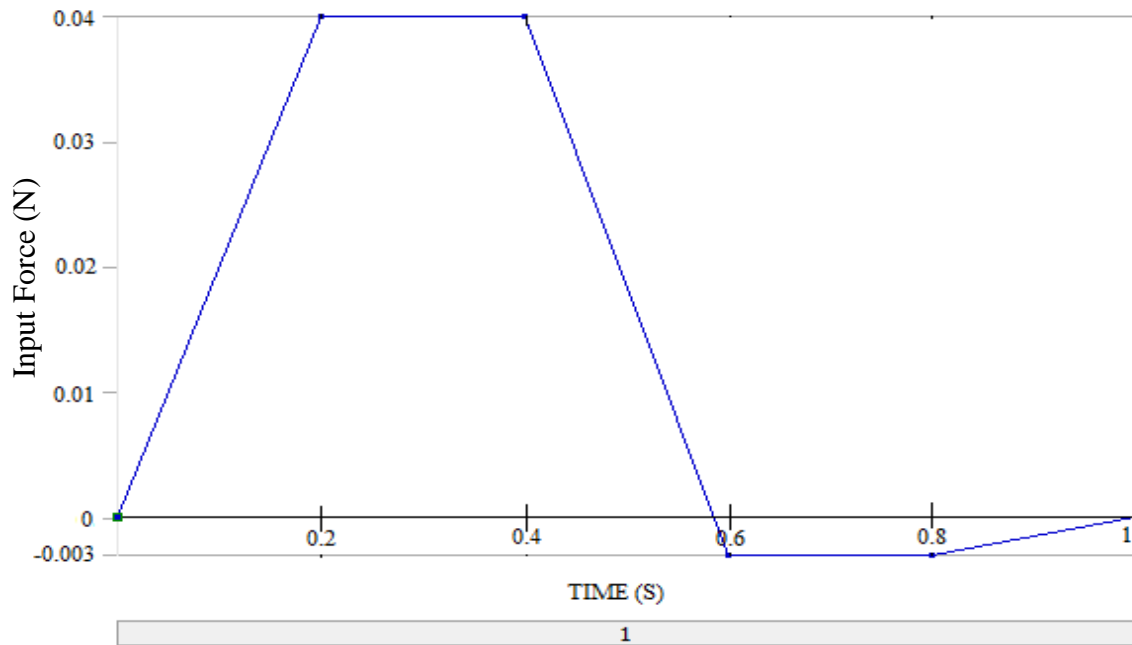
**4.1.2.5 Transient analysis.** Transient analysis is performed to simulate the behavior of gripper in terms of time response for opening and closing of finger tips under EM and PE actuation.

**Case-1:** Input EM load is applied on the central base with wings and bottom base fixed for the total time span of 1 second as given in Table 4.14 and Figure 4.35. Input displacement of 3mm and force of 0.04N is applied in the upward direction (Figure 4.10) from 0.2 – 0.4 sec, which results in **Open mode** of gripper. Input displacement of 0.225mm and force of 0.003N (critical load obtained in section 4.1.2.2 [b]) is applied in the downward direction (Figure 4.15) from 0.6

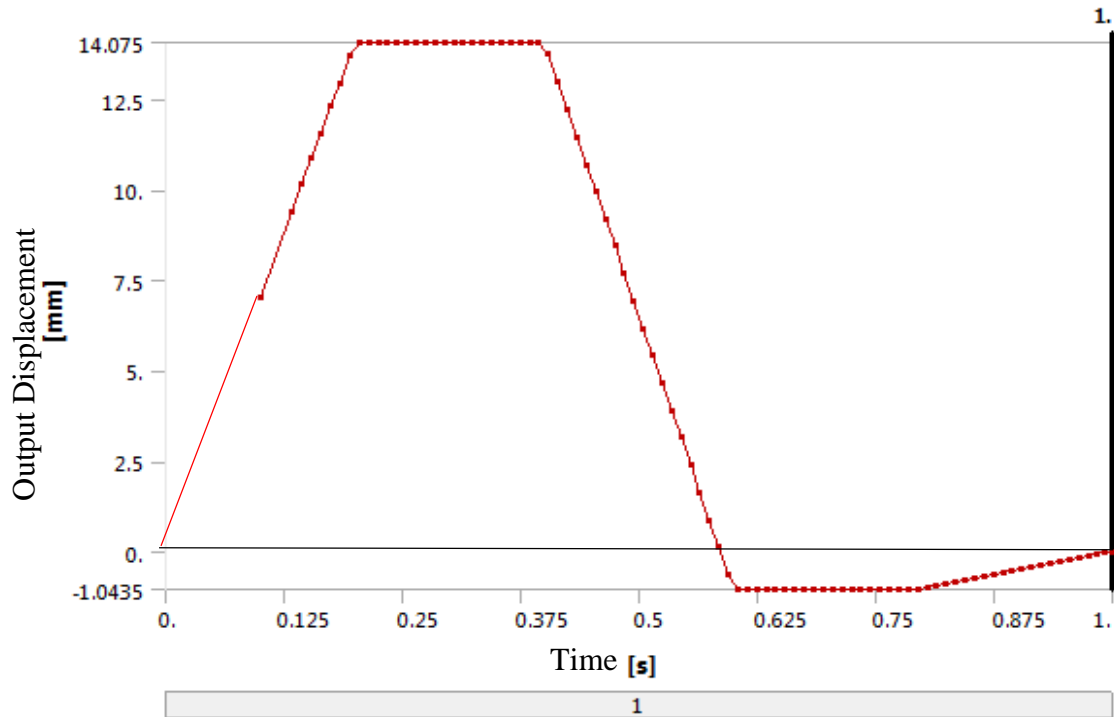
– 0.8 sec, which results in **Close mode** of gripper. Output horizontal deformation of the tip is represented against time on a plot as shown in Figure 4.36.

**Table 4.14:** Input EM load for transient analysis (Case-1).

Time [s]	Input Force [N]	Input Displacement [mm]
0	0	0
0.2	4.00E-02	3
0.4		
0.6	-3.00E-03	-0.225
0.8		
1	0	0



**Figure 4.35:** Input force vs time (Case-1).



**Figure 4.36:** Output horizontal tip displacement vs time (Case-1).

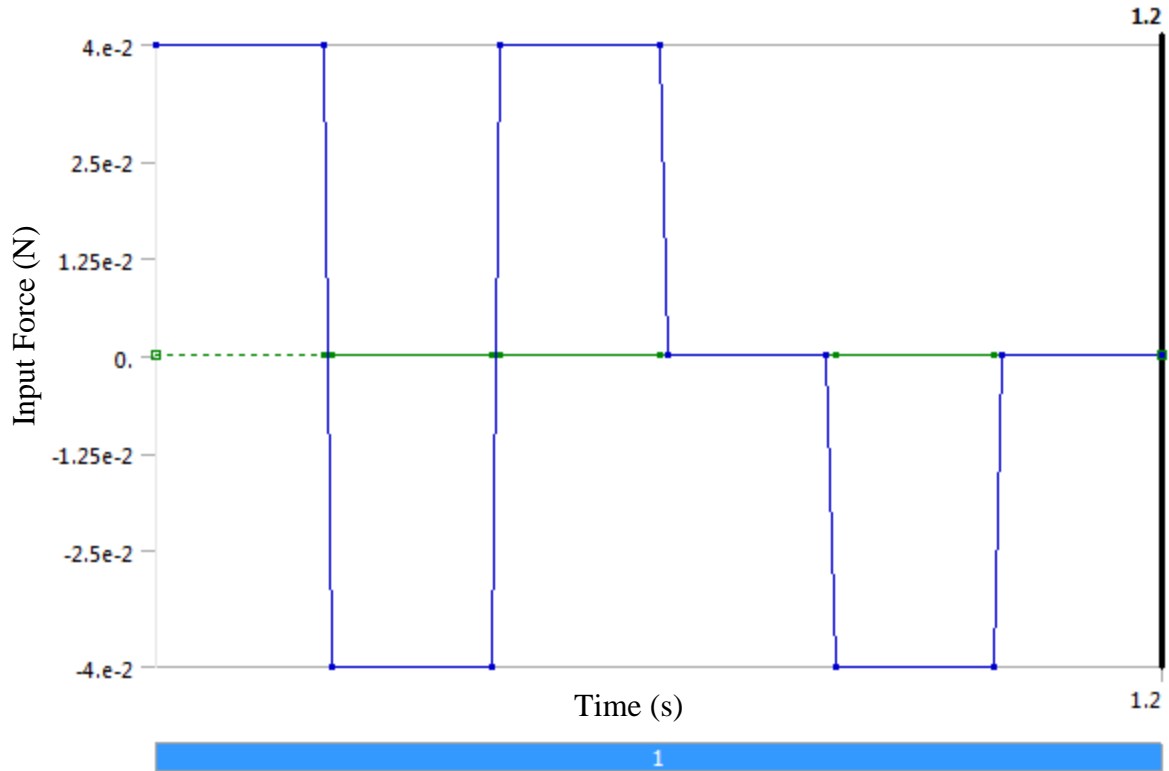
From 0 sec to 0.2 sec, EM input load is applied gradually in the upward direction, which results in the gradual opening of gripper. It is observed that maximum opening occurs at 0.2 sec which stays open till 0.4 sec with the maximum opening of 14.075 mm. From 0.4 sec, load is removed gradually, which facilitates to reach its neutral position at 0.6 sec. At 0.6 sec, EM input load is applied in the downward direction till 0.8 sec due to which, gripper closes gradually until 0.60044 sec, and then reaches its stable displacement of 1.0435 mm. From 0.8sec till 1 sec, load is gradually removed which facilitates in returning to its neutral position. It is observed that at 1sec, even upon complete removal of load, it didn't reach its neutral position, and the minute displacement at this point is found to be  $1.92e-5$  mm.

Static structural (section 4.1.2.2 [a]) and transient analysis resulted the same output directional deformation of 14.074 mm under EM loading in open mode.

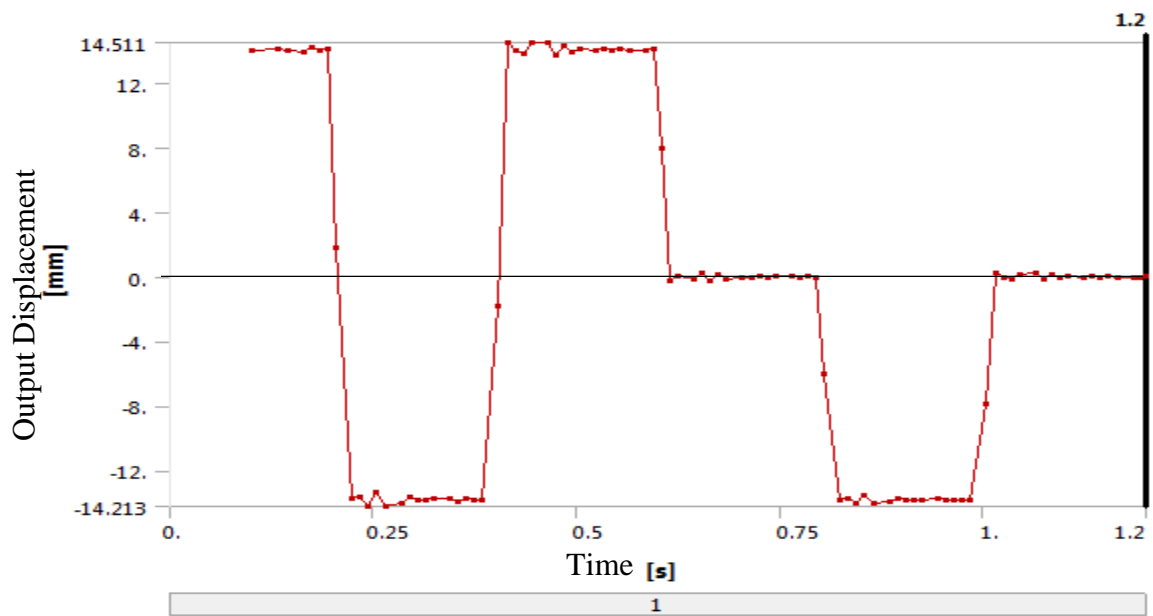
**Case-2:** Input EM load is applied on the central base with wings and bottom base fixed, for the total time span of 1.2 seconds as given in Table 4.15 and Figure 4.37. Input displacement of 3 mm and force of 0.04N is applied in the upward direction from (0 - 0.2) sec and (0.41 – 0.6) sec, which results in **Open mode** of gripper. Input displacement of 3mm and force of 0.004N is applied in the downward direction from (0.21 – 0.4) sec and (0.81 – 1) sec, which results in **Close mode** of gripper. Output horizontal deformation of the tip is represented against time on a plot as shown in Figure 4.38.

**Table 4.15:** Input EM load for transient analysis (Case-2).

Time [s]	Input Force [N]	Input Displacement [mm]
0	4.00E-02	3
0.2		
0.21	-4.00E-02	-3
0.4		
0.41	4.00E-02	3
0.6		
0.61	0	0
0.8		
0.81	-4.00E-02	-3
1		
1.01	0	0
1.2		



**Figure 4.37:** Input force vs time (Case-2).



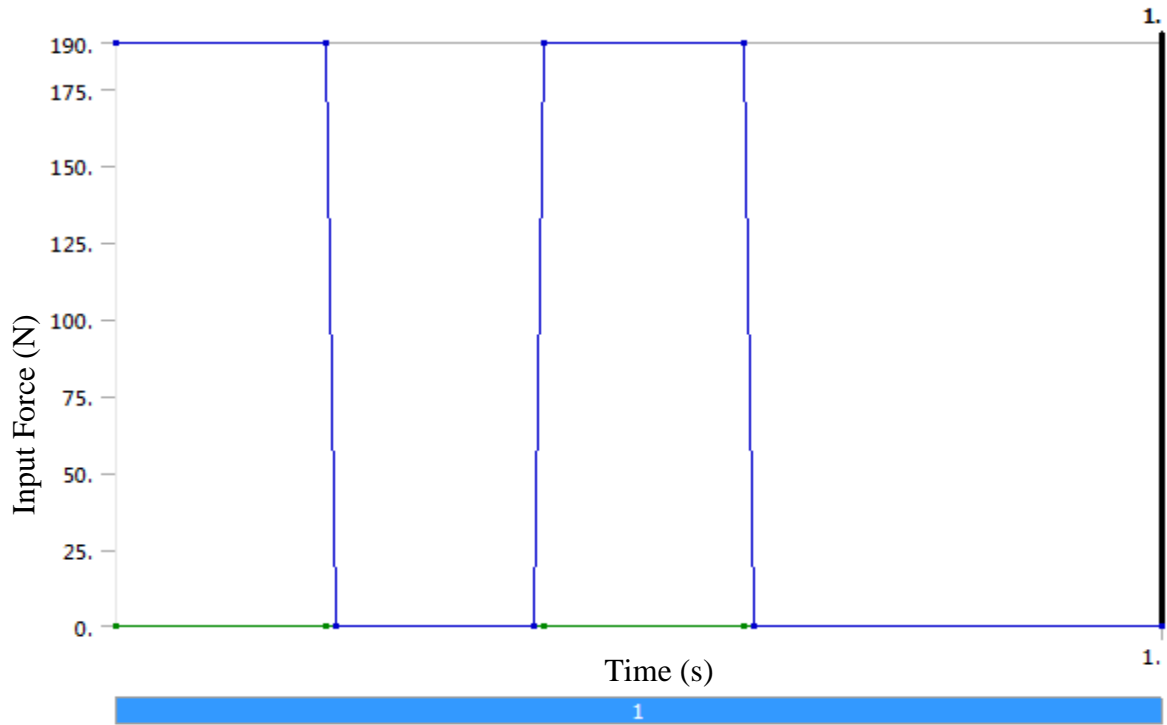
**Figure 4.38:** Output horizontal tip displacement vs time (Case-2).

At 1.2 sec, output tip displacement is not zero but it is  $4.29 \times 10^{-3}$  mm under input force of 0N. So, there existed some output displacement at 1.2 sec even if the actuation load is removed earlier at 1.01 sec.

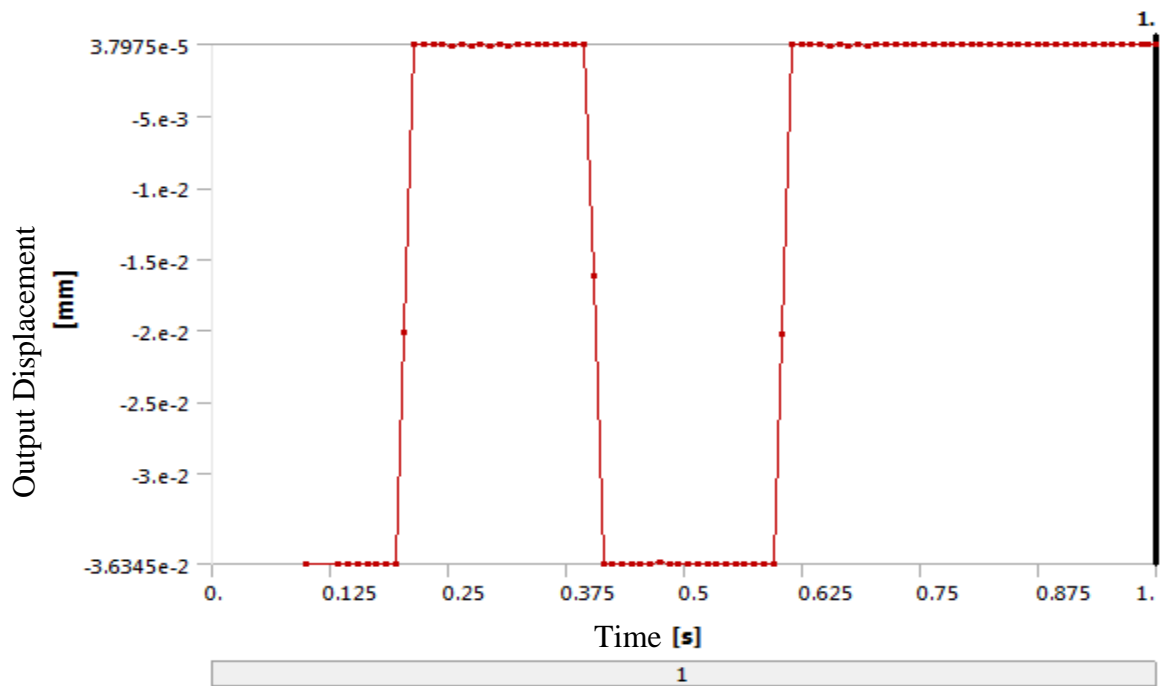
**Case-3:** Input PE load is applied on wings in the upward direction with central and bottom base fixed, for the total time span of 1 second as given in Table 4.16 and Figure 4.39. This results in **Close mode** of the gripper. Input displacement of 0.008 mm and force of 190N is applied from (0 – 0.2) sec and (0.41 – 0.6) sec. Output total deformation of the tip is represented against time on a plot as shown in Figure 4.40.

**Table 4.16:** Input PE load for transient analysis (Case-3).

Time [s]	Input Force [N]	Input Displacement [mm]
0	190	0.008
0.2		
0.21	0	0
0.4		
0.41	190	0.008
0.6		
0.61	0	0
1		



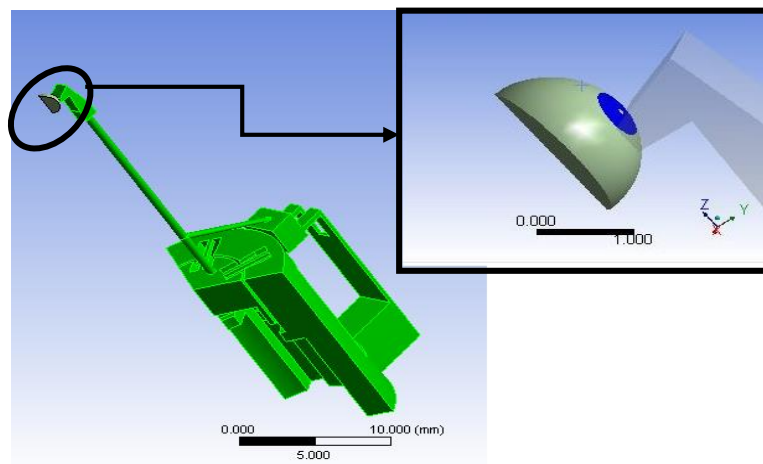
**Figure 4.39:** Input force vs time (Case-3).



**Figure 4.40:** Output horizontal tip displacement vs time (Case-3).

At the end of 1 second, output tip displacement is not zero but it is  $4.71e-8$  mm under input PE force of 0N. So, there existed some output displacement at the end of 1second even if the actuation load is removed earlier at 0.61 sec. Static structural and transient analysis resulted in the same horizontal tip displacement of 0.036 mm under PE loading in **Close mode**.

**4.1.2.6 Static structural analysis with the object grasped.** In this section, a rigid bead of diameter 1.88 mm is built with frictionless contact at the gripper tip. Contact pressure is then calculated. Symmetrical part of gripper is taken as shown in the Figure 4.41, to reduce the size of the problem.



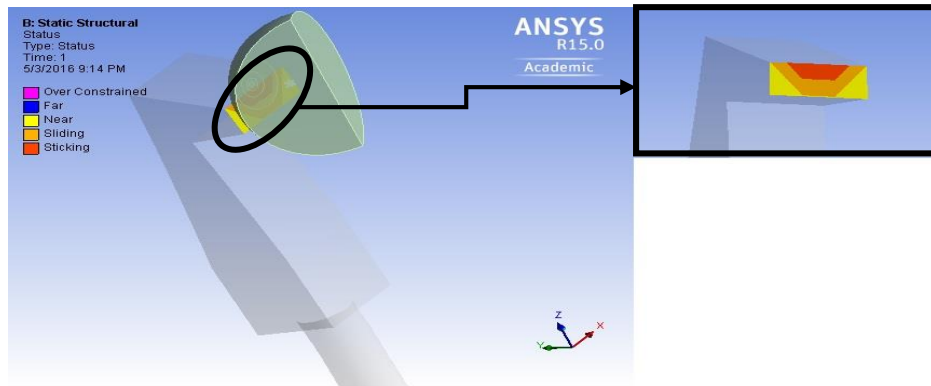
**Figure 4.41:** Gripper with the bead and its contact region.

Input force of  $-0.002784\text{N}$  and displacement of  $-0.20881\text{mm}$  (safe load obtained from section 4.1.2.2 [b]) is applied on the central base as shown in Figure 4.15. Wings and the bottom base are fixed.

Output results are discussed by the status and pressure at the contact region.

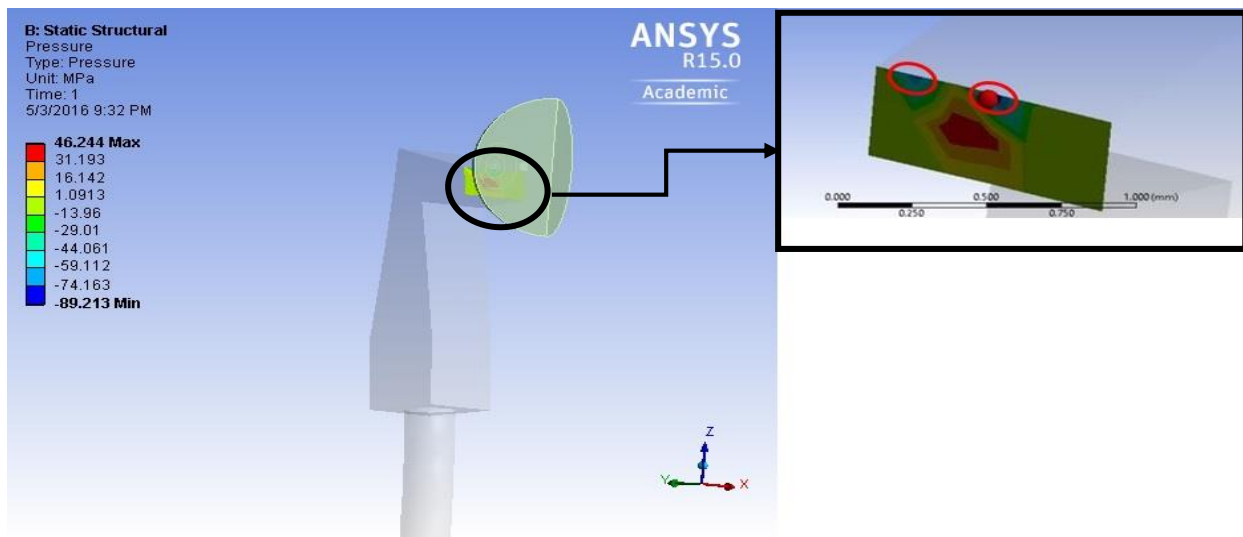
- a) **Contact status:** Status of the contact region is obtained as given below in Figure 4.42, which clearly shows that it is sticky at the contact region, and becomes sliding contact as it moves away from this region.





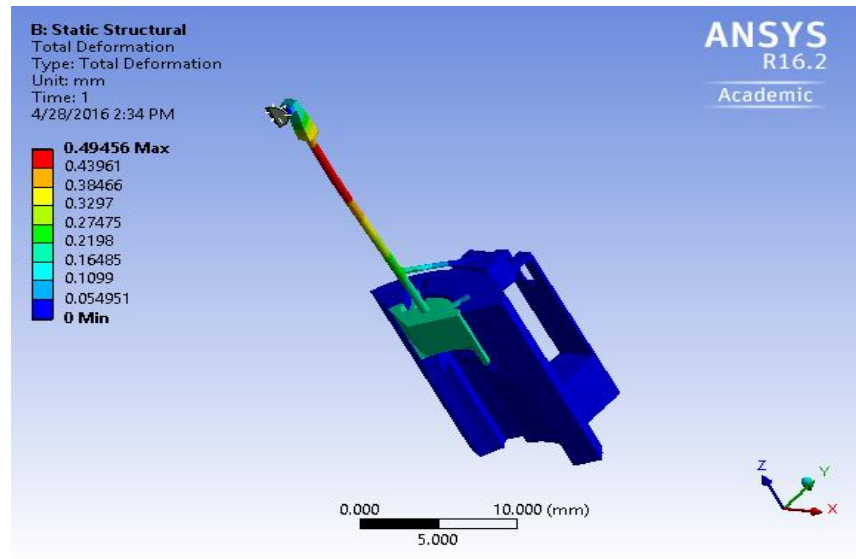
**Figure 4.42:** Contact status.

- b) **Contact pressure:** Pressure at the contact region is also evaluated, which is illustrated in Figure 4.43. It shows that more negative pressure (blue color region) is generated at the contact region and at a point in the surrounding as indicated below.



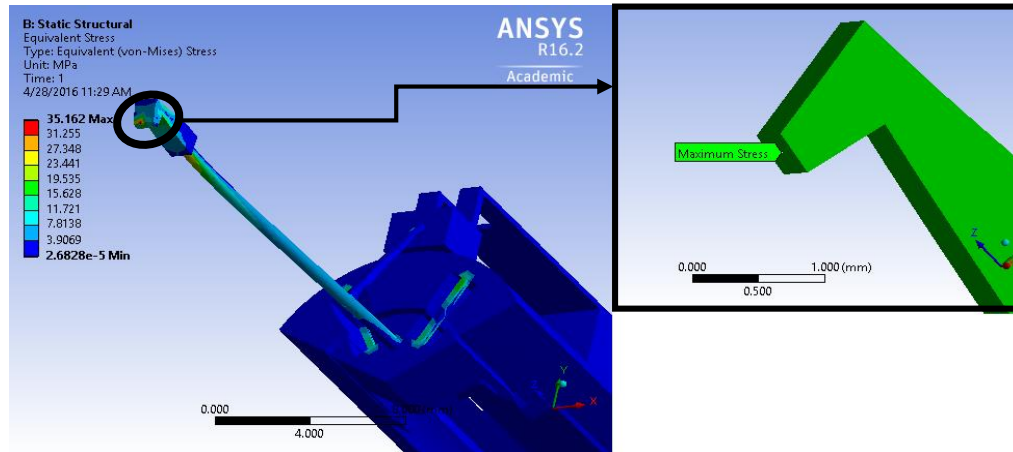
**Figure 4.43:** Contact pressure.

- c) **Total Deformation:** Maximum deformation here indicates the bending of finger at the region shown in red in the Figure 4.44, and as the bead is rigid there is zero deformation at the fingertip.



**Figure 4.44:** Output total deformation with the bead grasped.

- d) **Equivalent stress:** As the bead is rigid, the contact region at the tip of finger acts as the fixed point resulting in high stress generation in that region as shown in the Figure 4.45 below.



**Figure 4.45:** Output equivalent stress with the bead grasped.

## 4.2 Flexibility

This section deals with the scenarios which prove the flexibility of the proposed gripper. The capability of gripper for grasping small size to large size objects has been discussed. Small

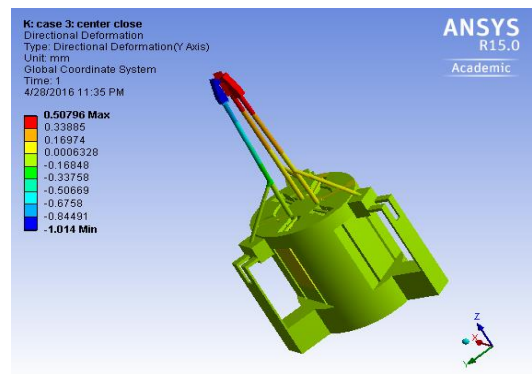
sized objects have been considered to have a size ranging from  $1\mu\text{m}$  to  $5\mu\text{m}$ , while large sized objects with the size ranging from 1mm to 5mm.

**4.2.1 Grasping small size object.** Grasping a smaller size object, such as radius  $2\mu\text{m}$ , i.e., 0.002 mm. The distance of the finger tip from its neutral position is 1.016 mm. Therefore, the tip has to displace horizontally by 1.014 mm, which is obtained by subtracting object size from 1.016 mm.

### Under EM actuation

Input of only EM actuation is applied on the central base in downward direction as shown in Figure 4.15, with fixed support on the wings and bottom base.

For the desired output displacement of 1.014 mm, using equation (4.7) from static-structural analysis, input displacement and force are given by 0.211734 mm and 0.002823N respectively. The required horizontal tip displacement of 1.014 mm is simulated, which will be able to grasp a bead of radius 0.002 mm as shown in Figure 4.46.



**Figure 4.46:** Gripper capable of grasping small sized object under EM actuation.

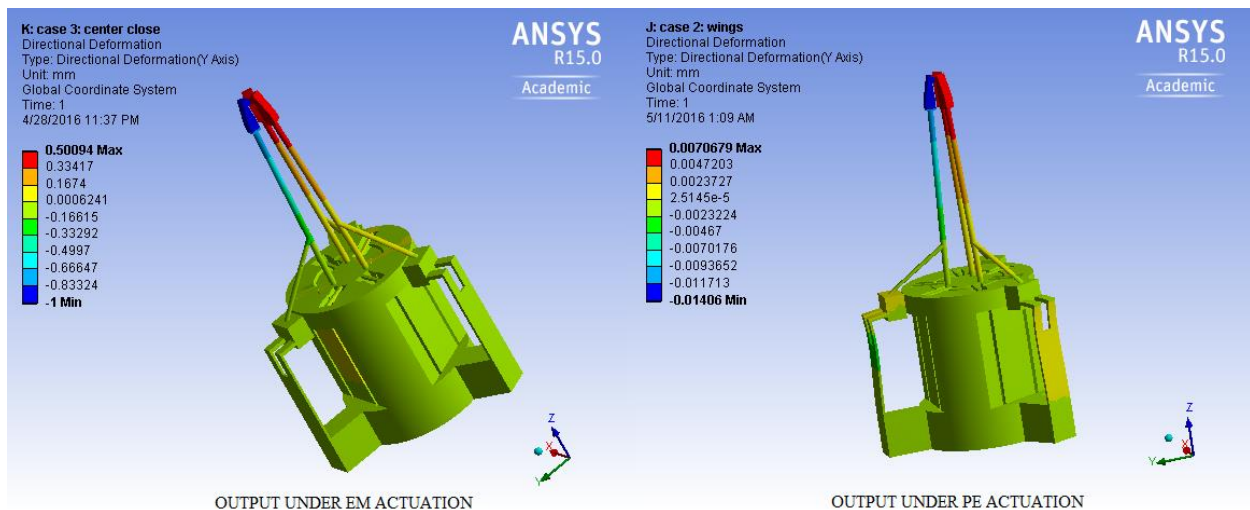
### Under EM and PE actuation

EM actuation is applied to achieve a displacement of 1mm (coarse movement), and the fine movement is achieved through PE actuation by displacing it 0.014 mm, giving us a total displacement of 1.014 mm.

EM actuation force of 0.002784N and displacement of 0.208811 mm applied on the central base in downward direction with the bottom base and three wings fixed. These values are calculated according to equation (4.7), for which output tip displacement is 1 mm.

PE actuation force of 69.9998N and displacement of 0.00295 mm is applied on the wings in upward direction with central and bottom base fixed. These values are calculated according to equation (4.9), for which output tip displacement is 0.014 mm.

The required horizontal tip displacement of 1mm through EM actuation and a displacement of 0.014 mm is simulated as shown in the Figure 4.47.



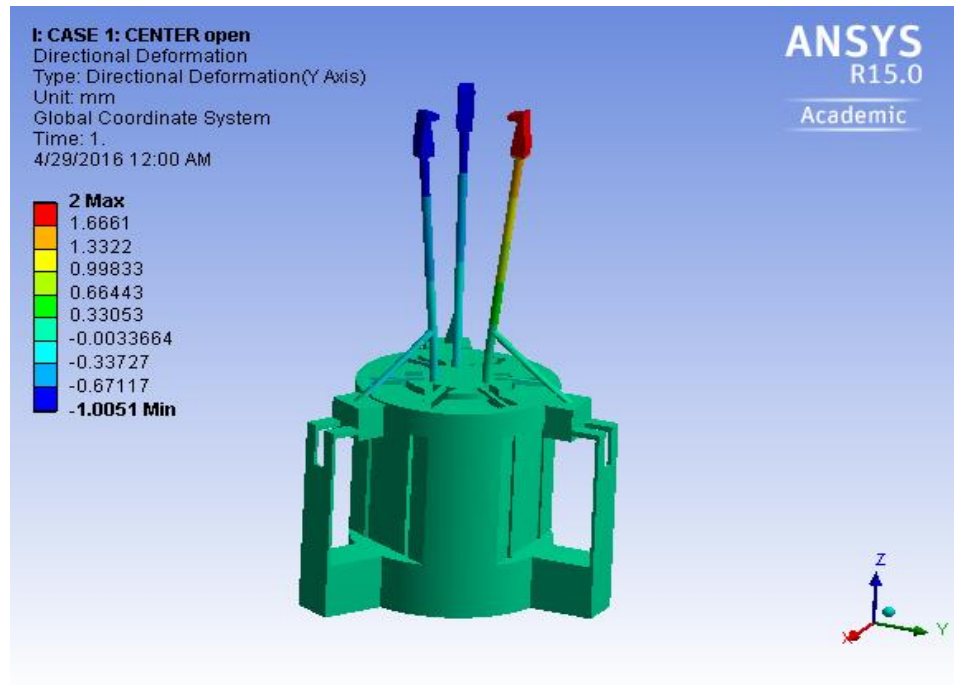
**Figure 4.47:** Gripper capable of grasping small sized under EM and PE actuation.

**4.2.2 Grasping large size object.** Let us consider grasping a larger size bead of radius 3 mm. The distance of the finger tip from its neutral position is 1.016 mm. Therefore, the tip has to open by 1.984 mm, which is obtained by subtracting 1.016 mm from the object size.

Only EM actuation is applied at the central base in upward direction with fixed support on the wings and bottom base.

For the desired output displacement of 1.984 mm, using equation (4.7) from static-structural analysis, input displacement and force are given by 0.417848 mm and 0.00571N respectively.

The required horizontal tip displacement of 1.984 mm is simulated (as shown in the following Figure 4.48), which will be able to grasp a bead of radius 3 mm.



**Figure 4.48:** Gripper capable of grasping large sized object under EM actuation.

From the above two scenarios, it is evident that gripper is flexible to grasp objects of sizes varying from micrometer size objects to millimeter size objects.

### 4.3 Scalability

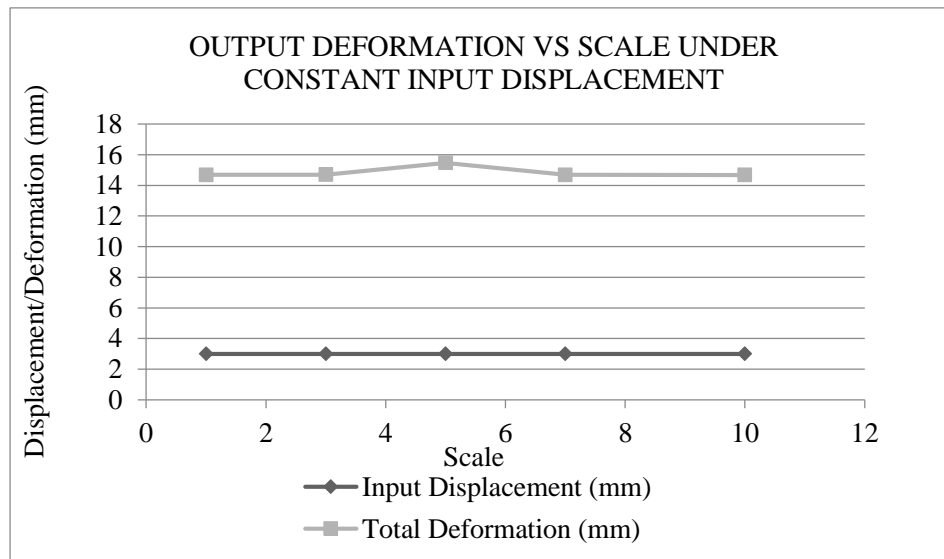
Test for scalability is performed by scaling up the gripper dimensions by a factor of 3, 5, 7, and 10. Input displacement is applied at the central base in upward direction for **Open mode** as shown in Figure 4.10, with wings and bottom base fixed. Two cases are considered. In ‘case-1’, constant input displacement is applied at each scale, while in ‘case-2’, input displacement is

scaled by the scale factor as shown in Table 4.17. Output total deformation and equivalent stress are then compared with the original scale, i.e., '1:1' for case-1 and case-2. Table 4.17 details the dimensions and the input displacement for different scales.

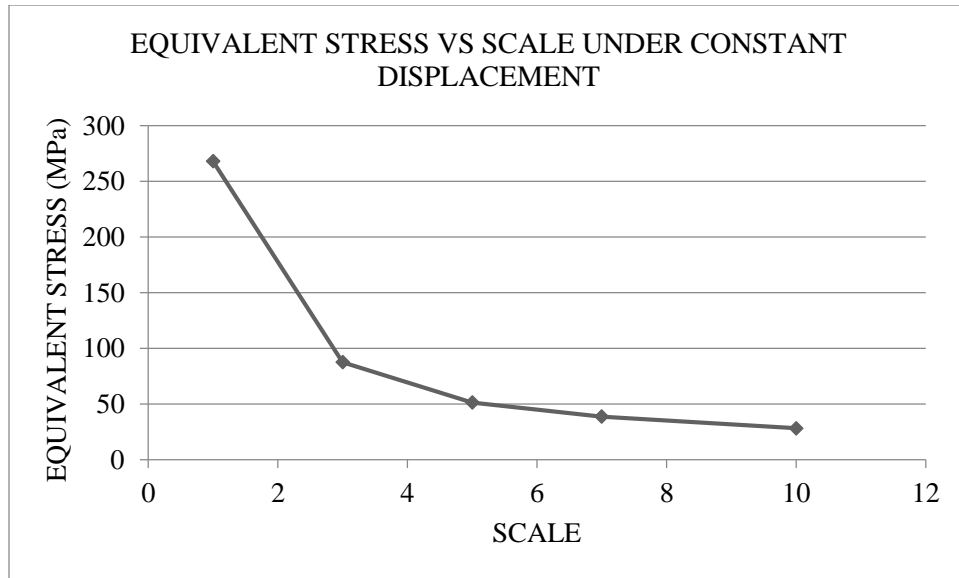
**Table 4.17:** Input parameters – scalability.

Scale	Dimensions (mm)	Case 1: Input Displacement (mm)	Case 2: Input Displacement (mm)
1:1	20.553 x 17.799 x 37.557	3	3
3:1	61.658 x 53.397 x 112.67	3	9
5:1	102.76 x 88.995 x 187.78	3	15
7:1	143.87 x 124.59 x 262.9	3	21
10:1	205.53 x 177.99 x 375.57	3	30

**4.3.1 Scalability under constant input displacement.** Output total deformation and equivalent stress at chosen scale factors for the constant input displacement of 3 mm are represented by the graphs in Figure 4.49 and Figure 4.50 respectively.



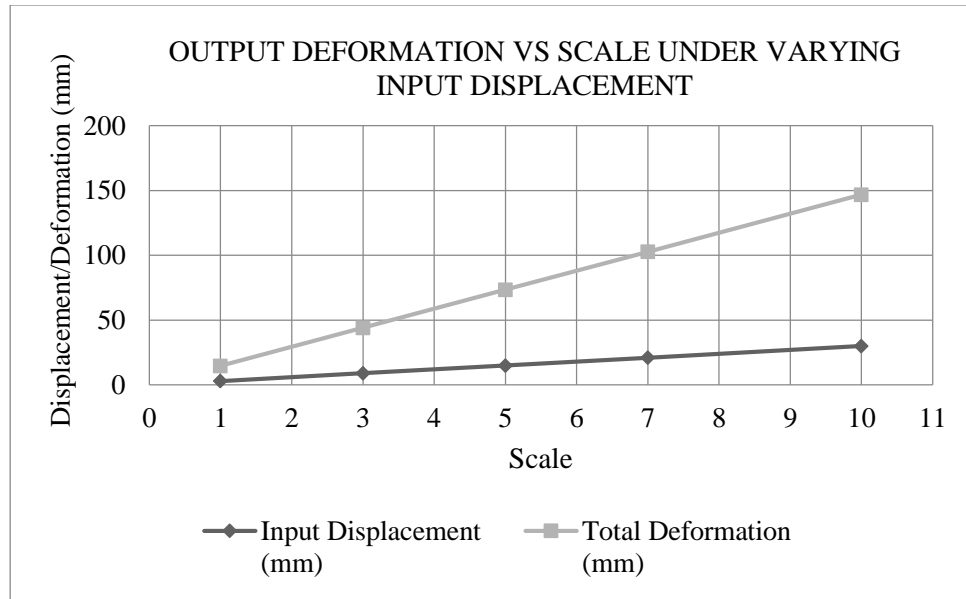
**Figure 4.49:** Effect of scalability on output deformation under constant input displacement.



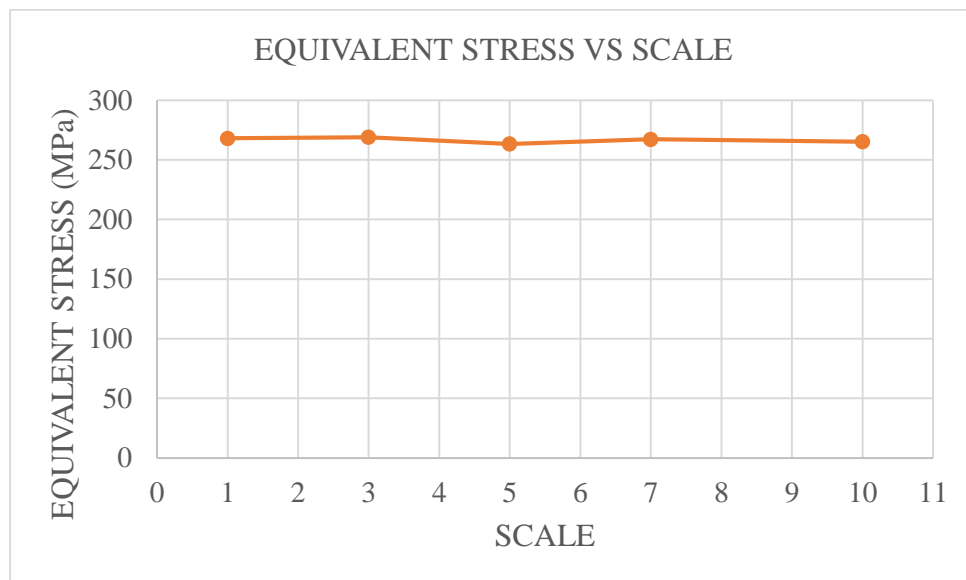
**Figure 4.50:** Effect of scalability on equivalent stress under constant input displacement.

It can be observed from the above graphs that output total deformation is almost the same for all scales, while the equivalent stress is found to decrease by its scale factor. For example, equivalent stress at scale factor of 3 is  $1/3^{\text{rd}}$  of the equivalent stress at original scale. Location of maximum stress is same at all scales.

**4.3.2 Scalability under varying input displacement.** Output total deformation and equivalent stress at chosen scale factors under varying input displacement as given in Table 4.17 are represented by the graphs in Figure 4.51 and Figure 4.52 respectively.



**Figure 4.51:** Effect of scalability on output deformation under varying input displacement.



**Figure 4.52:** Effect of scalability on equivalent stress under varying input displacement.

It can be observed from the above graphs that the equivalent stress is the same at all scales, while output total deformation got scaled up by the same factor. For example, total deformation at scale factor of 3 is three times the deformation at original scale. Location of maximum stress is the same at all cases.



## CHAPTER 5

### SUMMARY AND DISCUSSION

This chapter summarized the results of the project, and also conclusions have been discussed along with future work suggestions.

#### 5.1 Summary

Objectives of this study were to study the functionality, flexibility, and scalability of the gripper. ANSYS Workbench has been used to simulate the gripper performance to achieve the stated objectives. Specifications of EM and PE actuators are taken from their manufacturing website. A simplified line model is taken initially to optimize the link lengths for the best design resulting in maximum gripping range. Optimized gripper increased its tip displacement from 11.916 mm to 12.143 mm. Proposed 3-D model of the gripper has its bounding dimensions of 20.553 x 17.799 x 37.557 mm. Optimized link lengths are updated in the 3-D model of the gripper.

Functionality is tested by performing static structural analysis, buckling analysis, modal analysis, and transient analysis. Maximum safe EM load for gripper in open mode is 0.0063N and 2.2494 mm, while in close mode it is 0.0028N and 1 mm. Maximum safe PE load for gripper in close mode is 5753.42N and 0.5753 mm. Gripper parts affected by buckling are its fingers, thin connecting members on the top base, and the region at the connection of wings to bottom base. EM buckling load is 0.1026N, and for PE actuation it is 167498.3N.

Gripper has been tested for its flexibility in gripping capability and can grasp micrometer to millimeter size objects. Sensitivity of EM actuator chosen is found to be 359 mm/N, while for PE actuator it is 0.0001 mm/N. Effect of scaling gripper dimensions and input displacement resulted in scaling of output deformation also by the same factor with equivalent stress remaining

same, while at constant input displacement, equivalent stress got scaled down by the scale factor with the deformation remaining same at all scales. So, we can say that gripper can be scaled.

## **5.2 Future work**

Suggestions for future work include reducing the buckling effects in thin structures such as the fingers, connecting members on top base, and the links connecting wings and bottom base. Strength can be increased by increasing the thickness of these members. Fabrication can be done by 3-D printing to obtain a compliant structure. More research can be done to avoid failures observed in the gripper and in fabrication.

Control system can be integrated with robot to control the motion of the gripper. Path planning which involves kinematic modeling of the gripper can be studied along with sensitivity of gripper.

## REFERENCES

- Amend, J. R., Jr., Brown, E., Rodenberg, N., Jaeger, H. M., & Lipson, H. (2012). A positive pressure universal gripper based on the jamming of granular material. *Robotics, IEEE Transactions*, 28, 341–350.
- Appleton, E., & Williams, D. (2012). *Industrial robot applications*. New York, NY: Springer Science & Business Media.
- Belfiore, N. P., & Pennestrì, E. (1997). An atlas of linkage-type robotic grippers. *Mechanism and Machine Theory*, 32, 811–833.
- Boeraeve, D. I. P. (2010). Introduction to the Finite Element Method (FEM). *Institutgramme Liege*, 2–68.
- Buzuayene, M. (2008). Rise time vs. bandwidth and applications. Retrieved from <http://www.interferencetechnology.com/rise-time-vs-bandwidth-and-applications/>
- Castillo-León, J., Svendsen, W. E., & Dimaki, M. (2011). *Micro and nano techniques for the handling of biological samples*. Boca Raton, FL: CRC Press.
- Daerden, F., & Lefeber, D. (2002). Pneumatic artificial muscles: Actuators for robotics and automation. *European journal of mechanical and environmental engineering*, 47, 11–21.
- Datta, R., Pradhan, S., & Bhattacharya, B. (2016). Analysis and design optimization of a robotic gripper using multiobjective genetic algorithm. *Systems, Man, and Cybernetics: Systems, IEEE Transactions*, 46, 16–26.
- Eitel, E. (2010). A history of gripping and gripper technologies and the available options for today's engineer. *Machine Design*.

- Felippa, C. A. (2004). Introduction to finite element methods. Course notes, Department of Aerospace Engineering Sciences, University of Colorado at Boulder, retrieved from <http://www.colorado.edu/engineering/Aerospace/CAS/courses>
- Goradia, A., Xi, N., & Elhaji, I. H. (2005). Internet based robots: Applications, impacts, challenges and future directions. In *Advanced Robotics and its Social Impacts, 2005. IEEE Workshop*, 73–78.
- Groover, M. P., Weiss, M., & Nagel, R. N. (1986). *Industrial robotics: Technology, programming and application*. Columbus, OH: McGraw-Hill Higher Education.
- Hoshizaki, J., & Bopp, E. (1990). *Robot applications design manual*. Hoboken, NJ: John Wiley & Sons.
- Huber, J., Fleck, N., & Ashby, M. (1997). The selection of mechanical actuators based on performance indices. In *Proceedings of the Royal Society of London A: Mathematical, Physical and Engineering Sciences* (pp. 2185–2205).
- Hunter, I. W., Hollerbach, J. M., & Ballantyne, J. (1991). A comparative analysis of actuator technologies for robotics. *Robotics Review*, 2, 299–342.
- Karabegović, I., Karabegović, E., & Husak, E. (2013). Industrial robot applications in manufacturing process in Asia and Australia. *Tehnički vjesnik*, 20, 365–370.
- Kim, J., Alspach, A., & Yamane, K. (2015). 3D printed soft skin for safe human-robot interaction. Retrieved from <http://www.disneyresearch.com/wp-content/uploads/3D-Printed-Soft-Skin-for-Safe-Human-Robot-Interaction-Paper.pdf>
- Lanni, C., & Ceccarelli, M. (2009). An optimization problem algorithm for kinematic design of mechanisms for two-finger grippers. *Open Mechanical Engineering Journal*, 3, 49–62.

- Lee, H.-H. (2015). *Finite element simulations with ANSYS Workbench 16*. Mission, KS: SDC Publications.
- MacDuffie, J. P., & Pil, F. K. (1997). *From fixed to flexible: Automation and work organization trends from the international assembly plant study*. New York, NY: Springer.
- MacDuffie, J. P., Sethuraman, K., & Fisher, M. L. (1996). Product variety and manufacturing performance: Evidence from the international automotive assembly plant study. *Management Science*, 42, 350–369.
- Materialise. (2015). Materialise grippers for assembly line automation.
- Miccoli, G. (2004). *Why and how do design optimization*. Presented at the Eleventh International Congress on Sound and Vibration, St. Petersburg, Russia.
- Monkman, G. J., Hesse, S., Steinmann, R., & Schunk, H. (2007). *Robot grippers*. Hoboken, NJ: John Wiley & Sons.
- Nair, P. (1997). Types of artificial gripper mechanisms. *Society of Robotics and Automation*.
- Nikoobin, A., & Niaki, M. H. (2012). Deriving and analyzing the effective parameters in microgrippers performance. *Scientia Iranica*, 19, 1554–1563.
- Parker, L. E., & Draper, J. V. (1998). Robotics applications in maintenance and repair. *Handbook of Industrial Robotics*, 1023–1036.
- Petković, D., Pavlović, N. D., Shamshirband, S., & Badrul Anuar, N. (2013). Development of a new type of passively adaptive compliant gripper. *Industrial Robot: An International Journal*, 40, 610–623.
- Pham, D., & Yeo, S. (1991). Strategies for gripper design and selection in robotic assembly. *The International Journal of Production Research*, 29, 303–316.

- Qingsong, X. (2015). Design of asymmetric flexible micro-gripper mechanism based on flexure hinges. *Advances in Mechanical Engineering*, 7(6), 1–8.
- Rao, R. V., & Savsani, V. J. (2012). *Mechanical design optimization using advanced optimization techniques*. New York, NY: Springer Science & Business Media.
- Reddy, P. V. P., & Suresh, V. (2013). A review on importance of universal gripper in industrial robot applications. *International Journal of Mechanical Engineering Robotics Research*, 2, 255–264.
- Robotiq. (2015). Why use a robot gripper with 3 fingers? *Robotics Industry News, Applications and Trends*, M. Belanger-Barrette.
- Romheld Automation. *Products Guide*. Retrieved from [http://www.romheld.com.au/pdf/Product\\_Guide\\_2012.pdf](http://www.romheld.com.au/pdf/Product_Guide_2012.pdf)
- Rubinstein, L. (2000). *A practical nanorobot for treatment of various medical problems*. Draft paper for the 8th Foresight Conference on Molecular Nanotechnology, Bethesda, MD.
- Sam, J., Kumar, J., Tetteh, E. A., & Braineard, E. P. (2014). A study of why electrostatic actuation is preferred and a simulation of an electrostatically actuated cantilever beam for MEMS applications. *International Journal of Engineering Sciences & Emerging Technologies*, 6(5), 441–446.
- Seidemann, V., Rabe, J., Feldmann, M., & Büttgenbach, S. (2002). SU8-micromechanical structures with in situ fabricated movable parts. *Microsystem Technologies*, 8, 348–350.
- Shahhosseini, A. M. (2015). *Design, Manufacturing and Mechatronics: Proceedings of the 2015 International Conference on Design, Manufacturing and Mechatronics (ICDMM2015)*. Singapore: World Scientific.

- Takemoto, M. (2002). Estimation of five elastic stiffness coefficients of unidirectional glass fiber reinforced plastic by laser generated ultrasonic. *Advanced Composite Materials*, 11(2), 121–135.
- Wu, C.-C., Lee, C.-C., Cao, G., & Shen, I. (2005). Effects of corner frequency on bandwidth and resonance amplitude in designing PZT thin-film actuators: An experimental demonstration. In *ASME 2005 International Mechanical Engineering Congress and Exposition* (pp. 437–441).
- Yan, H.-S. (1998). *Creative design of mechanical devices*. New York, NY: Springer Science & Business Media.